

DIGESTION OF TITANIFEROUS SLAGS WITH
SULPHURIC ACID

by
JEAN-FRANCOIS TURGEON

Department of Mining and Metallurgical Engineering
McGill University
Montreal, Canada

September 1992

A Thesis Submitted to the Faculty of
Graduate Studies and Research
in Partial Fulfillment of the Requirements
of the Degree of Master of Engineering

© J.F. Turgeon, 1992.

ABSTRACT

Digestion of titaniferous slag (Sorelslag) with sulphuric acid was studied in an effort to optimise the process and develop a better understanding of its chemistry.

Thermodynamic analysis of the digestion reaction was performed using the program F*A*C*T. A laboratory reactor was built to simulate the operation of an industrial slag digestion reactor. Microstructure examinations of digestion samples revealed the main phases present.

Statistically designed experiments using the Box-Behnken technique were performed in the laboratory to correlate the responses (digestion yield, maximum temperature, solidification time, degree of Ti_2O_3 oxidation, sulphuric acid loss in the gas, active acid/titanium ratio and cake height) to the four experimental variables (particle size of the slag, acid concentration, acid/slag weight ratio and baking time).

Model equations successfully tested were obtained for each response. The analysis of the figures obtained from those equations revealed the relative importance of the variables evaluated. In complement to these experimental results the qualitative mass and heat balances were calculated.

RESUME

La digestion de la scorie de titane (Sorelslag) avec de l'acide sulfurique a été étudiée dans un effort pour optimiser et développer une meilleure compréhension du procédé.

Une analyse thermodynamique des réactions de digestion a été réalisée en utilisant le programme F*A*C*T. Un réacteur de laboratoire a été construit pour simuler les conditions rencontrées dans les digesteurs de scorie industriels. Une observation microscopique des échantillons de digestion a permis d'en identifier les principaux composants.

Un plan d'expérimentation statistique utilisant la technique Box-Behnken a été réalisé en laboratoire afin de corréler les réponses (rendement de digestion, température maximale, temps écoulé avant la solidification, degré d'oxydation du Ti_2O_3 , acide sulfurique perdu dans les gaz, rapport acide actif/titane et la hauteur du solide) aux quatre variables expérimentales (granulométrie de la scorie, concentration d'acide, rapport acide/scorie et temps de mûrissement). Des équations statistiques testées avec succès ont été obtenues pour chaque réponse. L'analyse des graphiques, générés à partir des équations, montre l'importance relative des variables étudiées. Pour compléter ces résultats expérimentaux, des bilans de matière et d'énergie ont été calculés.

ACKNOWLEDGEMENTS

I would like to express my sincere gratitude and appreciation to professor G.P. Demopoulos for his inspiring supervision and his continual interest and encouragement throughout the course of this work.

I especially wish to thank Michel Guéguin, principal scientist at QIT-Fer et Titane, for his invaluable guidance, support and advice.

I would also like to thank all of the members of the Hydrometallurgy research group of McGill University and my working colleagues at QIT for their helpfulness and team-like disposition. In particular I want to thank Bruno Côté for his help he offered me at McGill, Cesar Gomez for the meticulous reading and fruitful discussions and Gabriel Falconi for his help with the chemical analysis.

Finally, I would like to express my gratitude to QIT-Fer et Titane Research for providing the equipment and personnel necessary to realize that work.

TABLE OF CONTENTS

	<u>Page</u>
ABSTRACT	i
RESUME	ii
ACKNOWLEDGEMENTS	iii
TABLE OF CONTENTS	iv
LIST OF FIGURES	vii
LIST OF TABLES	xi
1. INTRODUCTION	1
2. LITERATURE SURVEY	3
2.1 Production of the Titanium Slag "Sorelslag"	3
2.2 Characterization of "Sorelslag"	8
2.3 The Sulphate Process for Pigment Manufacture	9
2.4 The Digestion Process	13
2.5 Statistical Design	17
3. THERMODYNAMICS	18
3.1 The Program F*A*C*T	19
3.2 Estimation of the Entropy of Solid Compounds	21
3.3 Estimation of Heat Capacities	24
3.4 Estimation of the Heat of Formation	25
3.5 Thermodynamic Modelling Results	30
4. EXPERIMENTAL	36
4.1 Preparation of Materials	36
4.2 Apparatus	40
4.2.1 Reactor	40
4.2.2 Heating system	42

	<u>Page</u>
4.2.3 Mixing	42
4.2.4 Data acquisition	42
4.2.5 Gas collection system	43
4.2.6 Steam	43
4.2.7 Tachometer	44
4.2.8 Settling tank	44
4.3 Digestion Procedure	46
4.4 Analysis	50
5. STATISTICAL DESIGN METHODOLOGY	51
5.1 Selection of Process Variables	51
5.2 Selection of Statistical Design	52
5.3 Selection of Statistical Software	56
6. RESULTS AND DISCUSSION	59
6.1 Experimental Design Data	59
6.2 Heat and Mass Balances Calculations	60
6.3 Microscopic Examination of Sorelslag Prior and After Digestion	67
6.4 Study of the Digestion Response	75
6.4.1 Recovery of TiO_2	75
6.4.2 Maximum temperature obtained	91
6.4.3 Set-up time	94
6.4.4 Black liquor active acid / titanium ratio	96
6.4.5 Oxidation of Ti_2O_3 during digestion	97
6.4.6 Sulphuric acid - equivalent losses in the exit gas	105
6.4.7 Digestion cake height	108

	<u>Page</u>
6.5 Special Conditions and Recommendations	110
7. CONCLUSIONS AND FUTURE WORK	111
7.1 Conclusions	111
7.2 Further Investigations	115
REFERENCES	116
APPENDICES	122
APPENDIX A: EXAMPLE OF A TABLE PRODUCED BY "INSPECT"	122
APPENDIX B: EXAMPLE OF A TABULAR PRINT-OUT FROM "REACTION"	124
APPENDIX C: EXAMPLE OF THE RESULTS OBTAINED BY RUNNING "EQUILIBRIUM"	126
APPENDIX D: EXAMPLE OF A TEST SPREADSHEET	132
APPENDIX E: DETAILS OF THE MASS AND HEAT BALANCES CALCULATIONS	137

LIST OF FIGURES

<u>Figure</u>	<u>Page</u>
2.1 Map Showing the Location of the Lac Tio Deposit in Relation to Sorel, Québec.	4
2.2 Process Flow Chart of QIT-Fer et Titane Inc	5
2.3 Production of Pigment from Sorelslag by the Sulphate Process	10
2.4 Sulphate Process for the Production of Titanium Dioxide Pigment	11
3.1 Comparison of Heats of Formation for Titanium and Vanadium Compounds	29
3.2 Equilibrium Product Comparison Derived from the Reaction $\text{TiO}_2 + x \text{H}_2\text{SO}_4$ at 100 to 250°C	32
3.3 Products Obtained by the Reaction of Sorelslag with Sulphuric Acid at Different Ratios	34
4.1 Sedigraph Particle Size Distribution of the Three Slag Samples Used	39
4.2 Digestion Reactor	41
4.3 Schematic Representation of Digestion Equipment	45
4.4 Temperature Profile of a Digestion Test	47
4.5 Thermocouple Locations in Digestion Reactor	49
6.1 SE Image of Polished Section of the Milled Sorelslag Powder	69
6.2 EDS Spectrum of the A Phase Containing Strong Ti and Weak Fe, Mg and Al Contributions.	69
6.3 EDS Spectrum of the B Phase, a Silicate Containing Some Al, Ca and Ti Oxides.	70
6.4 EDS Spectrum of the C Phase, Which is Metallic Iron	70
6.5 SE Image of the Sorelslag Digestion Cake Produced by the Sulphate Process.	71

<u>Figure</u>	<u>Page</u>
6.6 Typical EDS Spectra Collected at Different Spots on Particle A of Figure 6.5.	71
6.7 EDS Spectrum Collected on Point B in Figure 6.5 Suggesting the Titanium Sulphate Matrix.	72
6.8 EDS Spectrum Collected on Particle C of Figure 6.5. Phases Present are Considered to be Titanium, Aluminium and Magnesium Sulphate.	72
6.9 SE Image of the Titanium Sulphate Matrix Showing Submicroscopic White (A) and Gray Phases (B).	73
6.10 EDS Spectra of the White Phase (A) and the Gray Phase (B), Respectively, Both Shown in Figure 6.9. The Ti:S Molar Ratio are Nearly 1 and 2 for (A) and (B), Respectively, Suggesting They Consist of TiOSO_4 and $\text{Ti}(\text{SO}_4)_2$.	73
6.11 SE Image of Polished Section of Sorelslag Digestion Cake Showing Numerous Particles Surrounded by the Titanium Sulphate Matrix.	74
6.12 EDS Spectra of the Large Particles Observed in Figure 6.11. They Consist of Two Populations (a) a Ti Rich Phase Which is Most Likely TiO_2 and (b) a Silicate Phase.	74
6.13 Standardized Pareto Chart for Yield	76
6.14 Standardized Pareto Chart for Yield with Significant Effects	77
6.15 Diagnostic Plot of the Predicted Versus Observed Values for Yield	80
6.16 Diagnostic Plot of the Residuals Versus Predicted Values for Yield	80
6.17 Diagnostic Plot of the Residuals Versus Run Order for Yield	82
6.18 Normal Probability Plot of Residuals for Yield	82
6.19 Surface Plot of the Response Function for Yield with a Fixed Particle Size and Concentration Particle Size = 15 μm , $[\text{H}_2\text{SO}_4]$ = 91 %	84

<u>Figure</u>	<u>Page</u>
6.20 Contour Plot of the Response Function for Yield with a Fixed Particle Size and Concentration Particle Size = 15 μm , $[\text{H}_2\text{SO}_4]$ = 91 %	84
6.21 Effect of Baking Time on the Yield of Digestion	86
6.22 Surface Plot of the Response Function for Yield with a Fixed Acid/Slag Ratio and Baking Time Acid/Slag Ratio = 1.7, Baking Time = 4 hours	87
6.23 Contour Plot of the Response Function for Yield with a Fixed Acid/Slag Ratio and Baking Time Acid/Slag Ratio = 1.7, Baking Time = 4 hours	87
6.24 Surface Plot of the Response Function for Yield with a Fixed Particle Size and Baking Time Particle Size = 11 μm , Baking Time = 5 hours	89
6.25 Contour Plot of the Response Function for Yield with a Fixed Particle Size and Baking Time Particle Size = 11 μm , Baking Time = 5 hours	89
6.26 Surface Plot of the Response Function for Yield with a Fixed Particle Size and Acid/Slag Ratio Particle Size = 11 μm , Acid/Slag Ratio = 1.75	90
6.27 Contour Plot of the Response Function for Yield with a Fixed Particle Size and Acid/Slag Ratio Particle Size = 11 μm , Acid/Slag Ratio = 1.75	90
6.28 Response Function for Maximum Temperature	92
6.29 Optimization of Yield and Maximum Temperature with a Fixed Particle Size and Baking Time	93
6.30 Surface Plot of the Response Function for Set-up Time	95
6.31 Contour Plot of the Response Function for Set-up Time	95
6.32 Surface Plot of the Response Function for Active Acid / Titanium Ratio	98
6.33 Contour Plot of the Response Function for Active Acid / Titanium Ratio	98
6.34 Surface Plot of the Response Function for Oxidation with a Fixed Ratio and Concentration Acid/Slag Ratio = 1.75, $[\text{H}_2\text{SO}_4]$ = 91 %	102

<u>Figure</u>	<u>Page</u>
6.35 Contour Plot of the Response Function for Oxidation with a Fixed Ratio and Concentration Acid/Slag Ratio = 1.75, $[H_2SO_4]$ = 91 %	102
6.36 Surface Plot of the Response Function for Oxidation with a Fixed Ratio and Baking Time Acid/Slag Ratio = 1.75, Baking Time = 5 hours	103
6.37 Contour Plot of the Response Function for Oxidation with a Fixed Ratio and Baking Time Acid/Slag Ratio = 1.75, Baking Time = 5 hours	103
6.38 Surface Plot of the Response Function for Oxidation with a Fixed Concentration and Baking $[H_2SO_4]$ = 91 %, Baking Time = 5 hours	104
6.39 Contour Plot of the Response Function for Oxidation with a Fixed Concentration and Baking $[H_2SO_4]$ = 91 %, Baking Time = 5 hours	104
6.40 Response Function for H_2SO_4 Equivalent	107
6.41 Surface Plot of the Response Function for Cake Height	109
6.42 Contour Plot of the Response Function for Cake Height	109

LIST OF TABLES

<u>Table</u>	<u>Page</u>
3.1 Entropies of the Elements in Solid Compounds at 25°C	22
3.2 Summary of Entropy Contribution of Negative Ions in Solid Compounds at 25°C	23
3.3 Atomic Contributions to C_p at 25°C	26
3.4 Anion Contributions to C_p at 25°C	27
3.5 Summary of Estimated Thermodynamic Properties	30
3.6 Heat Generated by the Reaction of 1 kg of Oxide with Sulphuric Acid at 180°C	35
4.1 Chemical Analysis of the Three Slag Samples Used	37
4.2 Size Distribution Analysis of the Three Slag Samples Used	38
5.1 Range of Process Variables Investigated	52
5.2 Four-Variable Box-Behnken Design	55
6.1 Four-Variable Design Response Surface: Data of the Digestion of Sorelslag with Sulphuric Acid	61
6.2 Mass Balance of Titanium Oxide	62
6.3 Stoichiometric Amounts of Reactants and Products Obtained for 95 % Digestion Efficiency	64
6.4 Mass Balance for 95 % Digestion Efficiency	65
6.5 Heat Balance for 95 % Digestion Efficiency	65
6.6 Estimated Effects for Yield	76
6.7 Estimated Significant Effects for Yield	77
6.8 ANOVA for Yield with Significant Effects	78
6.9 Estimated Significant Regression Coefficients for Yield (in real units)	78

<u>Table</u>	<u>Page</u>
6.10 Percentage of the Ti_2O_3 Reacting in Each of the Four Possible Reactions and Total Oxidation Measured in Each Experiment	100
6.11 Analysis of the Digestion Fumes	106
G.1 Heats of Reaction Obtained with F*A*C*T at 175°C	140

CHAPTER 1

INTRODUCTION

Titanium dioxide pigment is produced industrially by two processes: the chloride process and the sulphate process. QIT-Fer et Titane Inc. produces a titanium rich slag which is used as feedstock in the sulphate process. The slag is processed by reacting it with sulphuric acid. This reaction is known as "digestion" and is the first step in the sulphate process for the production of titanium dioxide pigment. During the digestion process, the titanium oxides, as well as other oxides, are transformed into sulphates. The process is exothermic.

Digestion is carried out in large batch reactors with conical bottoms through which air is injected to produce agitation while steam and water are injected to control temperature and acid concentration. However the actual process is much more complex than described above.

In an effort to optimise the digestion process and develop a better understanding of its chemistry a statistically designed experimental program was under taken at the QIT-Fer et Titane Research laboratory. This research program involved:

The thermodynamic analysis of the complex reactions of digestion with F*A*C*T.

The design and construction of a laboratory scale reactor as an exact physical model of the large commercial digestion vessel in order to perform the experiments under truly simulated industrial conditions.

The execution of the statistically designed experiments in which the digestion yield (i.e. the % conversion of titanium oxide to titanium sulphate) was obtained along with several other responses such as maximum reactor temperature, solidification time, degree of oxidation of Ti(III) compounds, sulphuric acid loss in the gas and digestion cake height. The variables studied were particle size of the slag (11 to 23 microns), acid/slag weight ratio (1.5 to 1.9), acid concentration (88 to 94 wt %) and baking time (2 to 6 hours). In complement to this experimental data a detailed microscopic examination of the solids was carried out before and after digestion.

The thesis is constructed as follow: Chapter II gives a literature review of the subject; Chapter III gives the results of the thermodynamic calculations; Chapter IV describes in detail the reactor built and the procedure followed; Chapter V refers to the statistical design methodology; Chapter VI gives the results and discusses the findings; Conclusions and recommendations for future work are summarized in Chapter VII; References; And finally, in Appendices additional information is reported.

CHAPTER 2

LITERATURE SURVEY

In this chapter, all technical information relevant to the subject matter of this thesis is reviewed. More particularly, the origin of the titaniferous slag which constitutes the feed material of the digestion process is described and previous studies on characterizing this slag material are reviewed. This section will be followed by a description of the sulphate digestion process and finally a brief reference to statistical design is made.

2.1 Production of the Titanium Slag "Sorelslag"

The slag is produced from the reduction of ilmenite ore with coal in electric arc furnaces (1). The ore is primarily a coarse-grained ilmenite, ($\text{FeO} \cdot \text{TiO}_2$) with fine lenses of hematite (Fe_2O_3) disseminated within the ilmenite grain structure (2,3). The gangue which accompanies the ilmenite ore is mainly anorthosite, a complex silicate. Conventional open pit mining methods are employed in a horseshoe-shaped mine, located in the Allard lake region, 43.5 km inland from Havre St-Pierre, Quebec.

A primary jaw crusher breaks the ore down to 18 cm size, and a secondary cone crusher breaks it down further to minus 7.5 cm. The minus 7.5 cm material is then transported to Sorel by

train and ship. A simplified map of the location of the mine and Sorel is shown in Figure 2.1.

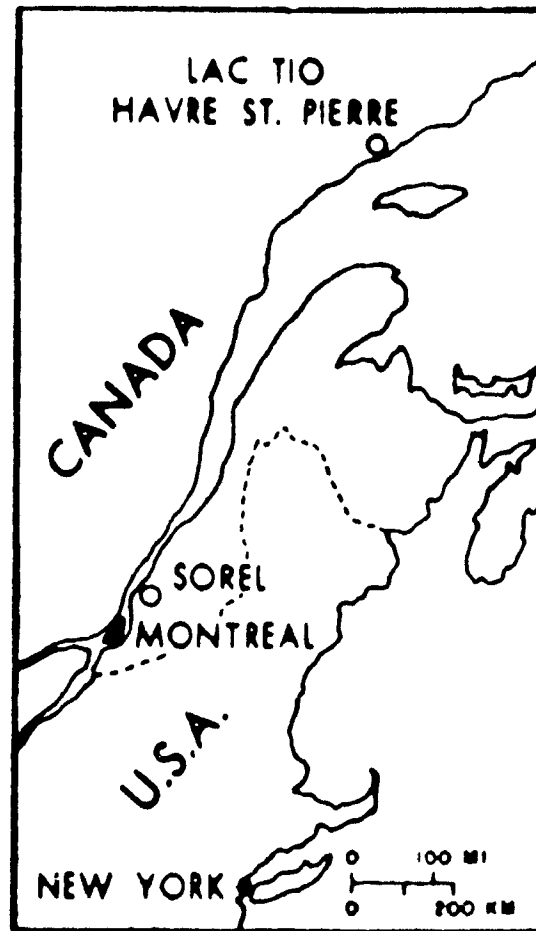
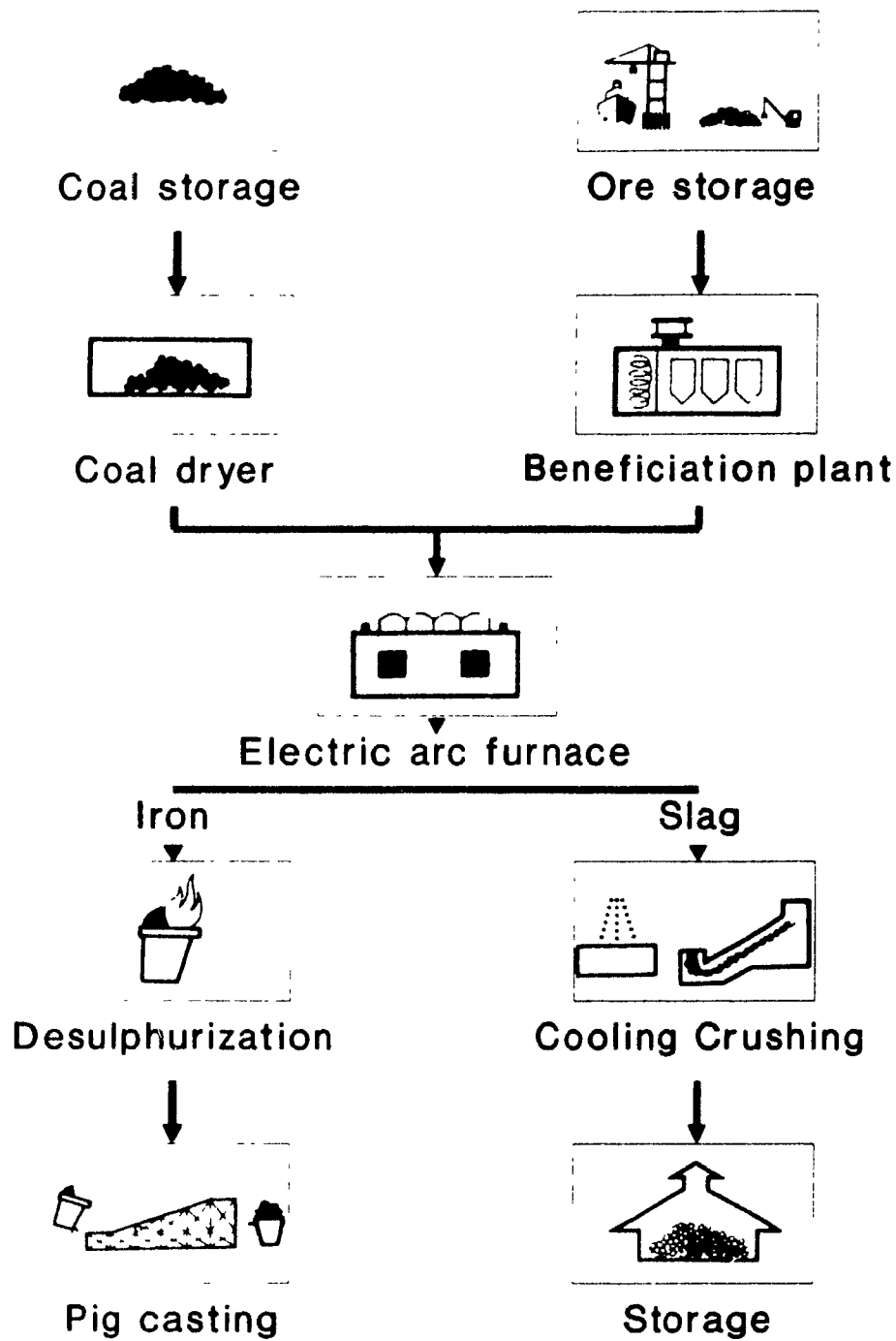


Figure 2.1 : Map Showing the Location of the Lac Tio Deposit in Relation to Sorel, Québec.

On the plant site in Sorel, the ilmenite ore and coal, the two principal bulk raw materials are unloaded at the dock, conveyed to their respective stockpiles, and stored in sufficient quantity to maintain operations during the winter months when shipping is no longer practical. The process flow chart of the QIT Sorelslag production plant is presented in Figure 2.2 (4).

Figure 2.2 : Process Flow Chart of QIT-Fer et Titane Inc.

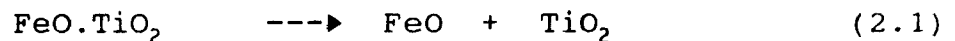


The minus 7.5 cm ore from the mine is crushed to minus 1 cm in cone crushers. The incoming ore grade, where grade is defined as the combined content of iron and titanium oxides, varies between 82 and 87 percent. The purpose of the beneficiation plant is to raise the ore grade to about 95.5 percent by discarding the worthless fraction or gangue. However, an additional advantage ensues from beneficiation, since the ore is not only more concentrated, but also far more consistent in composition, which helps to ensure a smooth smelting operation (5,6,7).

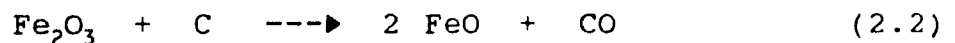
The smelting of the ore and coal mixture takes place in a line of electric furnaces with power ratings up to 60 megawatts. Operating temperatures exceed 1600°C thus enabling the required chemical reactions to occur (8,9,10,11).

The principal reactions are (12):

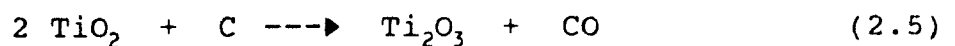
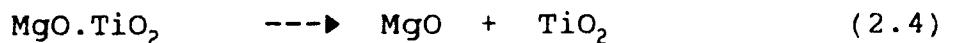
i) Decomposition of the complex oxide phase



ii) Two stage reduction of iron oxides



The minor reactions that occur simultaneously are:



To a lesser degree some reduction of SiO_2 , MnO , Cr_2O_3 and V_2O_5 also takes place.

The ratio of coal to ore is controlled so that most of the iron oxides are reduced to an exceptionally high purity metallic iron which sinks through the molten slag (13). Large volumes of CO gas which are generated from the chemical reactions are withdrawn through the furnace roof, and used within the plant as fuel.

Slag is tapped from the furnaces, cooled, crushed to minus 1.6 cm and stored for bulk shipment to the pigment producer (14).

2.2 Characterization of "Sorelslag"

The phases identified, in order of abundance, in Sorelslag are ferrous pseudobrookite solid solution (AB_2O_5), silicate (both crystalline and glass), rutile (TiO_2), anatase (TiO_2), metallic iron, iron sulphide (FeS), ilmenite ($FeTiO_3$), and ulvospinel ($TiFe_2O_4$) (15). The ferrous pseudobrookite solid solution is the principal phase. The silicate phase make up 3 to 4 percent of the sample and metallic iron and iron sulphide together contribute about one percent of its mass.

The main constituents of QIT's slag can be represented as one of the two following basic chemical formulae (16): $RO.2TiO_2$, where R may be Mg^{2+} , Fe^{2+} and Mn^{2+} , or $R_2O_3.TiO_2$, where R may be Fe^{3+} , Al^{3+} and Ti^{3+} . However, the pseudobrookite structure (AB_2O_5) is actually $(Mn_{0.05}Fe_{0.43}Ti_{0.52})(Ti_{2.0})O_5$ and $(Mg_{0.21}Fe_{0.33}Ti_{0.46})(Ti_{1.9}Mg_{0.1})O_5$ (17,18).

The siliceous portion of the slag is composed of solid solutions of anorthite ($CaO.Al_2O_3.2SiO_2$) and albites ($Na_2O.Al_2O_3.6SiO_2$), a small amount of orthoclase ($K_2O.Al_2O_3.6SiO_2$), and a considerable amount of mixed metasilicates of iron ($FeO.SiO_2$), calcium ($CaO.SiO_2$) and magnesium ($MgO.SiO_2$). A large amount of this portion is in the amorphous or glassy state (19,20).

2.3 The Sulphate Process for Pigment Manufacture

There are two principal routes by which TiO_2 pigment can be produced: the H_2SO_4 digestion process (sulphate process) applied to titanium slag and ilmenite ore and the chlorination process applied to natural or artificial rutile, high grade ilmenites and low alkali-earth slags (21).

The production of pigment from Sorelslag by the sulphate process involves the following steps (Figure 2.3 and 2.4) (22). First the titanium slag is ground in ball mills into fine powder. Then, in order to extract titanium in the form of titanyl sulphate, the powder is reacted with sulphuric acid in digesters, huge tanks lined with lead and acid bricks, to obtain a soluble salt. The dissolution of the product in water yields a solution of titanyl sulphate containing some iron sulphate and other soluble impurities in addition to an unreacted suspension of slag. Settling tanks and filtration remove the unreacted solids from the solution. After adjustment of the absolute and relative concentration of the components, which may involve crystallization and vacuum concentration, the proper seeding is added and the precipitation started (23,24,25,26,27). The precipitation step is an important part of the process as several key properties of the pigment are determined in this stage. Precipitation takes place under carefully monitored conditions where the solution of titanyl sulphate is forced by boiling in

Figure 2.3 : Production of Pigment from Sorelslag
by the Sulphate Process

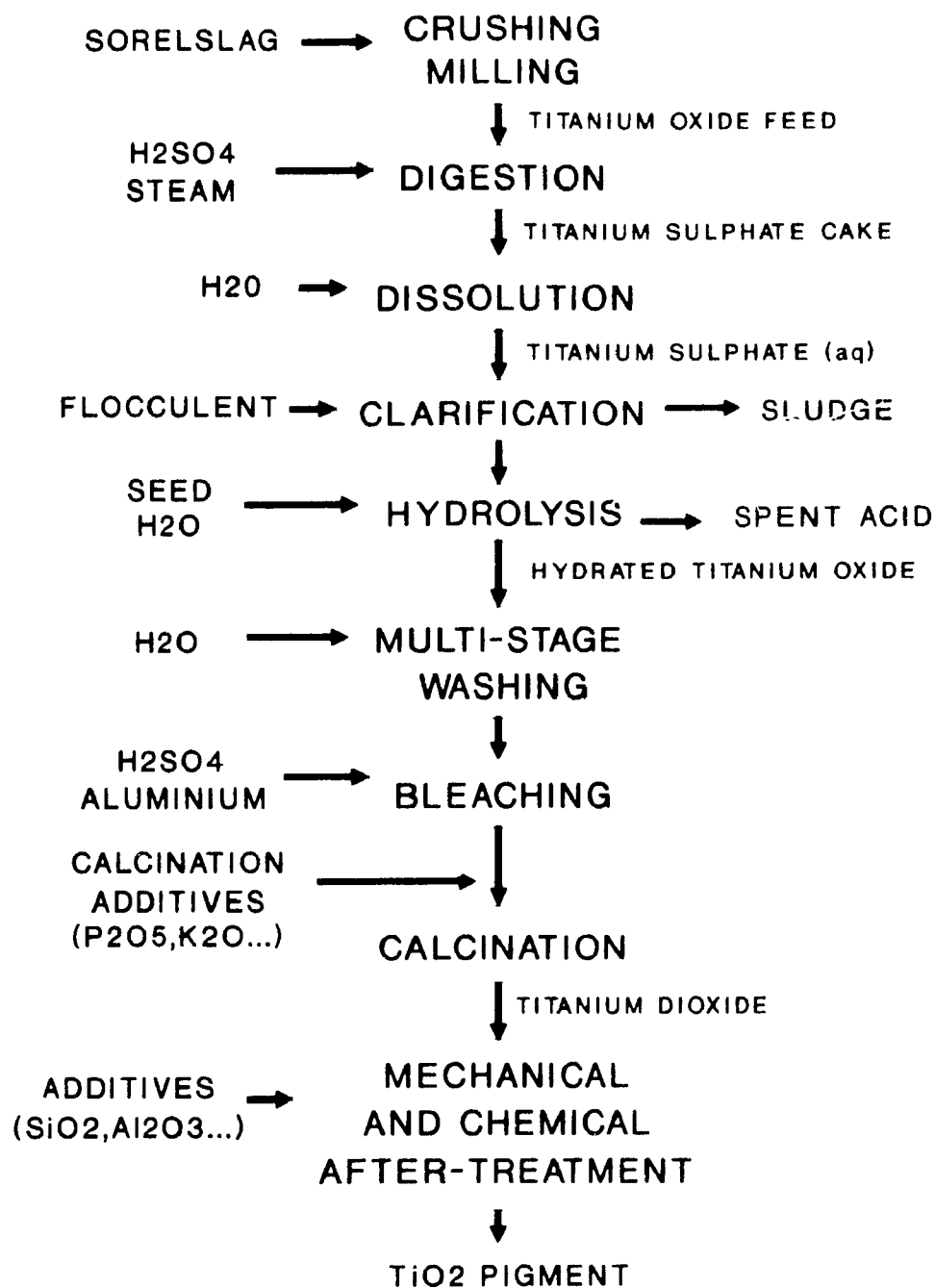
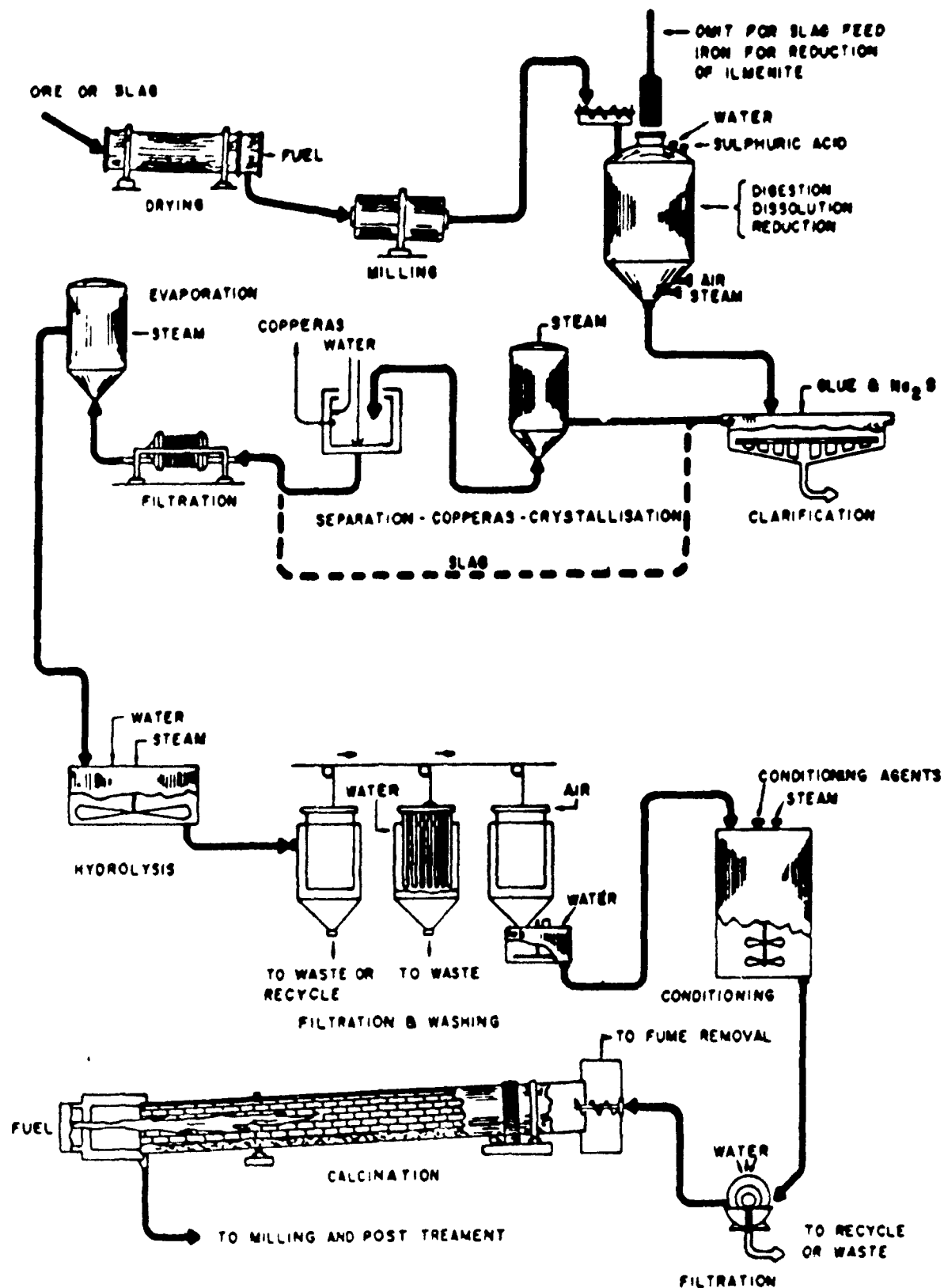


Figure 2.4 : Sulphate Process for the Production of Titanium Dioxide Pigment.



tanks to hydrolyse and produce hydrated titanium oxide as a very fine precipitate (28,29,30). The precipitated pulp of titanium oxide is washed thoroughly several times, passing through a sequence of filters to reduce all impurities to a low level. The pulp is treated with conditioning agents to prevent sintering during calcination. Potassium is the conditioning agent for anatase (23).

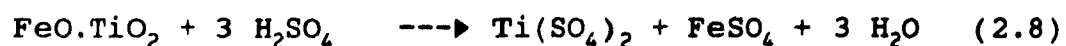
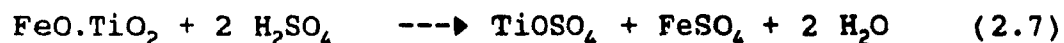
The process continues with calcination, to convert the amorphous hydrous oxide to a crystalline form with the desired pigment properties. The washed titanium oxide pulp is subjected to heat treatment in large rotary kilns fired by natural gas. The crystal structure, anatase or rutile (31), and the crystal size distribution are determined. The crystalline TiO_2 is ground by intensive dry and wet milling, followed by classification to eliminate the oversize particles.

The pigment, now in aqueous suspension, is coated with various additives to produce precise grades. Each grade has the pigmentary properties required for its particular application (32).

Flowsheets of the process are given by Forbath (25) as well as Coates (26), and have been included in a U.S. Bureau of Mines publication (23).

2.4 The Digestion Process

In the digestion step, the titanium oxides in the feedstock react with sulphuric acid to produce titanium sulphates and water. The following reactions have been suggested to describe the digestion process (33):



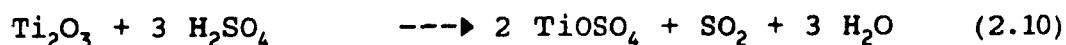
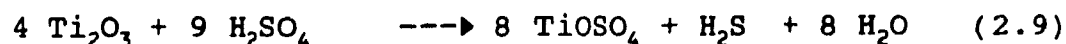
To control the rate of the digestion reaction the slag is grounded so that all of the material passes through a 200 mesh screen (74 micron), but not more than 30 per cent of the particles have an average diameter smaller than 8 microns, and at least 90 per cent of the particles are smaller than 44 microns in average diameter (32). Sulphuric acid of a concentration of 92 to 98 per cent by weight is added (34). The slag-acid mixture is heated with steam to 120 to 160°C before reaction takes place. Heat is liberated and drives the reaction to completion. The solid digestion cake is blown with air to hasten cooling and to produce a porous mass (24). This cake is then retained at elevated temperatures in the digestion tank for several hours in order to cure the cake (35).

A previous study (36) of the digestion of high titania slags (TiO_2 content greater than 70% by weight) has determined that

optimum digestion is obtained when two parts (weight ratio) of 92 wt. % sulphuric acid to one part of slag having a particle size range of 40 to 60 microns are employed. The same study has indicated that the initial temperature should be at least 115°C and the maximum reaction temperature at least 180°C. Digestion time ranges from 2 to 3 hours.

It is important, during the reaction of slag with sulphuric acid, to produce a porous, water-permeable, solid product which can be dissolved readily in the reaction tank. Several procedures have been described (32), but in general the desired texture of the solid product is obtained by blowing air through the reacting mass as it solidifies.

During the digestion of the titanium-bearing slag with sulphuric acid, the titanium (III) present in the slag undergoes an oxidation-reduction reaction with the liberation of hydrogen sulphide and sulphur dioxide (37).



Furthermore, trivalent titanium is believed to be oxidized to the tetravalent state by the air which is blown through the porous solid mass (38,39).



The conversion of Ti(III) into Ti(IV) during the digestion process is promoted by the addition of very small quantities of lignosulfonate, an inexpensive by-product of the pulp and paper industry, into the acid-slag mixture (40). The role of the lignosulfonate is to promote the oxidizing properties of sulphuric acid.

The reaction product, soluble sulphates, obtained by digesting finely divided ilmenite or slag with sulphuric acid is leached with water or dilute sulphuric acid to obtain a solution of sulphates. The leaching liquor is introduced at the bottom of the porous mass. The temperature should be held relatively low (below 75°C) to avoid hydrolysis, but at the same time it should be maintained as high as practical (but not above 85°C) to speed the rate of dissolution. Farup (41) employed dilute solutions of sulphuric acid as the solvent instead of water. This method was also followed by Washburn (42) and others. In general, it has been found beneficial to use dilute sulphuric acid followed by water addition.

After leaching, which takes 4 to 16 hours, the aqueous slurry is clarified. The solution is highly acidic and contains finely disseminated, siliceous material, insoluble TiO_2 and undissolved slag, that are in part in a colloidal suspension. The colloidal material is first coagulated by introducing a coagulant of opposite electrical charge (32), such as synthetic cationic polyelectrolytes or a polymer like glue,

after which the liquor is passed through a series of settling tanks and finally filtered to yield a clear solution of a density of 1.4 to 1.5 (24).

After clarification is complete, the sulphate solution is prepared for hydrolysis. The black liquor should contain 200 to 250 g/l of titanium sulphate (39). All of the iron present as a contaminant in the titanium sulphate solution must be in the ferrous state. This is necessary to avoid any precipitation of iron oxide and other miscellaneous oxides such as vanadium oxide with the titanium dioxide during the hydrolysis stage. If some ferric ions are present, scrap iron is added to reduce ferric to ferrous, while containing about 3 to 6 g/l of trivalent titanium expressed as TiO_2 . If $Ti(III)$ exceeds 6 g/l, the excess $Ti(III)$ has to be oxidized to avoid losses of titanium as $Ti(III)$, which does not hydrolyse (40).

The digestion of Sorelslag is similar to the digestion of ilmenite. However two costly processing steps (crystallization and vacuum concentration) can be eliminated when slag is used (25,43). According to Irkov and Reznichenko (44) slag from smelting of titanomagnetites dissolves more readily in sulphuric acid yielding higher overall recoveries of titanium dioxide.

2.5 Statistical Design

Frequently the mechanism underlying a process is not understood sufficiently well, or it is too complicated, to allow an exact model to be postulated from theory. In such circumstances an empirical model may be utilized. Empirical models can be built by applying statistical design methodology (45) in the execution of the experiments. By changing the significant process variables in a systematic way, one response (for example yield) is studied. Response surface methodology (46) is one of the experimental design methodologies which is particularly useful in the study of complex process systems such as the one studied here.

Kondos gives references to many successful uses of statistical design in hydrochemical processing (47).

CHAPTER 3

THERMODYNAMICS

The thermodynamics of the reactions involved in the transformation of the titanium and other oxides into sulphates is analyzed here. The reactions of the basic constituent components of the "Sorelslag" with sulphuric acid can be represented by the following equations:



To proceed with this thermodynamic analysis , it was decided to use F*A*C*T. F*A*C*T stands for Facility for the Analysis of Chemical Thermodynamics. Primarily two sub-programs of F*A*C*T, Reaction and Equilibrium were used.

This analysis focused on establishing what reactions are the

most probable, which reactions are exothermic and what is the effect of varying the sulphuric acid to Sorels slag ratio on the equilibrium product mixture.

Although F*A*C*T contains a large data bank, properties for the titanium sulphates were missing and had to be estimated. The estimation of these properties is presented in the following section.

3.1 The Program F*A*C*T.

F*A*C*T is a computer system which performs commonly encountered thermochemical calculations. The program incorporates extensive prompting which is readily understood by those with a background in the principles of chemical thermodynamics. Moreover, all inputs are extensively checked both for logical and numerical validity. The system has its own database which includes the thermodynamic properties for more than 3800 compounds and a number of binary solutions. The scope of the system is useful in many branches of fundamental or applied chemistry (48).

In this study, three of the several features of F*A*C*T were used: "Inspect", "Reaction" and "Equilibrium".

"Inspect": This program locates and displays thermodynamic

data for compounds stored in the main F*A*C*T file or in the user's data files if such files have been set up. If data exist for a selected compound, tables are generated with references. An example of a table produced by this program is included in Appendix A.

"Reaction": This program calculates changes in extensive thermochemical functions (H,G,V,S,U,A) for a specified change in state of a system. The user indicates the chemical make-up of the initial and final states by entering a balanced chemical equation. Temperatures, pressures, phases and activities of each reactant and product are specified on a second line. This line forms, in effect, subscripts for the reactants and products included in the chemical equation specified in the previous line. Data is then automatically retrieved from the main F*A*C*T file or from the user's file or a combination of both and a tabular print-out is generated. An example of one of these print-outs is shown in Appendix B.

"Equilibrium": This program determines the concentrations of chemical species when specified elements or compounds (in typically known proportions) react or partially react to reach a state of chemical equilibrium. The user supplies the reactants of a chemical equation. The products are not specified, typically only the temperature and total pressure of the products are entered. A list of all possible compounds found in the database as well as in the user's data file is

then automatically produced. The user then specifies what species should be considered in the equilibrium calculation (often all of them). The program then produces the solution by finding the most stable product of the reaction in equilibrium at the user's specified temperature and pressure. Appendix C includes an example of the results obtained by running the "Equilibrium" program.

3.2 Estimation of the Entropy of Solid Compounds

Latimer (49) described a method for estimating the entropy of solid compounds. Where by the entropy of a solid compound is a function of the mass of the constituent atoms and the force acting between these atoms. That is, the greater the mass and the lower the force, the larger the entropy.

To estimate the entropy of a compound, the contribution of the metallic elements given in Table 3.1 is added to the contribution of the negative ions given in Table 3.2, which depends on the charge of the metallic element (positive ion).

Table 3.1 : Entropies of the Elements in Solid
Compounds at 25°C (49)
(values in cal/°C)

Ag	12.8	Dy	14.4	Mn	10.3	Se	(11.6)
Al	8.0	Br	14.5	Mo	12.3	Si	8.1
As	11.45	Eu	14.1	N	5.8	Sm	14.1
Au	15.3	F	(6.9)	Na	7.5	Sn	13.1
B	4.9	Fe	10.4	Nd	13.9	Sr	12.0
Ba	13.7	Ga	11.2	Ni	10.5	Ta	14.9
Be	4.3	Gd	14.3	Os	15.1	Tb	14.3
Bi	15.6	Ge	11.4	Pb	15.5	Te	(13.4)
Br	(11.7)	Hf	14.8	Pd	12.7	Th	15.9
C	5.2	Hg	15.4	Pr	13.8	Ti	9.8
Ca	9.3	Ho	14.5	Pt	15.2	Tl	15.4
Cb	12.2	I	(13.4)	Ra	15.8	Tm	14.6
Cd	12.9	In	13.0	Rb	11.9	U	16.0
Ce	13.8	Ir	15.2	Re	15.0	V	10.1
Cl	(8.8)	K	9.2	Rh	12.5	W	15.0
Co	10.6	La	13.8	Ru	12.5	Y	12.0
Cr	10.2	Li	3.5	S	(8.5)	Yb	14.7
Cs	13.6	Lu	14.8	Sb	13.2	Zn	10.9
Cu	10.8	Mg	7.6	Sc	9.7	Zr	12.1

Table 3.2 : Summary of Entropy Contribution of Negative Ions in Solid Compounds at 25°C (49)
(values in cal/mol .°C)

Negative Ion	Charge on Positive Ion			
	+1	+2	+3	+4
F ⁻	(5.5)	4.7	(4.0)	5.0
Cl ⁻	10.0	8.1	6.9	8.1
Br ⁻	13.0	10.9	(9.)	(10.)
I ⁻	14.6	13.6	12.5	13.0
CN ⁻	7.2	(6.)		
OH ⁻	(5.0)	4.5	3.0	
ClO ⁻	(14.)	(10.)	(8.)	
ClO ₂ ⁻	19.2	(17.)	(14.)	
ClO ₃ ⁻	24.9	(20.)		
ClO ₄ ⁻	26.0	(22.)		
BrO ₃ ⁻	26.5	22.9	(19.)	
IO ₃ ⁻	25.5	(22.)		
H ₄ IO ₆ ⁻	33.9	(30.)		
NO ₂ ⁻	17.8	(15.)		
NO ₃ ⁻	21.7	17.7	(15.)	(14.)
VO ₃ ⁻	20.0	(18.)		
MnO ₄ ⁻	31.8	(28.)		
O ²⁻	2.4	0.5	0.5	1.0
S ²⁻	8.2	5.0	1.3	2.5
Se ²⁻	(16.)	11.4	(8.)	
Te ²⁻	(16.5)	12.1	(9.)	
CO ₃ ²⁻	15.2	11.4	(8.)	
SO ₃ ²⁻	(19.)	14.9	(11.)	
C ₂ O ₄ ²⁻	(22.)	17.7	(14.)	
SO ₄ ²⁻	22.	17.2	13.7	(12.)
CrO ₄ ²⁻	26.2	(21.)		
SiO ₄ ²⁻	(19.)	13.8	(9.)	7.9
SiO ₃ ²⁻	16.8	10.5	(7.)	
PO ₄ ²⁻	(24.)	17.0	(12.)	
HCO ₃ ⁻	17.4	(13.)	(10.)	
H ₂ PO ₄ ⁻	22.8	(18.)		
H ₃ AsO ₄ ⁻	25.1	(21.)		

Using this method, the entropies of TiOSO_4 , $\text{Ti}(\text{SO}_4)_2$ and $\text{Ti}_2(\text{SO}_4)_3$ were calculated.

$$\begin{aligned} \text{TiOSO}_4 & : 9.8 \text{ cal/}^\circ\text{C} + 1 \text{ cal/}^\circ\text{C} + 12 \text{ cal/}^\circ\text{C} & (3.12) \\ & = 22.8 \text{ cal/}^\circ\text{C} \text{ or } 95.5 \text{ J/}^\circ\text{C} \end{aligned}$$

$$\begin{aligned} \text{Ti}(\text{SO}_4)_2 & : 9.8 \text{ cal/}^\circ\text{C} + 2(12 \text{ cal/}^\circ\text{C}) & (3.13) \\ & = 33.8 \text{ cal/}^\circ\text{C} \text{ or } 141.5 \text{ J/}^\circ\text{C} \end{aligned}$$

$$\begin{aligned} \text{Ti}_2(\text{SO}_4)_3 & : 2(9.8 \text{ cal/}^\circ\text{C}) + 3(13.7 \text{ cal/}^\circ\text{C}) & (3.14) \\ & = 60.7 \text{ cal/}^\circ\text{C} \text{ or } 254.1 \text{ J/}^\circ\text{C} \end{aligned}$$

3.3 Estimation of Heat Capacities

The Kopp-Neumann (50) rule provides a means of estimating C_p for solid substances at room temperature. According to this rule, the heat capacity C_p for compounds at room temperature is approximately equal to the sum of the heat capacities of the constituent elements. The value of C_p at 25°C is obtained by adding $25.9 \text{ J/}^\circ\text{C}$ for each atom of the compound.

With this rule, we calculated:

$$\text{TiOSO}_4 : 181.3 \text{ J/gmol}^\circ\text{C} \quad (3.15)$$

$$\text{Ti}(\text{SO}_4)_2 : 284.9 \text{ J/gmol}^\circ\text{C} \quad (3.16)$$

$$\text{Ti}_2(\text{SO}_4)_3 : 440.3 \text{ J/gmol}^\circ\text{C} \quad (3.17)$$

Kellogg (51) developed an improved method for estimating the

heat capacities of solid compounds at 25°C which consists of adding up the contributions from the cationic and anionic groups in the compound. The individual contributions of cations and anions are listed in Tables 3.3 and 3.4.

Estimation of the heat capacities of titanium sulphates with this method gives:

$$\text{TiOSO}_4 : 23.8 + 15.9 + 72.8 = 112.5 \text{ J/gmol}^\circ\text{C} \quad (3.18)$$

$$\text{Ti}(\text{SO}_4)_2 : 23.8 + 2(72.8) = 169.4 \text{ J/gmol}^\circ\text{C} \quad (3.19)$$

$$\text{Ti}_2(\text{SO}_4)_3 : 2(23.8) + 3(74.9) = 272.3 \text{ J/gmol}^\circ\text{C} \quad (3.20)$$

For this work, the heat capacities calculated with the Kellogg improved method were used.

3.4 Estimation of the Heat of Formation

One approach for the estimation of heat of formation of simple inorganic compounds is to assign a characteristic parameter (or parameters) to each element making up the compound. Wilcox (52) used this approach and developed a method for estimating the heat of formation of inorganic compounds. Using a computer program he found:

$$\text{Ti}(\text{SO}_4)_2 : 2181 \pm 126 \text{ kJ/mole} \quad (3.21)$$

$$\text{Ti}_2(\text{SO}_4)_3 : 3387 \pm 63 \text{ kJ/mole} \quad (3.22)$$

Table 3.3 : Atomic Contributions to C_p at 25°C (51)

Ag 25.5	H 6.3	Pt 26.4
Al 14.6 (23.4)	Hf 26.4	Rb 26.4
As 21.3	Hg 26.4	Rb 25.9
Au 26.4	I [28.5]	S [20.9]
B 5.4 (10.9)	In 23.4	Sb 25.5
Ba 27.2	Ir 26.4	Sc 20.1
Be 7.5 (11.7)	K 25.9	Se [27.2]
Bi 27.2	La 27.2	Si 12.6 (20.1)
Br [27.6]	Lanthanides 26.4	Sn 25.5
C [8.4][10.5]	Li 20.5	Sr 25.5
Ca 23.4[25.1]	Mg 18.4 (23.8)	Ta 26.4
Cd 25.1	Mn 25.1	Te ?
Cl [25.1]	Mo 25.5	Th 28.0
Co 25.1	N 18.8 (18.8)	Ti 23.8
Cr 25.1	Na 25.1	Tl 25.5
Cs 26.8	Nb 25.9	U 28.9
Cu 25.1	Ni 25.1	V 25.1
F[22.2]	O[16.7]	W 27.2
Fe 25.5	P 15.1	Y 23.4
Ga 20.1	Pb 27.2	Zn 22.6 (25.1)
Ge 21.8	Pd 25.5	Zr 25.5

Note: Units are J/g.atom.°C

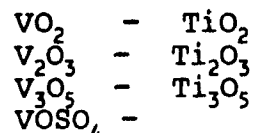
Table 3.4 : Anion Contributions to C_p at 25°C (51)

Species	Cation charge					
	+1	+2	+3	+4	+5	+6
F^-	23.0	22.2	21.3	20.9	21.3	(22.6)
Cl^-	25.5	25.1	24.3	23.8		(23.8)
Br^-	27.6	27.6	27.6	27.6	26.4	
I^-	28.5	28.5	(29.3)	(28.5)		
O^{2-}	17.6	19.3	17.2	15.9	15.1	17.2
S^{2-}	29.3	23.8	23.0	20.9		
Se^{2-}	(31.4)	(27.2)				
Te^{2-}		(46.0)	(36.8)	(25.1)		
N^{3-}	(15.9)	22.2	16.7	16.7	(19.7)	
OH^-	(32.2)	(29.7)				
SH^-	(52.7)					
SeH^-	(46.9)					
CO_3^{2-}	60.7	57.7				
NO_3^-	69.0	62.8	(58.6)			
SO_3^{2-}	(69.9)	(68.2)				
ClO_3^-	75.7	(71.1)				
BrO_3^-	(79.1)	75.3				
IO_3^-	(79.5)					
SO_4^{2-}	79.1	76.2	74.9	(72.8)		
ClO_4^-	80.3					
CrO_4^{2-}	92.9					
$Cr_2O_4^{2-}$		107.5				
BH_4^-	64.9					
CN^-	(37.7)	(37.7)	(33.5)			

Note : The values in parentheses are based on scant evidence.

The units are J/g.atom.°C

For TiOSO_4 , however, the method was not reliable and a comparative method was used instead which consisted of comparing the compound with another of a similar atomic weight (53). As an illustration of the method Figure 3.1 was constructed which compares the heats of formation for titanium and vanadium compounds. Vanadium was chosen because of its similarity with titanium. There was data available in F*A*C*T for:



But not for TiOSO_4 . By interpolation we estimated the following heat of formation for:

$$\text{TiOSO}_4 : 1637 \text{ kJ/mole} \quad (3.23)$$

This compares well with the estimation made by Bobyrenko (54) who used zirconium compounds as a comparison base. He found respectively:

$$\text{TiOSO}_4 : 1870 \text{ kJ/mole} \quad \text{and} \quad (3.24)$$

$$\text{Ti}(\text{SO}_4)_2 : 2310 \text{ kJ/mole} \quad (3.25)$$

Figure 3.1 : Comparison of Heats of Formation for Titanium and Vanadium Compounds

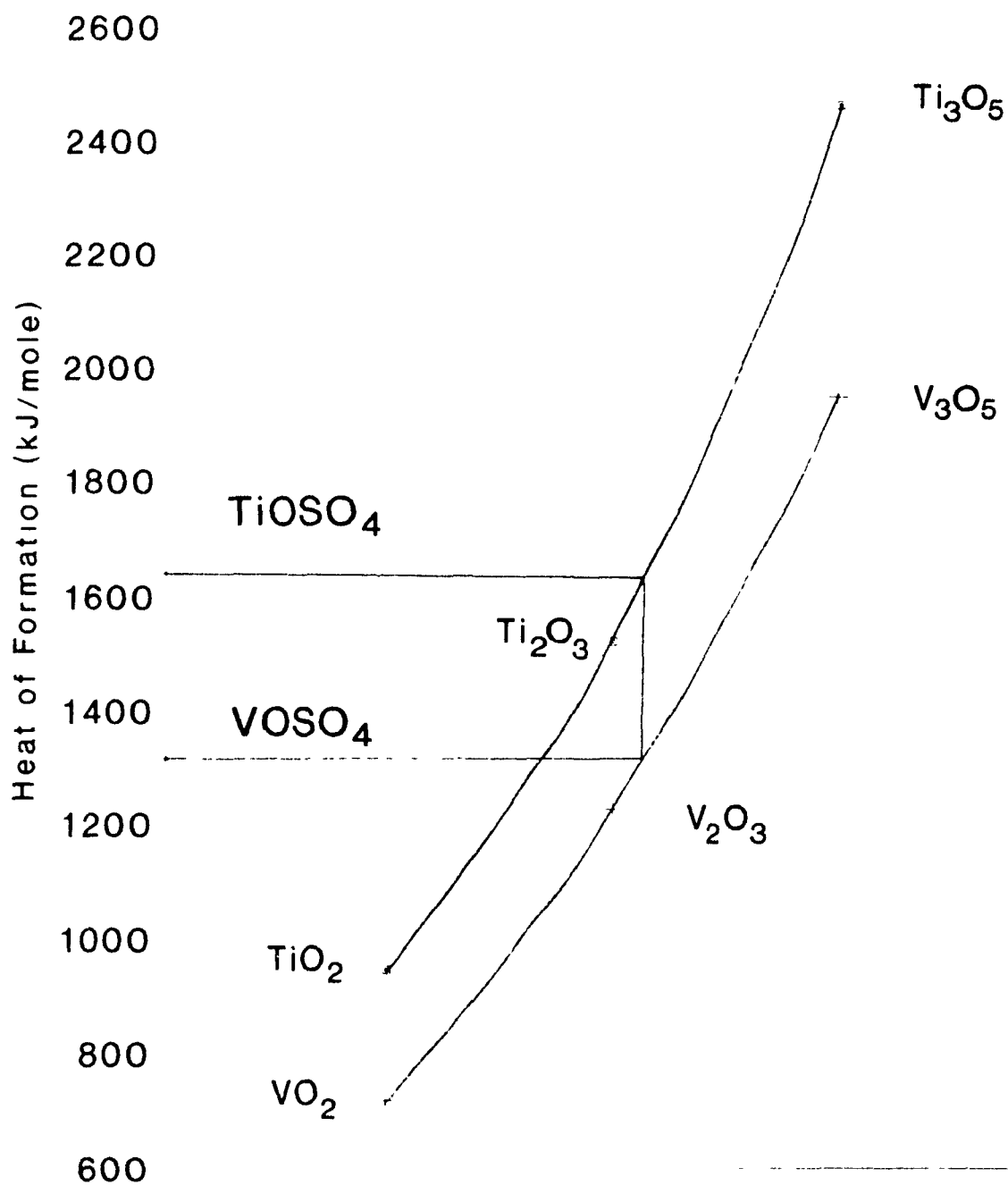


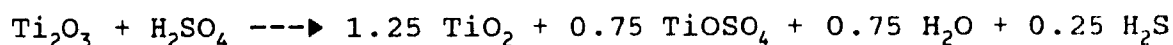
Table 3.5 : Summary of Estimated Thermodynamic Properties

Compounds	Entropy J/°C	Heat capacities J/gmol°C	Heat of formation kJ/mole
TiOSO ₄	95.5	112.5	1637
Ti(SO ₄) ₂	141.5	169.4	2181
Ti ₂ (SO ₄) ₃	254.1	272.3	3387

3.5 Thermodynamic Modelling Results

The estimated thermodynamic properties (summarized in Table 3.5) of the titanium sulphates were added into our database. "Equilibrium" was used to define which of the three Ti₂O₃ reactions with sulphuric acid was favourable (Reaction 3.3, 3.4 or 3.5). In the full temperature range of the digestion process, 25 to 250°C, F*A*C*T Equilibrium determined the following product mixture when Ti₂O₃ and H₂SO₄ react at 1:1 ratio:

(3.26)



This reaction is a combination of the following two:



In this particular case, more sulphuric acid is necessary to convert all the titanium oxide into titanium sulphates. If the same reactants are used, but with the addition of water to simulate a 92 % sulphuric acid, the same products are obtained. However, when oxygen is included in the reaction, reaction (3.6) is favoured.

To determine the effect of the sulphuric acid to TiO_2 ratio on equilibrium product composition the two reactants were mixed in varying ratios (i.e. x was varied).

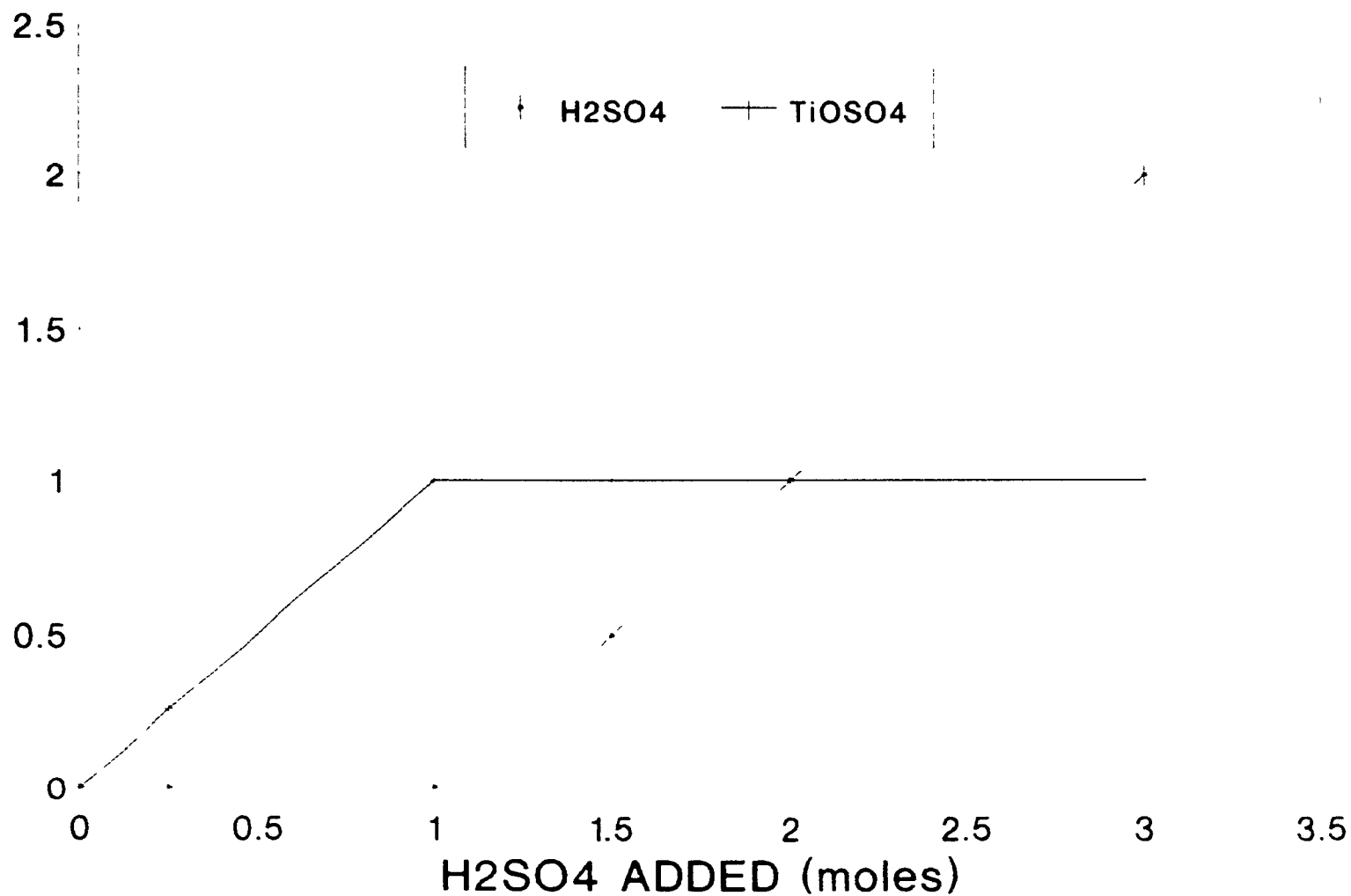


Using "Equilibrium" the data reported in Figure 3.2 was generated. According to these results all TiO_2 is found to be transformed into TiOSO_4 with no signs of $\text{Ti}(\text{SO}_4)_2$ formation even if more acid is used. All excess acid is found in the product as free acid.

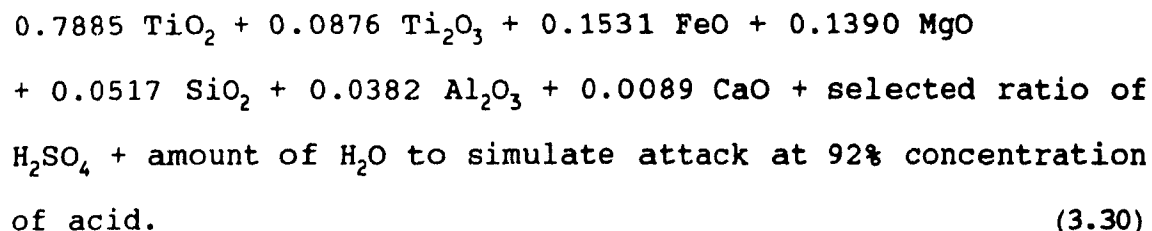
The reactions of more complex compounds closer to those present in slag (55), such as Ti_3O_5 , $\text{MgO} \cdot 2\text{TiO}_2$, $\text{FeO} \cdot \text{TiO}_2$, $\text{Al}_2\text{O}_3 \cdot \text{TiO}_2$ and $\text{CaO} \cdot \text{Al}_2\text{O}_3 \cdot \text{TiO}_2$ were analyzed to establish whether or not a difference existed in their reaction with sulphuric acid. F*A*C*T showed that the same products were the most stable.

Figure 3.2 : Equilibrium Product Comparison Derived from
the Reaction $\text{TiO}_2 + x \text{H}_2\text{SO}_4$ at 100 to 250°C
(F*A*C*T EQUILI results)

EQUILIBRIUM PRODUCT
COMPOSITION (moles)



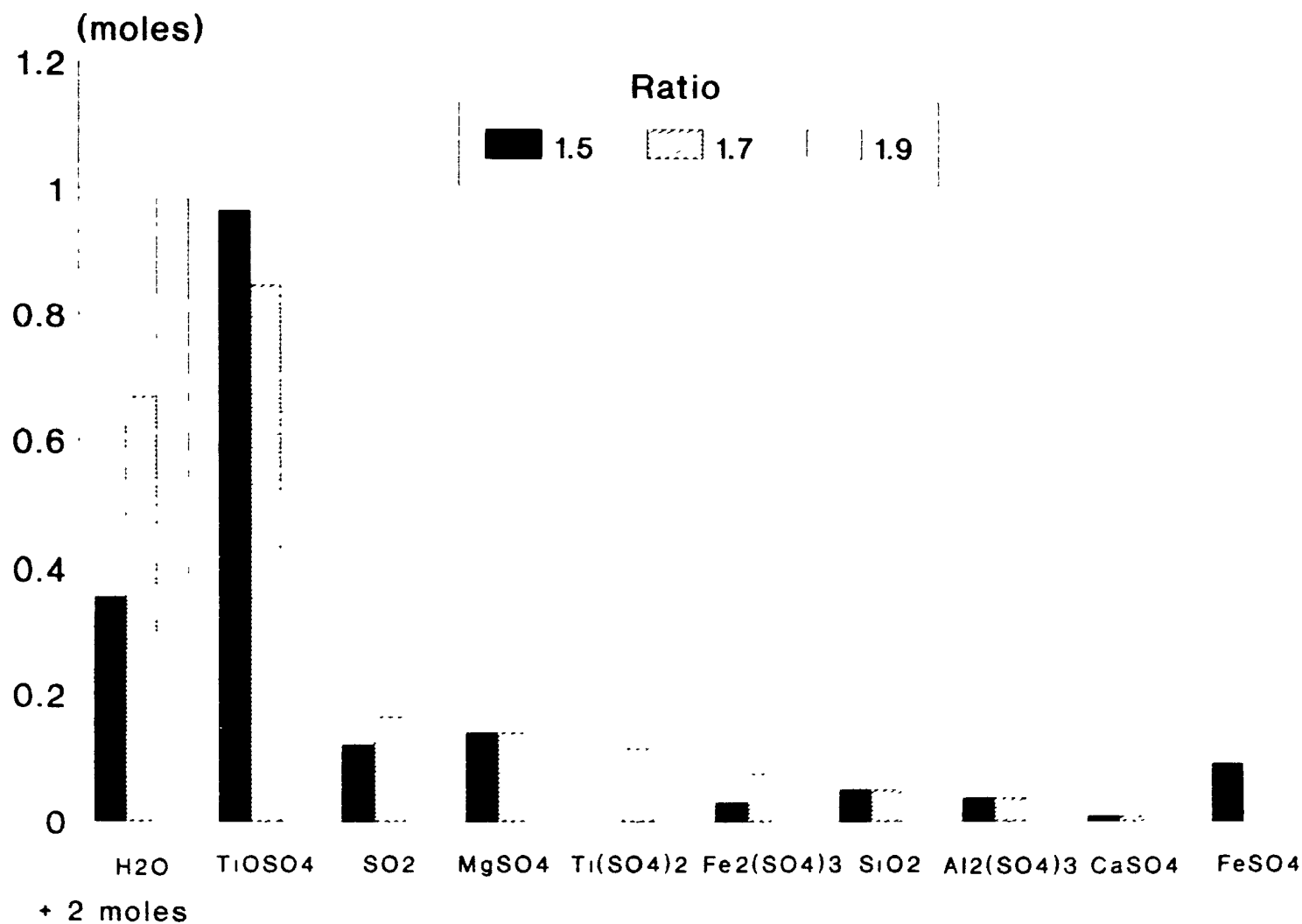
The sulphuric acid to Sorelslag ratio is an important variable in digestion. To predict its effect "Equilibrium" was run with three different acid/slag ratios: 1.5, 1.7 and 1.9 % wt. The corresponding molar ratios of each of the oxide phases present in the slag were as follows:



The products obtained from this reaction, at equilibrium temperature of 200°C, are shown in Figure 3.3. The results indicated that all the oxides contained in the slag are transformed into sulphates, even with a ratio of 1.5. With a ratio of 1.9, the extra amount of sulphuric acid is used to convert the titanyl sulphate (TiOSO_4) into titanium bisulphate ($\text{Ti}(\text{SO}_4)_2$). For the three acid/slag ratios used, all the acid is transformed into sulphates and SO_2 gas. The reaction oxidizes all the Ti(III) present in the slag before the reaction converts the Fe(II) into Fe(III).

The reactions were tried at different temperatures. At low temperature (below 100°C) hydrated sulphates are produced. At high temperature sulphates and steam are produced.

Figure 3.3 : Products Obtained by the Reaction of SORELSLAG
with Sulphuric Acid at Different Ratios



The sub-programm "Reaction" was used to calculate the heat of reaction generated in the digestion of the different oxides with sulphuric acid. Table 3.6 gives the heat generated per kg of oxides reacting with sulphuric acid. We can see that the oxidation of Ti(III) into Ti(IV) (reaction 3.4 to 3.6) is the most important source of heat. The reaction involving CaO is less significant, due to its low content in the Sorels slag.

Table 3.6 : Heat Generated by the Reaction of 1 kg of Oxide with Sulphuric Acid at 180°C

Oxides	Heat Generated (kJ/kg)	Reaction
TiO ₂	1606.06	3.1
TiO ₂	1359.75	3.2
Ti ₂ O ₃	1220.29	3.3
Ti ₂ O ₃	2994.32	3.4
Ti ₂ O ₃	2503.65	3.5
Ti ₂ O ₃	4359.67	3.6
FeO	1295.15	3.7
Fe ₂ O ₃	406.93	3.8
MgO	2970.25	3.9
Al ₂ O ₃	614.37	3.10
CaO	4208.47	3.11

CHAPTER 4

EXPERIMENTAL

This chapter covers the preparation of materials, the description of the apparatus, the standard digestion procedure and the analytical techniques used.

4.1 Preparation of Materials

The titanium slag supplied by QIT-Fer et Titane was the regular Sorelslag type, as shipped to pigment producers.

The slag was ground in a dry ball mill. Three different samples were prepared to study the effect of particle size on the digestion.

The size analysis of a fine material like the one used in the sulphate process is not easy. Three different techniques of analysis were used: wet sieves, sedigraph and diffraction. Tables 4.1 and 4.2 show the chemical analysis and the size distribution analysis of the three samples used (coded respectively SQ1A, SQ1B and SQ1C). The sedigraph particle size distribution plots are shown in Figure 4.1.

Table 4.1 : Chemical Analysis of the Three Slag Samples Used

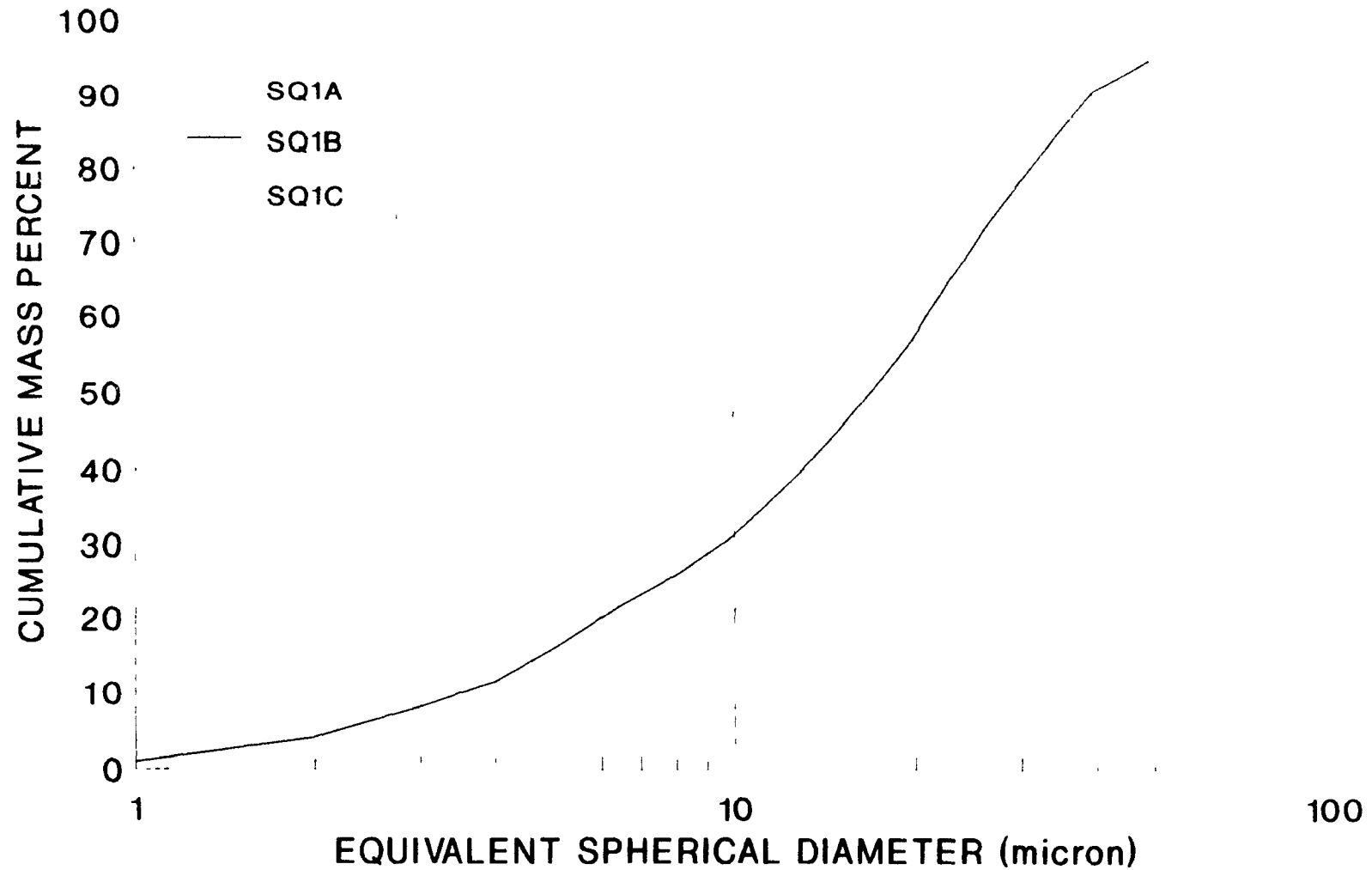
	SQ1A (%)	SQ1B (%)	SQ1C (%)
TiO ₂	77.0	77.3	77.3
Ti ₂ O ₃ *	13.7	14.2	15.7
Fe Total	8.8	8.8	8.53
Fe Metal	0.16	0.17	0.39
FeO	11.11	11.12	10.45
Al ₂ O ₃	3.70	3.69	3.73
CaO	0.56	0.56	0.57
MgO	5.38	5.40	5.40
C	0.022	0.022	0.022
S	0.080	0.077	0.084
P ₂ O ₅	0.006	0.010	0.004
MnO	0.26	0.27	0.26
SiO ₂	3.15	3.16	3.16
Cr ₂ O ₃	0.17	0.18	0.16
V ₂ O ₅	0.62	0.60	0.60

*Express as TiO₂

Table 4.2 : Size Distribution Analysis of the Three Slag Samples Used

	SQ1A	SQ1B	SQ1C
<u>Wet sieve</u>			
+200 Mesh (74 μm)	0.6 %	3.0 %	19.6 %
-200, +325 Mesh	6.0 %	10.5 %	14.0 %
-325 Mesh (43 μm)	93.4 %	86.5 %	66.4 %
<u>Sedigraph</u> $d_{50\%}$	11 μm	17 μm	23 μm
<u>Diffraction</u> $d_{50\%}$	10.2 μm	16.4 μm	17.4 μm

Figure 4.1 : Sedigraph Particle Size Distribution of the Three Slag Samples Used



Sulphuric acid at an initial concentration of 96 to 97 % by weight was used to digest the slag. This concentration was verified by standard analytical methods.

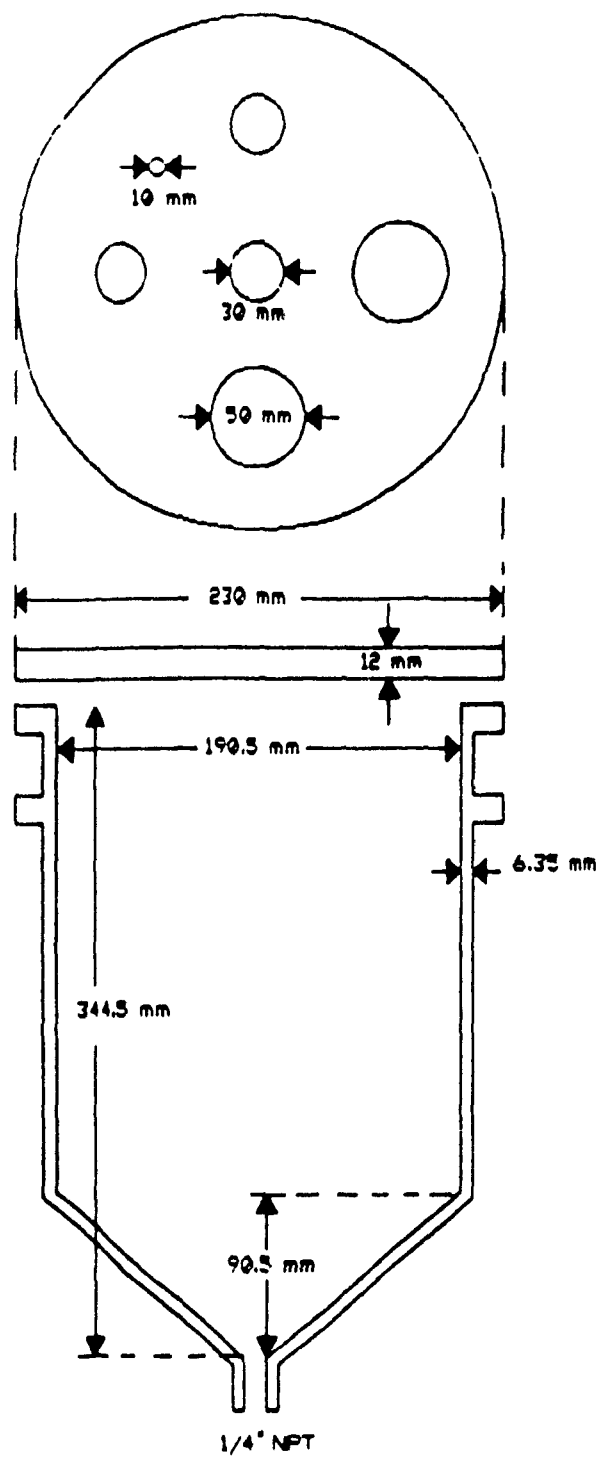
4.2 Apparatus

The equipment used for these tests has been designed and constructed to simulate in the best possible way the conditions encountered in commercial digesters, i.e. air agitation, steam heating, curing, and dissolution. Its construction was based on the experience obtained with less sophisticated experimental devices previously developed at QIT (56,57). The reactor had a design capacity of 1500 g of slag per batch.

4.2.1 Reactor

The reactor was made of 316 stainless steel and had a volume of 8.1 litres. The internal surface was covered with a 1 mm thick lead coating that was electrolytically applied (58). This lead coating was used for anti-corrosion protection, as stainless steel is not resistant to dilute sulphuric acid and liquors containing Ti(III) (59). The cover of the reactor was flat. Detailed data on the reactor sizes and shape are shown in Figure 4.2.

Figure 4.2 : Digestion Reactor



4.2.2 Heating system

The reactor was supported by a steel cylindrical structure which was insulated but allowed hot air circulation around the reactor. Hot air temperature was controlled so as to follow the temperature evolution in the reactor. External heating of the reactor with hot air was necessary to compensate for the heat losses. With this system, it was made possible to reach the same temperatures as in industrial reactors for which no external heating is used. It is well known that even with insulation, pilot plant heat losses are much greater than found in commercial units (60).

4.2.3 Mixing

The mixture was agitated by an air flow injected through the bottom of the reactor, as in commercial digesters. Air flow and pressure were controlled throughout each complete digestion cycle (mixing, attack, curing and dissolution).

4.2.4 Data acquisition

An IBM-compatible microcomputer equipped with a 16 channel Optomux card was used for data acquisition. This system was used to monitor the temperature of the reacting mass, of the exit gas stream, of the heating system and of the steam. Iron-constantan thermocouples of 0.16 cm (1/16") diameter were

connected to the card. The thermocouple installed in the reactor was coated with teflon for protection against acid. The evolution of the reaction temperature was displayed on the screen of the microcomputer. The Labtech Notebook software was used during the experiments to draw the temperature flowchart.

4.2.5 Gas collection system

The exit gases were cooled by two condensers at the reactor outlet and were then passed through four traps containing sodium hydroxide. By analysing the contents of these traps it was possible to follow the amounts of sulphur (S), hydrogen sulphide (H_2S), sulphur dioxide (SO_2) and sulphur trioxide (SO_3) produced during digestion (61).

4.2.6 Steam

A Cole-Parmer Chromalox electrical steam generator having a capacity of 4 kg/hr supplied the steam required for starting the reaction. The steam line was heated by an electric wire. Steam line temperature and pressure were kept constant by controllers. The resulting condensed water (from the condensing tube on the steam line) was used to calibrate the steam flow rate before the test so as to determine the amount of steam introduced into the reactor and to calculate the sulphuric acid concentration for digestion.

4.2.7 Tachometer

The readings from a tachometer installed on the axis of a small agitator immersed into the mixture were used as an indirect measure of the viscosity of the slurry as well as an accurate measure of the set-up time*. The output of the tachometer was a 0-5 V analog signal that was recorded by the computer.

4.2.8 Settling tank

The settling tank consisted of a pyrex tank provided with an isothermal liner that permitted a flow of hot water in order to maintain the liquor temperature at 65°C. The lower section was graduated so the amount of settled residues could be measured. The installation of a valve at the bottom of the settling tank permitted the discharge of the liquor and sludge while still hot which made filtration much easier. The experimental set-up is schematically shown in Figure 4.3.

*Set-up, as explained later, indicates the conditions at which the viscous reacting mass becomes solid.

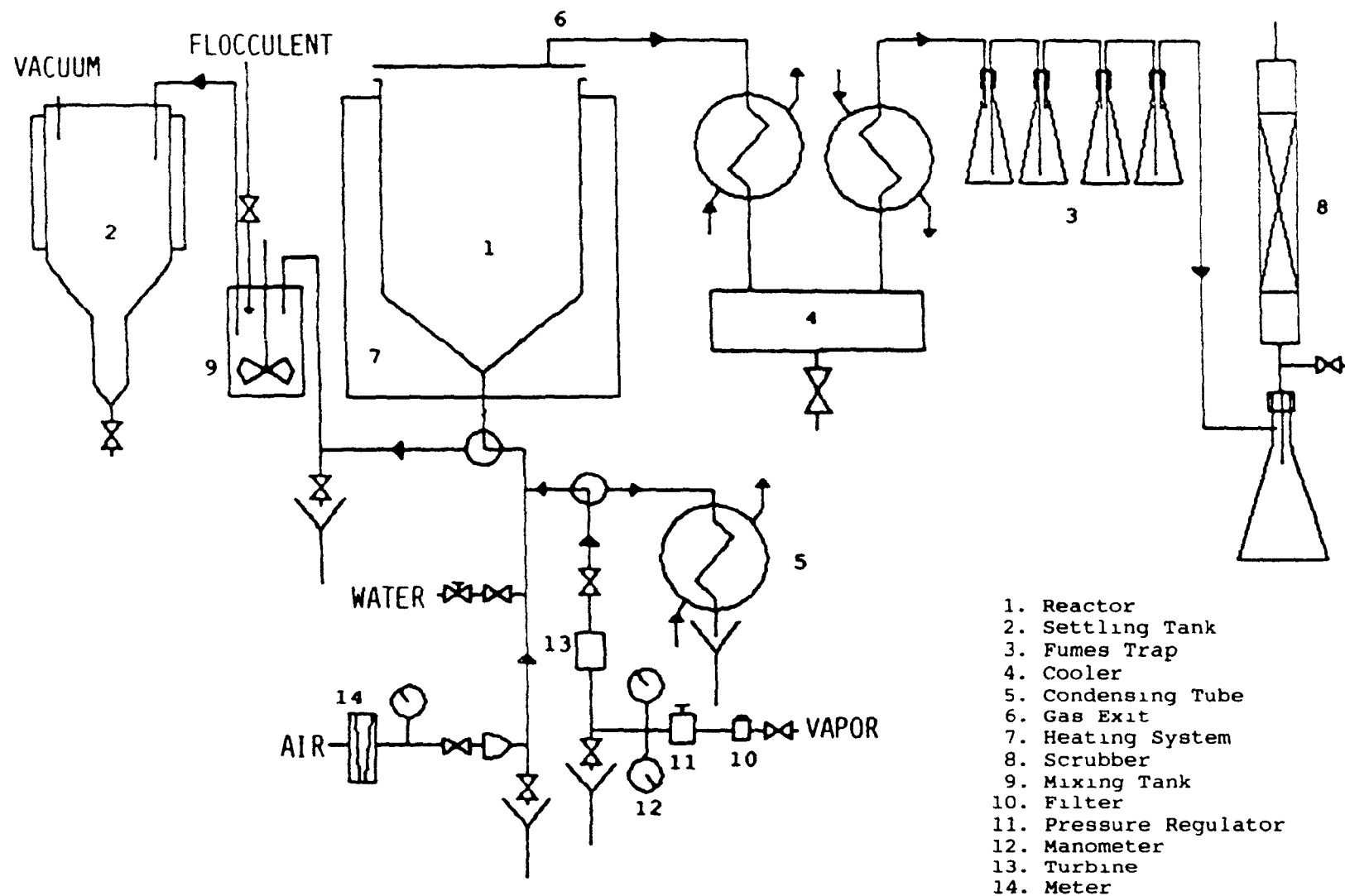


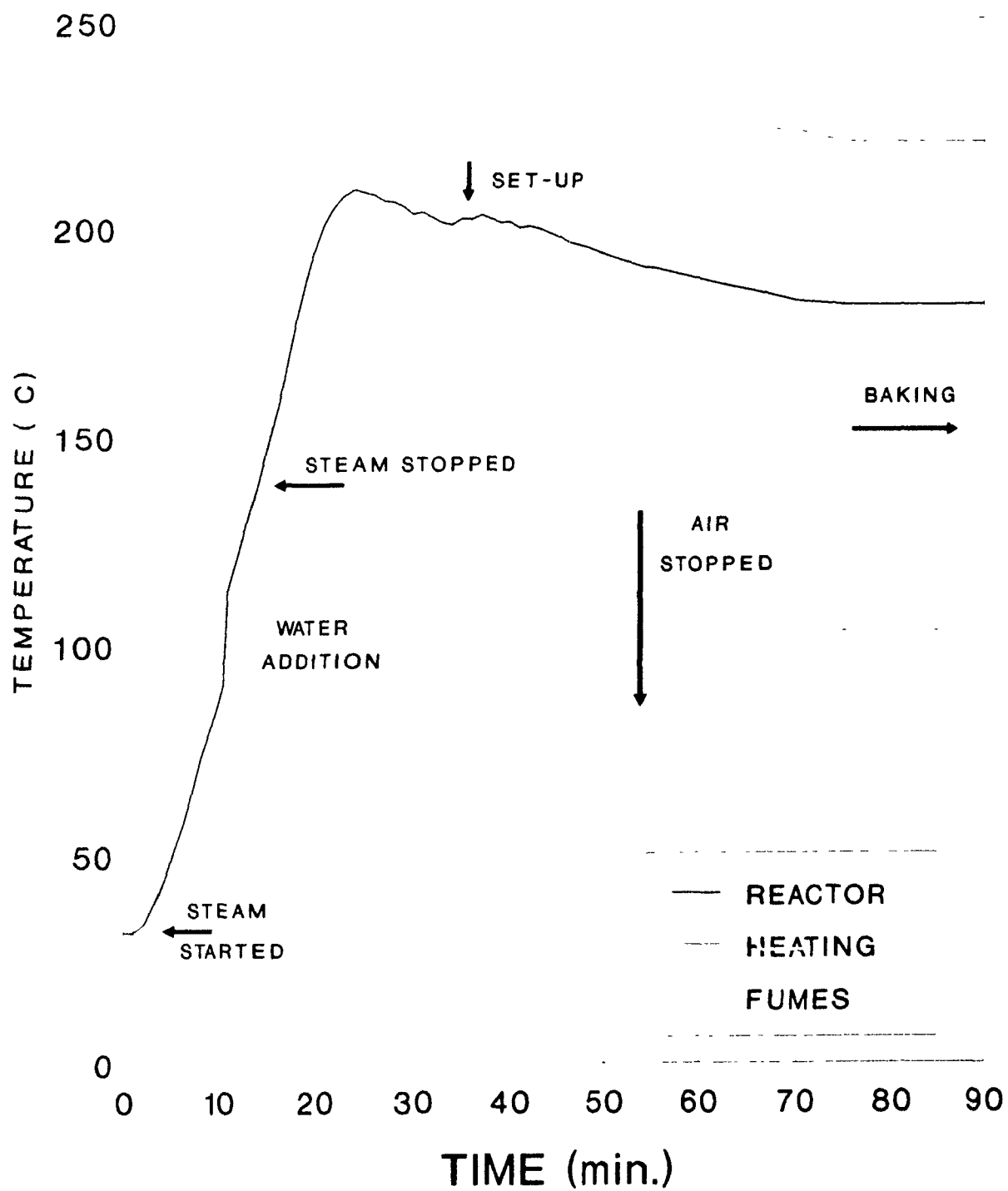
Figure 4.3 : Schematic Representation of Digestion Equipment

4.3 Digestion Procedure

The reactor was initially loaded with concentrated sulphuric acid and slag; by means of an air flow of 3.2 l/min. the contents of the reactor were mixed for 10 minutes; the air flow was then reduced to 2.7 l/min. Then the temperature was gradually increased by turning on the heating system surrounding the reactor and by injecting steam into the mixture. A quantity of demineralized water was poured into the reactor when the temperature reached 90°C in order to obtain the pre-determined acid concentration. This addition caused a sharp temperature increase and the reaction started.

Steam injection was stopped after 65 g of steam had been introduced. The temperature inside the reactor rose to a maximum. Meanwhile the temperature of the heating system was maintained as close as possible to that in the reactor. A tachometer was used to indicate the accurate set-up time (i.e. the time the reaction mass solidifies). Ten minutes after the set-up point the air flow was reduced by 50% and then was stopped completely after a further ten minutes. By then the mixture was very solid. A typical temperature evolution profile during digestion is shown in Figure 4.4 (test Run 4): for the reactor temperature, the external heating system temperature and the temperature of the exit fumes.

Figure 4.4 : Temperature Profile of a Digestion Test



The locations of the thermocouples used to monitor the three temperatures are shown in Figure 4.5.

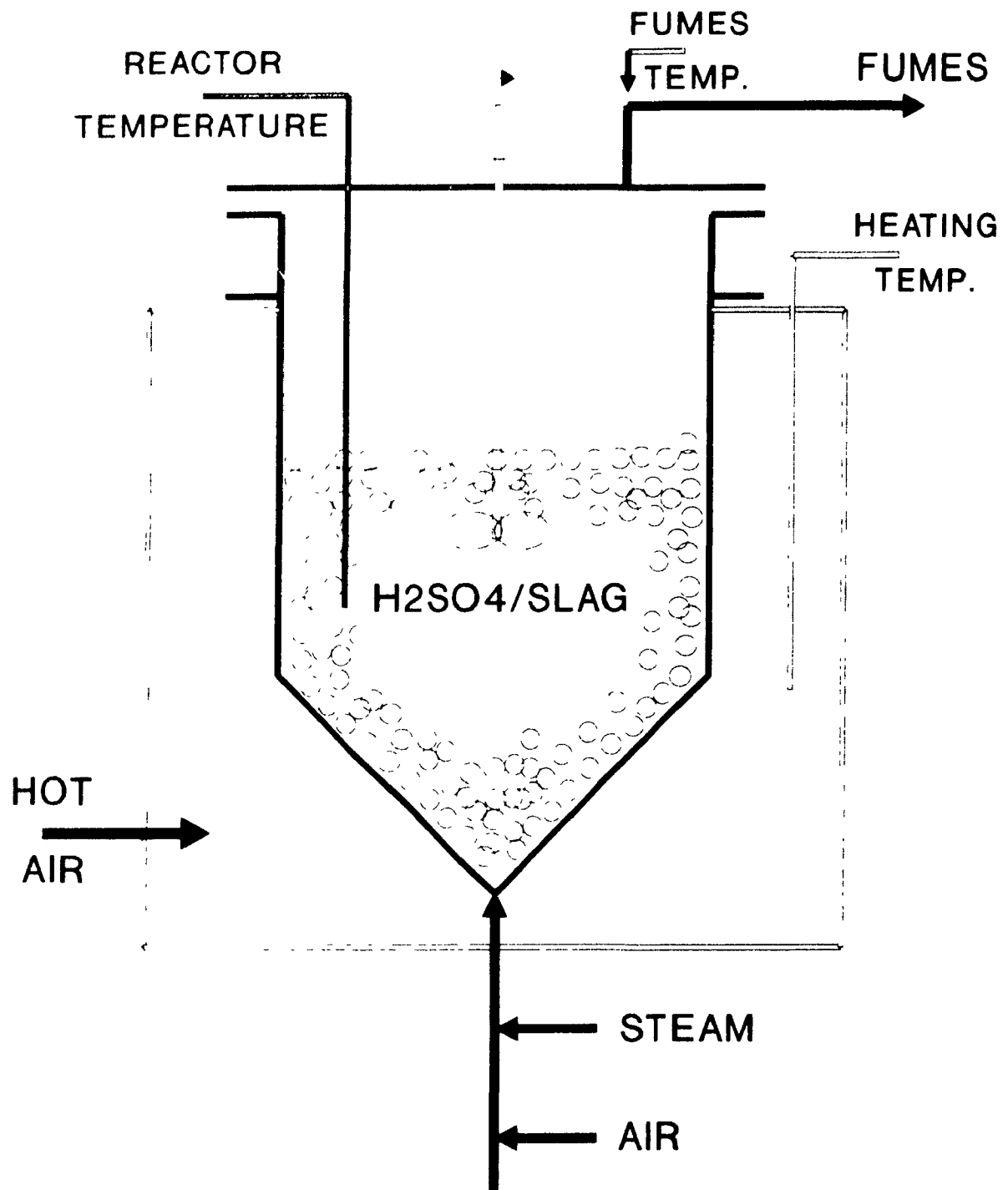
After solidification (set-up) the reaction mass was allowed to cure for a given time at 180°C. Upon completion of curing, the heating system temperature was set at 80°C and the cake allowed to cool overnight.

The following morning, the temperature of the cake was approximately 70°C making possible its dissolution with the introduction of water through the bottom of the reactor. During dissolution, the cake was agitated with an air flow of 2.8 l/min. For complete dissolution a retention time of 5 to 6 hours at 75°C was required.

At the end of dissolution, the reactor was emptied from the bottom; the liquor transferred into a small agitated tank where flocculant (Diafloc) was continuously added, then it was transferred into the settling tank.

After settling, the liquor was filtered under vacuum and three streams were recovered: sludge, liquor and washing water.

Figure 4.5 : Thermocouples Location in Digestion Reactor



For each digestion test a TiO_2 material balance was performed and several calculations were made to determine recovery, the amount of acid lost in the gases and the properties of the liquor for the following step (hydrolysis). These calculations were made and recorded on an electronic spreadsheet, Lotus 123 (See Appendix D).

4.4 Analysis

The analyses which were made at the research laboratory of QIT-Fer et Titane (61) included several complete analyses of the slag. The composition reported in Table 4.1 gives the average of these analyses.

The products resulting from these digestion tests, i.e. black liquor, digestion residue and wash water, were analyzed for TiO_2 content. The stability, the percentages of free acid, Ti_2O_3 , and Total Fe in black liquor were also analyzed using the standard analytical techniques developed at QIT-Fer et Titane (61).

CHAPTER 5

STATISTICAL DESIGN METHODOLOGY

5.1 Selection of Process Variables

Many variables influence the digestion process: slag composition, the particle size of the feed material, the sulphuric acid/slag ratio, the initial acid concentration, the acid concentration after dilution with water and steam, the temperature at which the addition of water and steam are stopped, the addition of organic material (40), the air flow used for agitation, the baking time, the baking temperature and the amount of air used during baking (38,39).

Because of the large number of parameters involved, it is understandable that only a few could be evaluated. The data from a previous investigation conducted at QIT (33) and the information collected from the literature formed the basis for the selection procedure. Four variables were considered the most important for the digestion of Sorels slag: the particle size of the slag, the sulphuric acid/slag weight ratio, the sulphuric acid concentration after dilution (at the attack) and the baking time. The range of conditions tested in this experimental program was chosen on the basis of operating conditions practised at commercial level. In Table 5.1, the ranges for the four process variables are summarized.

Table 5.1 : Range of Process Variables Investigated

PROCESS VARIABLE	RANGE OF CONDITIONS		
	LOW	MEDIUM	HIGH
d_{50} SIZE (micron)	11	17	23
RATIO acid/slag	1.5	1.7	1.9
H ₂ SO ₄ conc. (%)	88	91	94
BAKING TIME (hrs)	2	4	6

The other variables were kept constant at values which are normally used in commercial installations. The principal objective of this work was to characterize the effect of changes in the process variables on the extraction yield of TiO₂. However, other important effects that were followed closely included: the maximum temperature obtained in the reactor, the solidification time (set-up time), the active acid/titanium ratio*, the degree of oxidation of Ti₂O₃ during digestion, the sulphuric acid lost in the fumes, and the height of the digestion cake.

5.2 Selection of Statistical Design

The purpose of this study was to determine the response of the

*This term will be fully explained in section 6.4.4.

seven dependent variables (yield, maximum temperature, set-up time, active acid/titanium ratio, oxidation, fume losses and cake height) to changes in the four independent variables (particle size, acid/slag ratio, acid concentration and baking time) by an empirical model (mathematical equation). Polynomial approximations are widely used and have proven very valuable in modelling process data (62).

A polynomial has the same form as a Taylor Series that has been truncated after a specified number of terms. The first order Taylor Series is a linear approximation. In the operational region of most processes a second order Taylor Series is an adequate approximation. In this case, the digestion of Sorelslag by sulphuric acid was approximated by a second-degree polynomial. In its general form, the selected empirical model was:

$$\begin{aligned}
 Y = & b_0 + b_1X_1 + b_2X_2 + b_3X_3 + b_4X_4 + b_{11}X_1^2 + b_{22}X_2^2 + b_{33}X_3^2 + b_{44}X_4^2 \\
 & + b_{12}X_1X_2 + b_{13}X_1X_3 + b_{14}X_1X_4 + b_{23}X_2X_3 + b_{24}X_2X_4 + b_{34}X_3X_4 + e
 \end{aligned}
 \tag{5.1}$$

where,

- Y : Measured or calculated response
- X_i : Design variables
- b_i : First-order coefficients
- b_{ii} : Second-order coefficients
- b_{ij} : Interaction coefficients
- e : Residual (difference between the measured response and the corresponding value predicted by the polynomial model)

The polynomial coefficients are not those of the Taylor Series but are constants adjusted by least squares to give a small prediction error throughout the region of interest, which was assumed to be the region in which data have been obtained.

Second-order experimental designs that might be suitable to obtain the polynomial model are full three-level factorial designs, central composite designs, regular polygon designs and fractional designs (45).

A Box-Behnken design, which is an incomplete three-level factorial design, was chosen. The Box-Behnken design limits the number of runs for the different sets of conditions and produces estimates of first-order and interaction term coefficients uncorrelated with each other. Only the coefficients of the quadratic terms are correlated with each other and with the constant term b_0 .

Each Box-Behnken design employs a subset of the points in the corresponding full three-level factorial, with two extra replicates at the centre point which provide a measure of inherent experimental error. The four-variable Box-Behnken design used here is shown in Table 5.2 (62).

Symbols X_1 , X_2 , X_3 , and X_4 represent, respectively, the particle size of the slag, the sulphuric acid/slag ratio, the

Table 5.2 : Four-Variable Box-Behnken Design

Experiment Number	X ₁	X ₂	X ₃	X ₄	
1	+1	+1	0	0	Block 1
2	+1	-1	0	0	
3	-1	+1	0	0	
4	-1	-1	0	0	
5	0	0	+1	+1	
6	0	0	+1	-1	
7	0	0	-1	+1	
8	0	0	-1	-1	
9	0	0	0	0	
10	+1	0	0	+1	Block 2
11	+1	0	0	-1	
12	-1	0	0	+1	
13	-1	0	0	-1	
14	0	+1	+1	0	
15	0	+1	-1	0	
16	0	-1	+1	0	
17	0	-1	-1	0	
18	0	0	0	0	
19	+1	0	+1	0	Block 3
20	+1	0	-1	0	
21	-1	0	+1	0	
22	-1	0	-1	0	
23	0	+1	0	+1	
24	0	+1	0	-1	
25	0	-1	0	+1	
26	0	-1	0	-1	
27	0	0	0	0	

acid concentration and the baking time. The +1, 0 and -1 sign represents the high, medium and low coded values of the variables. The execution order was randomized to eliminate time effects as much as possible.

5.3 Selection of Statistical Software

To treat and analyze the Box-Behnken design output data, to obtain a representation of variable interactions; to obtain the polynomial equation and to check the statistical accuracy of the results, software especially developed for computer-aided design of experiments (CADOE) was used. CADOE Software packages automatically perform many of the calculations and manipulations required. Highly detailed graphic displays provide an easy-to-understand picture of exactly how the process performs.

Some of the personal computer software packages being used for these purposes today include ECHIP (63), RS/Discover, Design Ease (64), Design Expert (64), XStat and Statgraphics (65). The present work was performed using Statgraphics. This software package includes the Box-Behnken technique and it is user-friendly.

To create an experimental program with Statgraphics the following steps have to be performed:

-Design Specification	The number of independent variables and the number of response variables are set.
-Variables definition	Names for each independent and response variable are provided, specifying the units for each. The high and low levels for each factor are set.
-Design selection	A design from a list of designs that are available for the number of independent variables specified is selected (in this case, Box-Behnken design was selected).
-Design options specification	Centerpoints and randomization of the runs are specified.
-Experiment saving	The system is instructed to save the experiment in a file.

After the experimental program is completed, the data collected for each run are entered in the software and the analysis begins. First, the estimate effects are calculated. using:

$$\text{Effect} = (\text{response at high level}) - (\text{response at low level})$$

The display includes the standard error of the estimate for each effect. Once the estimated effects have been calculated, a standardized Pareto Chart is created. This chart is similar to a Pareto chart (65), except that it shows the effect divided by its standard error. The chart includes a vertical line at the critical t-value for an α of 0.05. An effect that exceeds the vertical line may be considered significant. The non-significant effects are removed and only the significant

ones are retained to build the model. The system produces an analysis of variance table, which is called the ANOVA table, that includes the sum of squares, degrees of freedom (DF), and mean square for each of the effects. The table also shows the F-ratio and significance level for each effect. Estimate regression coefficients are calculated to fit the data in its original units. These values are the coefficients of the polynomial equation used to plot the Response.

To determine whether the model, as estimated, adequately fits the data, a diagnostic plots section is available. When all the information has been verified, two or three dimensional graphs of the response over the selected design region for the process can be generated to visualize each response surface and to determine the optimum operating conditions.

CHAPTER 6

RESULTS AND DISCUSSION

6.1 Experimental Design Data

Statistically designed digestion experiments of Sorels slag were performed to establish optimum conditions for sulphation of titanium oxide and to have a better understanding of the effect of the variables. In total, 27 experiments were performed following the Box-Behnken statistical methodology described in section 5.2. The independent variables investigated were particle size of the slag (SIZE, $d_{50\%}$ in micron), acid/slag weight ratio (RATIO), sulphuric acid concentration at the attack* ([H₂SO₄], in wt% units) and baking time (BAKING, in hours). Initial sulphuric acid concentration (96 wt%), steam addition (65 g), set-off point** (135°C) and the baking temperature (180°C) were held constant throughout the experimental program.

The following responses were measured: yield of titanium oxide conversion (YIELD, %), maximum temperature obtained in the reactor (MAXIMUM, °C), set-up time (SETUP, minutes), active

*This corresponds to the acid concentration after dilution with water and steam as explained in section 4.3.

**This corresponds to the time where the steam addition is stopped. See Figure 4.3.

acid/titanium ratio (AAc/Ti), Ti_2O_3 oxidized (OXIDATION, %), mass of sulphuric acid gaseous products generated by the reaction (FUMES, g) and cake height (CAKE, cm). All the experimental data are given in Table 6.1. From this information, statistical model equations were developed for each of the responses and the results are discussed in section 6.4.

6.2 Heat and Mass Balances Calculations

The analysis of TiO_2 in the slag and the analysis of TiO_2 in the products, black liquor, residue and washing, provided a way to verify the validity of the experimental data. For each of the tests, a TiO_2 mass balance was performed. Table 6.2 gives the respective results for the 27 experiments. If run 15 is excluded because some of the product was lost during the test, an average discrepancy of 1.15 % between the TiO_2 fed and collected was consistently obtained. This difference is within the accuracy range of the analytical techniques.

TABLE 6.1 : FOUR-VARIABLE DESIGN RESPONSE SURFACE: DATA OF THE DIGESTION
OF SORELSLAG WITH SULPHURIC ACID

RUN #	SIZE (micron)	RATIO Ac/SI	[H ₂ SO ₄] (%)	BAKING (hrs)	YIELD (%)	MAXIMUM (°C)	SETUP (min)	AAc/T ₁	OXIDATION (%)	FUMES (g)	CAKE (cm)
1	17	1.7	91	4	92.2	208	24.5	1.725	62.3	27.5	15.5
2	11	1.504	91.24	4	87.7	210	15.3	1.526	68.6	34.0	15.5
3	23	1.5	91	4	85.7	201	27.2	1.522	57.4	34.0	17.5
4	11	1.9	91	4	94.6	206	29.5	1.959	79.8	46.3	15.0
5	23	1.9	91	4	93.1	204	27.5	1.963	52.2	35.2	17.5
6	17	1.7	88	2	93.1	193	40.7	1.896	67.4	34.1	16.8
7	17	1.7	94	2	91.6	217	20.5	1.780	54.8	25.8	15.3
8	17	1.7	88.7	6	94.7	198	32.2	1.666	68.8	39.0	16.5
9	17	1.7	94	6	94.4	218	19.5	1.581	68.0	41.7	16.0
10	11	1.7	91	2	90.0	205	10.2	1.897	65.0	36.0	15.8
11	23	1.7	91	2	88.3	202	21.0	1.859	50.3	17.7	18.5
12	11	1.7	91	6	92.0	204	26.4	1.799	83.5	35.0	
13	23	1.7	91	6	90.2	204	27.4	1.763	68.2	34.2	17.5
14	17	1.7	91	4	92.3	201	31.2	1.744	64.6	41.1	16.4
15	17	1.5	88	4	89.4	192	37.8	1.496	68.5	25.0	17.0
16	17	1.9	88	4	95.0	194	38.5	1.925	71.8	40.1	15.8
17	17	1.5	94	4	88.0	216	19.3	1.552	61.2	27.0	16.0
18	17	1.9	94	4	94.7	217	25.4	1.897	62.5	45.5	15.2
19	11	1.7	88	4	93.6	192	39.1	1.659	79.7	45.6	15.3
20	23	1.7	88	4	92.2	190	32.8	1.619	65.1	44.7	18.5
21	11	1.7	94	4	93.7	218	28.5	1.614	71.9	43.9	13.6
22	23	1.7	94	4	89.0	215	30.8	1.644	58.8	34.7	19.0
23	17	1.5	91	2	88.6	208	21.6	1.474	57.1	30.2	15.5
24	17	1.9	91	2	93.0	203	31.9	1.883	44.0	23.8	16.3
25	17	1.5	91	6	91.1	206	27.0	1.392	71.4	44.8	15.2
26	17	1.9	91	6	94.6	198	31.2	1.869	69.4	32.9	
27	17	1.7	91	4.5	93.1	195	28.3	1.644	61.6	37.4	16.2

Table 6.2 : Mass Balance of Titanium Oxide

RUN #	FEED	PRODUCT			LOSS	
	SLAG (g)	LIQUOR (g)	RESIDUE (g)	WASH (g)	(g)	(%)
1	1159.5	995.8	66.2	73.0	24.5	2.11
2	1155.0	965.6	141.0	36.6	11.8	1.03
3	1159.5	942.0	163.2	40.0	14.7	1.27
4	1155.0	1068.6	62.7	24.0	-0.3	-0.03
5	1159.5	1043.7	80.1	29.8	5.8	0.50
6	1159.5	1041.8	78.8	16.1	22.7	1.96
7	1159.5	1018.1	96.6	29.1	15.6	1.35
8	1159.5	1039.8	60.5	35.0	24.2	2.09
9	1159.5	1053.0	63.8	29.0	13.7	1.18
10	1155.0	1009.9	114.3	20.6	10.1	0.87
11	1159.5	983.8	133.7	28.1	13.9	1.20
12	1155.0	1044.7	92.8	22.7	-5.2	-0.45
13	1159.5	1023.9	113.0	18.9	3.7	0.32
14	1159.5	1036.2	88.4	30.2	4.7	0.41
15*	1159.5	860.8	108.0	50.1	141	12.13
16	1159.5	1069.4	57.3	17.9	14.8	1.28
17	1159.5	973.5	136.9	33.6	15.5	1.33
18	1159.5	1072.9	61.0	23.7	1.8	0.16
19	1155.0	1036.4	72.2	26.7	19.7	1.71
20	1159.5	1027.4	88.9	26.1	17.2	1.48
21	1155.0	1041.9	71.2	18.0	23.9	2.07
22	1159.5	1006.6	126.8	21.6	4.5	0.39
23	1159.5	981.7	130.2	31.3	16.2	1.40
24	1159.5	1041.2	79.9	21.3	17.1	1.48
25	1159.5	1014.1	101.1	24.1	20.2	1.74
26	1159.5	1055.7	61.9	24.7	17.3	1.49
27	1159.5	1058.2	79.4	14.7	7.2	0.62

*Problem with the reactor, loss of black liquor.

To have a better understanding of the digestion process a theoretical mass and heat balance was performed (details on how these calculations were performed and what kind of assumptions were used are given in Appendix E). Table 6.3 gives the stoichiometric amounts of reactants and products for 95 % digestion efficiency using the middle range values for the variables studied in this work. In this table the heat of reaction was calculated using $F \cdot A \cdot C \cdot T$ from the data for pure oxides.

Tables 6.4 and 6.5 contain, respectively, the mass and heat balance results. All the acid was converted into sulphate salts and the water produced by the sulphation reactions was approximately double the water contained in the dilute acid. During digestion, an average of 60 % of the water present was evaporated.

Table 6.3 : Stoichiometric Amounts of Reactants and Products Obtained for 95 %
Digestion Efficiency (The data correspond to the middle range values
of the process variables)

	SLAG	H ₂ SO ₄ 100 % *	SULFATES PRODUCED	H ₂ O PRODUCED	NON- REACTED FRACTION (g)	HEAT OF REACTION (kJ)	HEAT GENERATED (%)
	(g)	(g)	(g)	(g)			
TiO ₂ soluble	907 41	1641 32	2201 86	301 20	45 37	1267 21	54 0
Ti ₂ O ₃	189 75	319 27	451 54	58 16	0.00	563 15	24 0
Fe metal	2 52	4 42	6 85	0 81	0 00	16 40	0 0
FeO	165 12	213 51	331 15	39 22	8 26	203 16	8 7
Fe ₂ O ₃	0 00	0 00	0 00	0 00	0 00	0 00	0 0
Al ₂ O ₃	54 79	150 04	174 53	27 56	2 74	31 98	1 4
CaO	8 32	13 82	19 18	2 54	0 42	33 24	1 4
MgO	80 18	186 63	228 52	34 28	4 01	226 26	9 6
MnO	4 01	5 26	8 10	0 97	0 20	6 18	0 3
SiO ₂	46 92	0 00	0 00	0 00	46 92	0 00	0 0
Cr ₂ O ₃	2 67	4 91	6 55	0 90	0 13	1 42	0 1
V ₂ O ₃	8 76	10 88	18 09	2 00	0 44	14 79	0 6
TiO ₂ insoluble	29 55	0 00	0 00	0 00	29 55	0 00	0 0
Total.	1500	2550 0	3446 4	467 6	138 03	2347 38	100 0

* Calculated according to stoichiometry

Table 6.4 : Mass Balance for 95 % Digestion Efficiency

REACTANTS (g)	
SLAG	1500 0
H2SO4 96 %	2656 3
DILUTION WATER	145 9
OXYGEN	10.7
TOTAL	4313
PRODUCTS (g)	
SULPHATES	3446.4
RESIDUE	138 0
REACTION WATER	467.6
DILUTION WATER	252.2
SO2	8.4
H2S	0.9
TOTAL:	4313
EVAPORATION OF WATER DURING DIGESTION	
STEAM LOSS (g).	431.9

Table 6.5 : Heat Balance for 95 % Digestion Efficiency

HEAT GENERATED	
TOTAL HEAT OF REACTION AT 175 C	2347.4 kJ
SULPHURIC ACID DILUTION	243.4 kJ
STEAM AT 122 C	159.1 kJ
TOTAL	2749.9 kJ
HEAT ABSORBED	
SLAG FROM 20 TO 175 C	161.7 kJ
SULPHURIC ACID FROM 20 TO 175 C	601.1 kJ
WATER FROM 20 TO 175 C	94.6 kJ
AIR FROM 20 TO 175 C	24.5 kJ
VAPOUR (STEAM)	1077.4 kJ
TOTAL	1959.3 kJ

According to table 6.5 there is a surplus of heat generated. This is apparently an error and it is due mainly to the way the heats of reaction were calculated. The heat of reaction for the slag was calculated by adding the contribution of each oxide contained in the slag. As discussed in Chapter 2.2, slag components are not present as pure oxides but in a ferrous pseudobrookite structure. The heat liberated by pure oxides is higher than the heat liberated by the chemical compound composed of these oxides. Calculations to correct the heat of reaction for such compounds are complex and it was considered as out of the context of this work. The best way to determine the correct heat of reaction is direct measurement in a calorimetric bomb.

Previous experiments (66) showed that approximately 80 % of the heat produced by the pure oxides is generated by digestion of ferrous pseudobrookite. This fact together with the heat losses of the system (the system is not perfectly adiabatic as assumed in the calculations) can account therefore for most of the discrepancy in the heat balance of Table 6.5.

Despite the conceptual errors, the heat balance calculations obviously show that it is the heat of reaction which is the major source of heat generated in the system while the evaporation of water absorbs most of the generated heat.

6.3 Microscopic Examination of Sorelslag Prior and After Digestion

The microstructure of Sorelslag prior to and after digestion was examined to determine its phase distribution and chemical analysis. Scanning electron microscopy and energy dispersive X-ray analysis were used to characterize the finely ground Sorelslag powder, chunks of the digestion cake, as well as prepared metallographic sections of the cake.

The Sorelslag powder consisted mainly of a titaniferous oxide phase (best known as pseudobrookite) containing iron oxide and low amounts of magnesium and aluminium oxides with a particle size distribution between 5 and 40 μm . Some minor phases such as aluminium-calcium-silicates and metallic iron were also found on the polished sections. (Figures 6.1, 6.2, 6.3 and 6.4)

The cake produced by the sulphate process consisted of an aggregate of submicroscopic titanium sulphate particles structured as a highly porous network and characterized by a high specific surface area. (Figures 6.5, 6.9 and 6.11)

The size of the aggregates ranged from 10 to 40 μm ; this is similar to the particle size of the ground Sorelslag prior to digestion. (Figure 6.5)

Energy dispersive X-ray analysis of individual particles showed two distinct Ti to S molar ratios, 1:1 and 1:2, which correspond to TiOSO_4 and $\text{Ti}(\text{SO}_4)_2$. (Figures 6.9 and 6.10)

Among the impurities present in the slag, Fe, Mg, Al and Ca were found in two distinct forms in the digestion cake: as sulphates containing Ti and a silicate phase. (Figures 6.5, 6.6, 6.7 and 6.8)

Two types of unreacted phases were found: pure titanium oxide (called insoluble in the industry) and silicates. It is worth mentioning that the latter contains Ti as a minor element. (Figures 6.11 and 6.12)

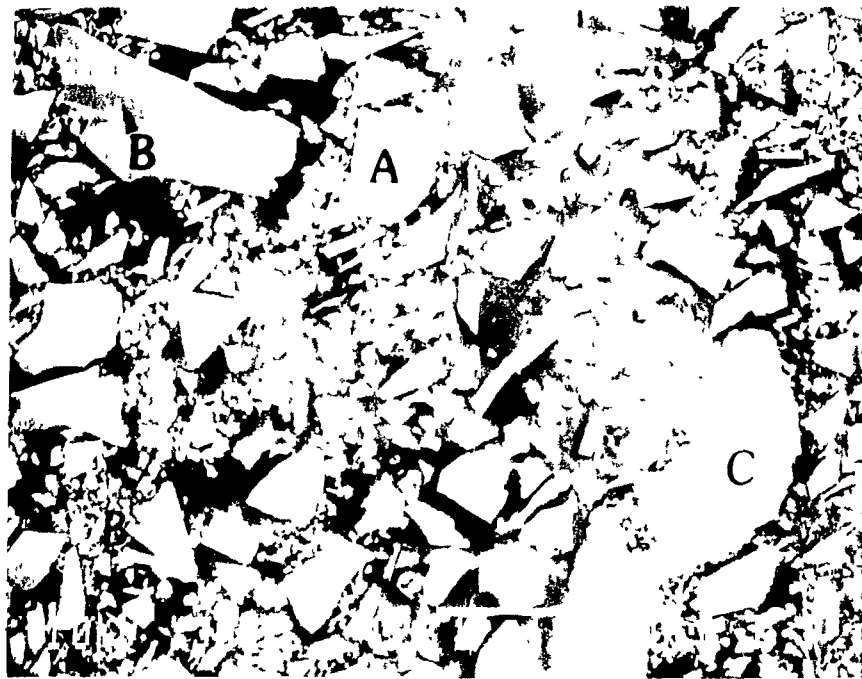
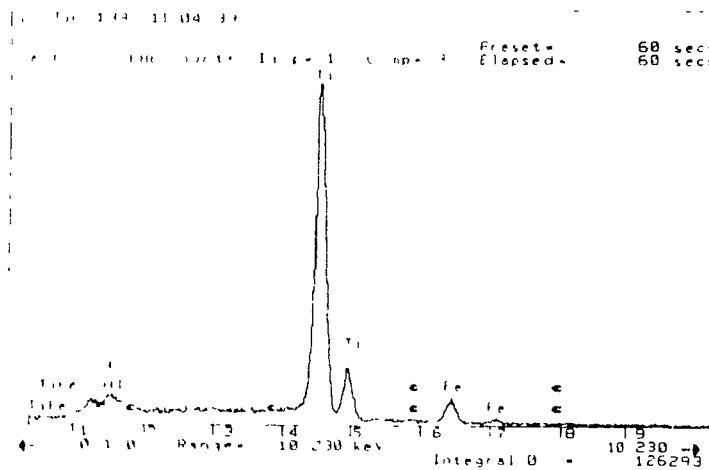


Figure 6.1 : SE Image of Polished Section of the Milled Sorelsag Powder
Showing a size distribution primarily between 5 and 40 μm . The main phase is identified as A and minor phases are identified as B and C.



TiO₂ : 87.0 % wt
FeO : 7.5 % wt
MgO : 3.0 % wt
Al₂O₃ : 2.5 % wt

Figure 6.2 : EDS Spectrum of the A Phase Containing Strong Ti and Weak Fe, Mg and Al Contributions.

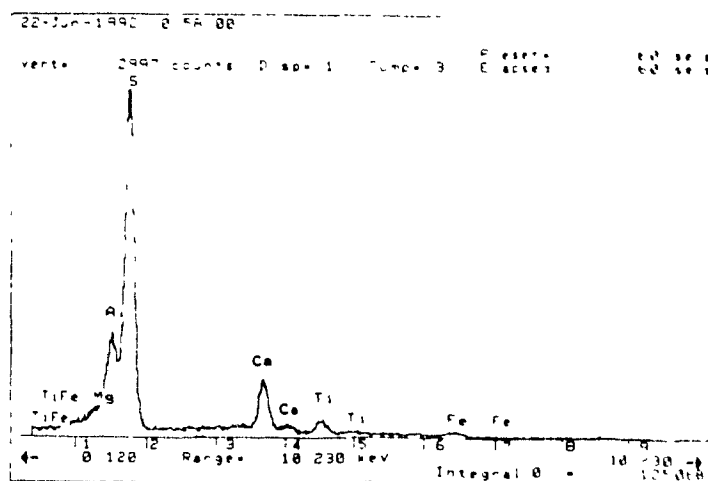


Figure 6.3 : EDS Spectrum of the B Phase, a Silicate Containing Some Al, Ca and Ti Oxides.

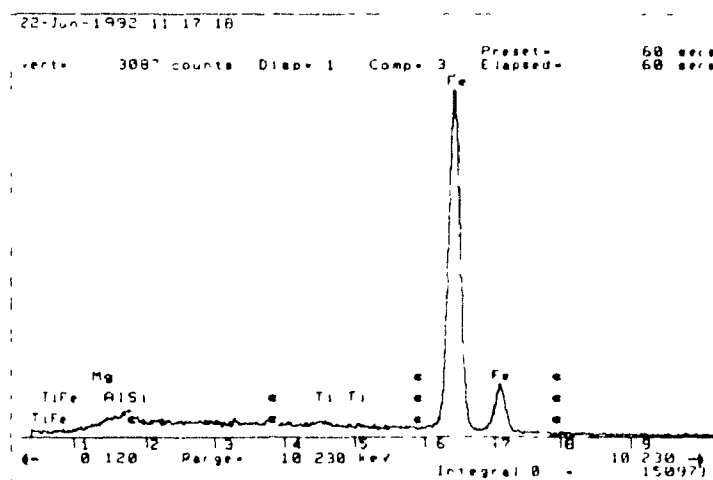


Figure 6.4 : EDS Spectrum of the C Phase, Which is Metallic Iron.

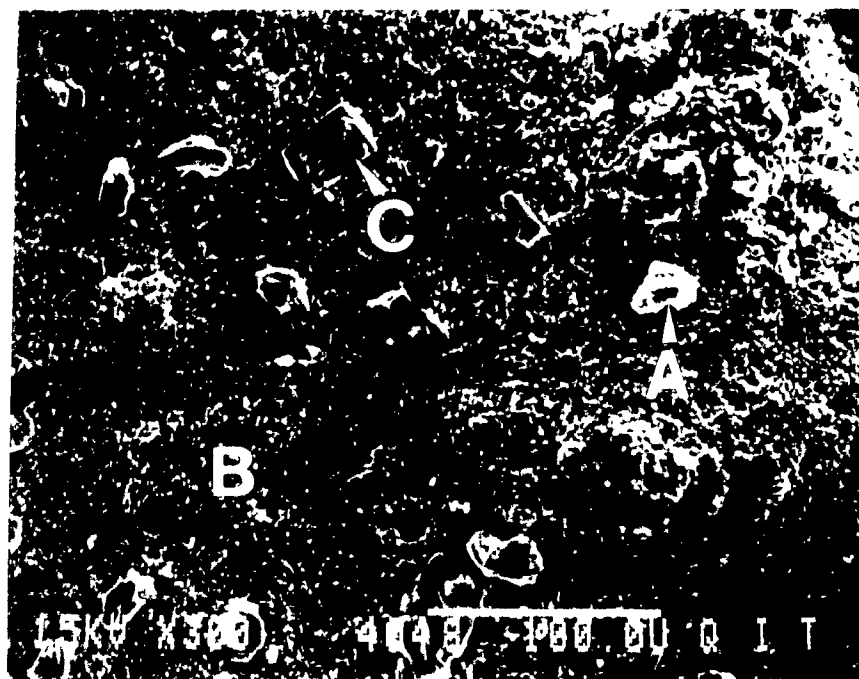


Figure 6.5 : SE Image of the Sorelslag Digestion Cake Produced by the Sulphate Process.

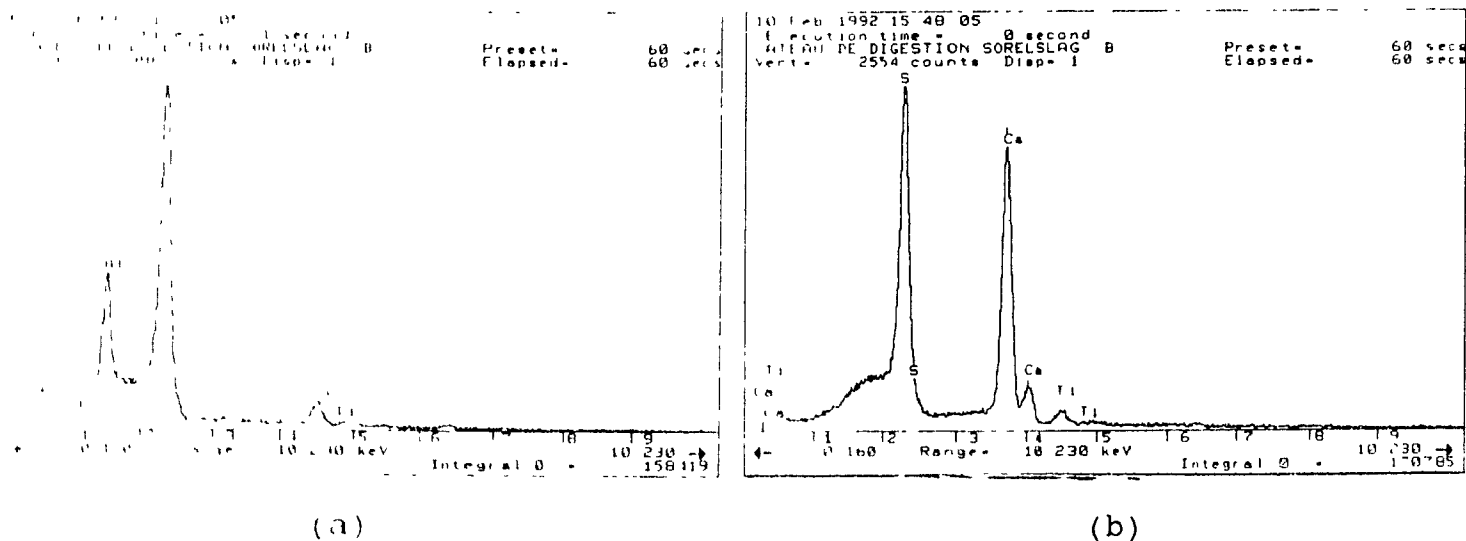


Figure 6.6 : Typical EDS Spectra Collected at Different Spots on Particle A of Figure 6.5. The Phases can be (a) Aluminium Sulphate or (b) Calcium Sulphate.

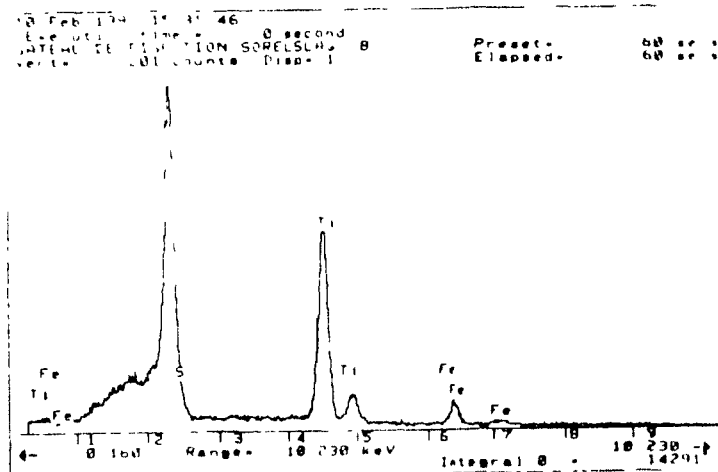


Figure 6.7 : EDS Spectrum Collected on Point B in Figure 6.5 Suggesting the Titanium Sulphate Matrix.

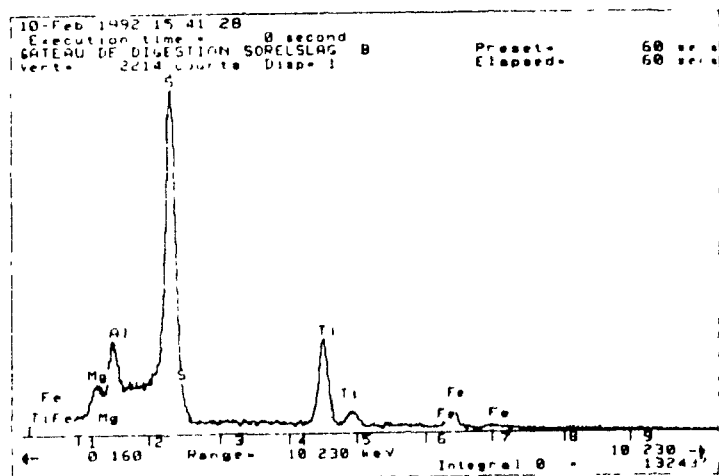


Figure 6.8 : EDS Spectrum Collected on Particle C of Figure 6.5. Phases Present are Considered to be Titanium, Aluminium and Magnesium Sulphate.

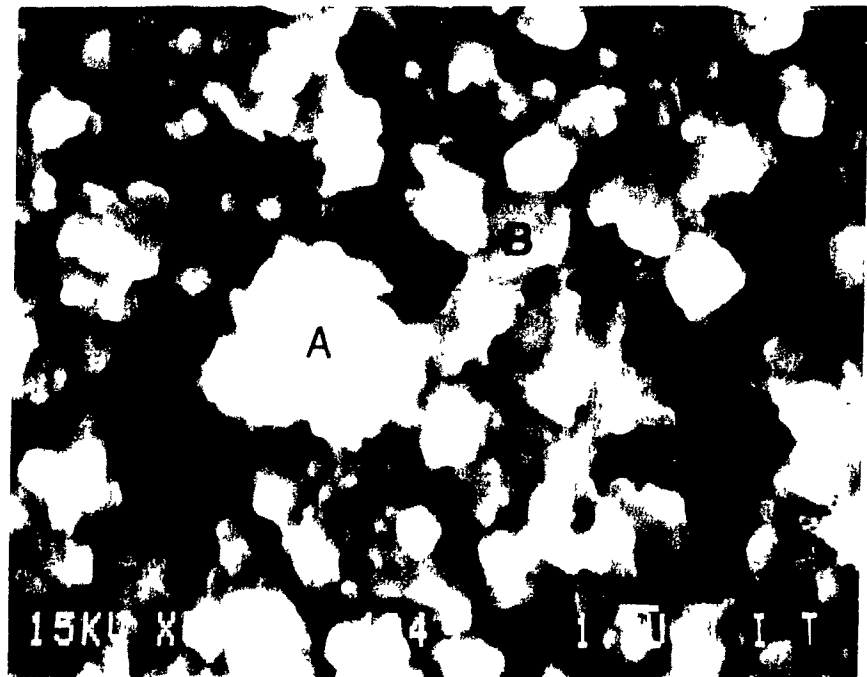


Figure 6.9 : SE Image of the Titanium Sulphate Matrix Showing Submicroscopic White (A) and Gray Phases (B).

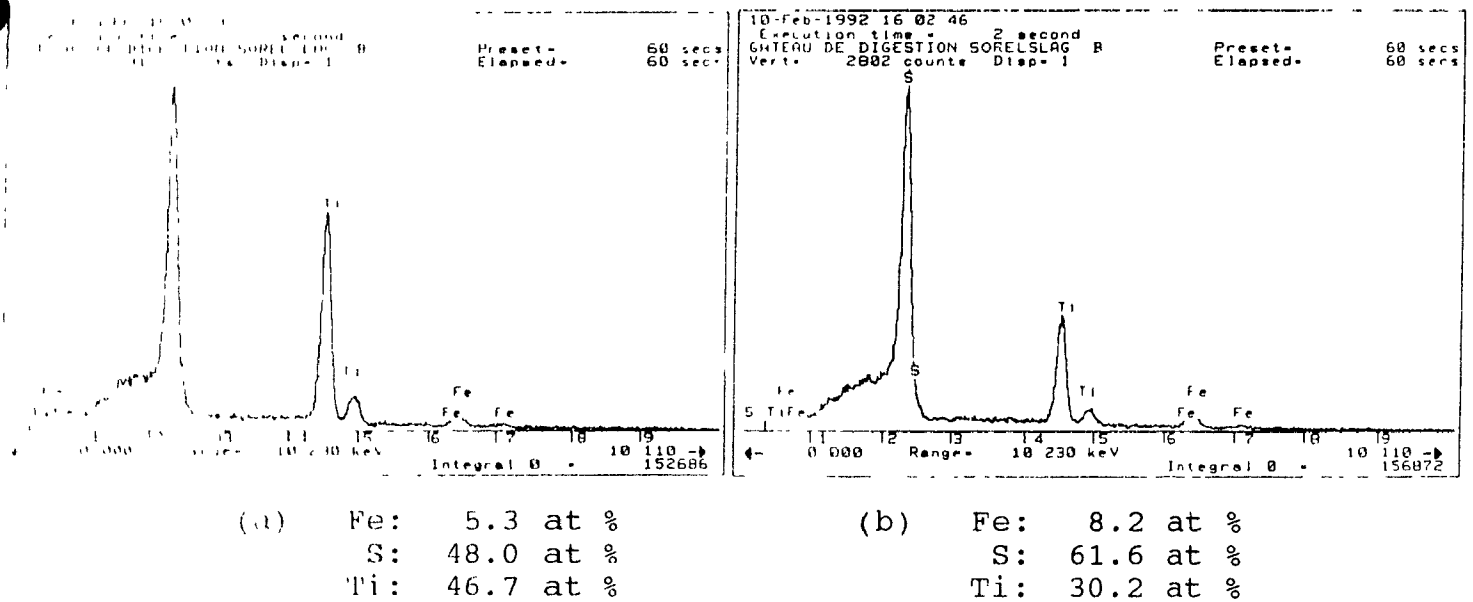


Figure 6.10 : EDS Spectra of the White Phase (A) and the Gray Phase (B), Respectively, Both Shown in Figure 6.9. The Ti:S Molar Ratio are Nearly 1 and 2 for (A) and (B), Respectively, Suggesting they Consist of TiOSO_4 and $\text{Ti}(\text{SO}_4)_2$.

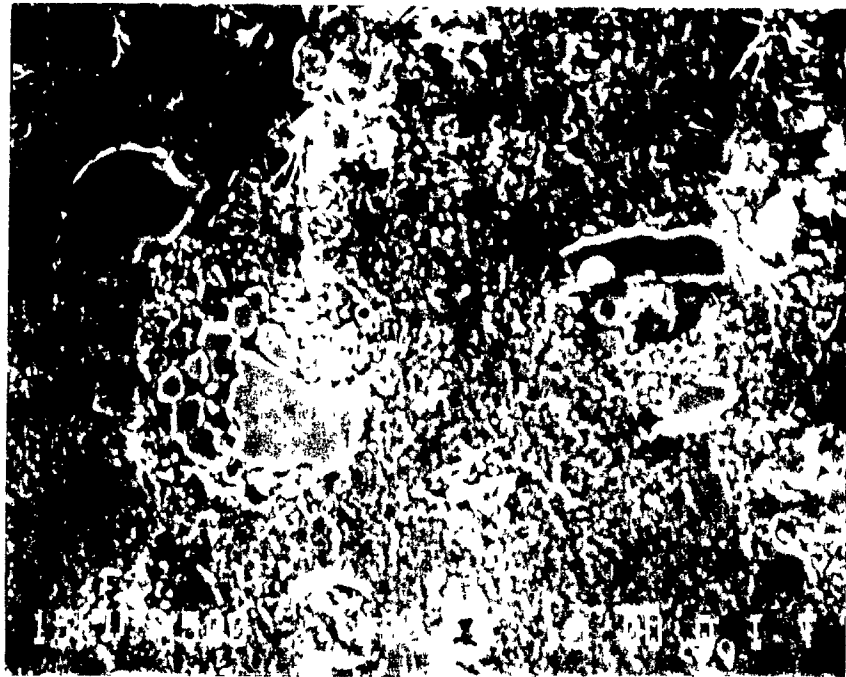


Figure 6.11 : SE Image of Polished Section of Sorelsdag Digestion Cake Showing Numerous Particles Surrounded by the Titanium Sulphate Matrix.

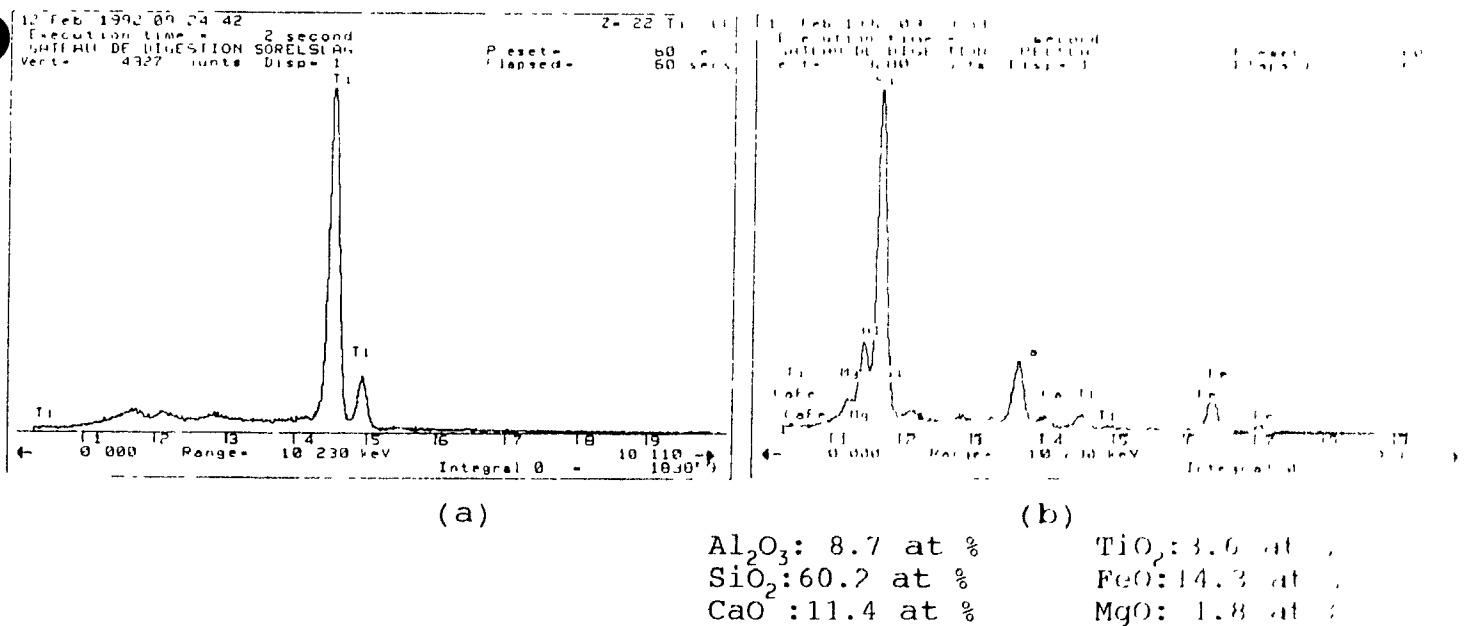


Figure 6.12 : EDS Spectra of the Large Particles Observed in Figure 6.11. They Consist of Two Populations (a) a Ti Rich Phase Which is Most Likely TiO_2 and (b) a Silicate Phase.

6.4 Study of the Digestion Response

This section includes: the building and validation of the model equations and the analysis of the results obtained.

6.4.1 Recovery of TiO_2

The yield of the titanium oxide reaction with sulphuric acid was calculated as:

$$\frac{TiO_{2\text{liquor}} + TiO_{2\text{wash}}}{TiO_{2\text{liquor}} + TiO_{2\text{wash}} + TiO_{2\text{residue}}} \times 100 \quad (6.1)$$

Using the data obtained from the 27 runs, the estimated effects were calculated (see Table 6.6). The standardized Pareto Chart, Figure 6.13, was created with these values. The vertical line at the critical t-value (2.179) for an α of 0.05 included in the Pareto Chart, indicates that some of the effects, specially the interaction ones, are not-significant. The non-significant effects were eliminated and a new table of estimated effects was produced, Table 6.7, as well as a new standardized Pareto Chart, Figure 6.14. ANOVA table and estimated regression coefficients table for the significant effects were produced. The ANOVA table contains the sum of squares, degrees of freedom and mean square for each of the effects (Table 6.8). The estimated regression coefficients table contains the regression coefficients calculated to fit the data in their original units (Table 6.9).

Table 6.6 : Estimated Effects for Yield

average	=	92.4685	+/-	0.595468
A:Size	=	-2.16784	+/-	0.590047
B:Ratio	=	5.76327	+/-	0.591033
C:H2SO4	=	-1.16517	+/-	0.602997
D:Baking	=	2.15567	+/-	0.591327
AB	=	0.210179	+/-	1.02746
AC	=	-1.62338	+/-	1.02147
AD	=	-0.05	+/-	1.02181
BC	=	0.576084	+/-	1.02148
BD	=	-0.45	+/-	1.02181
CD	=	0.431106	+/-	1.08942
AA	=	-3.18169	+/-	0.883514
BB	=	-1.8251	+/-	0.885392
CC	=	1.72992	+/-	0.916523
DD	=	-0.167164	+/-	0.906034

Standard error estimated from total error
with 12 d.f. (t = 2.17938)

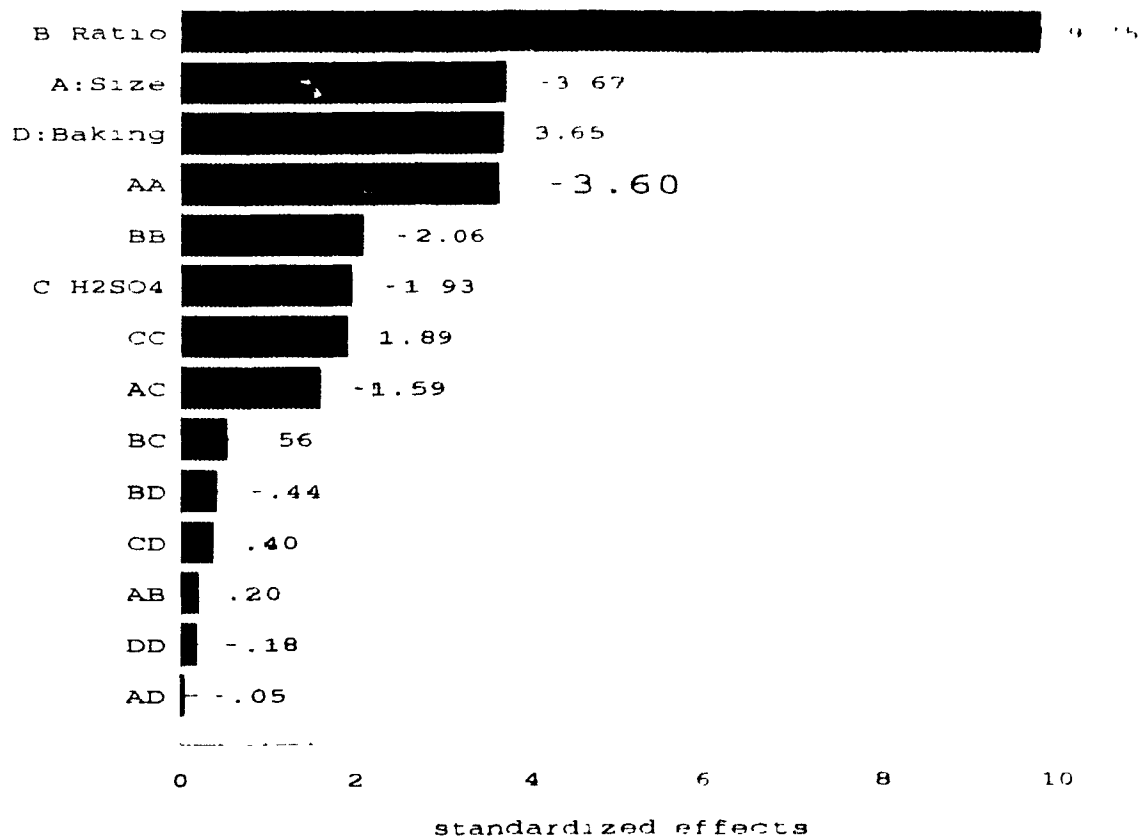


Figure 6.13 : Standardized Pareto Chart for Yield

Table 6.7 : Estimated Significant Effects for Yield

average	=	92.3876	+/-	0.386144
A:Size	=	-2.17483	+/-	0.528981
B:Ratio	=	5.75682	+/-	0.529861
C:H2SO4	=	-1.18305	+/-	0.539018
D:Baking	=	2.17061	+/-	0.52908
AA	=	-3.11939	+/-	0.743345
BB	=	-1.76438	+/-	0.745469
CC	=	1.82135	+/-	0.75847

Standard error estimated from total error
with 19 d.f. (t = 2.09353)

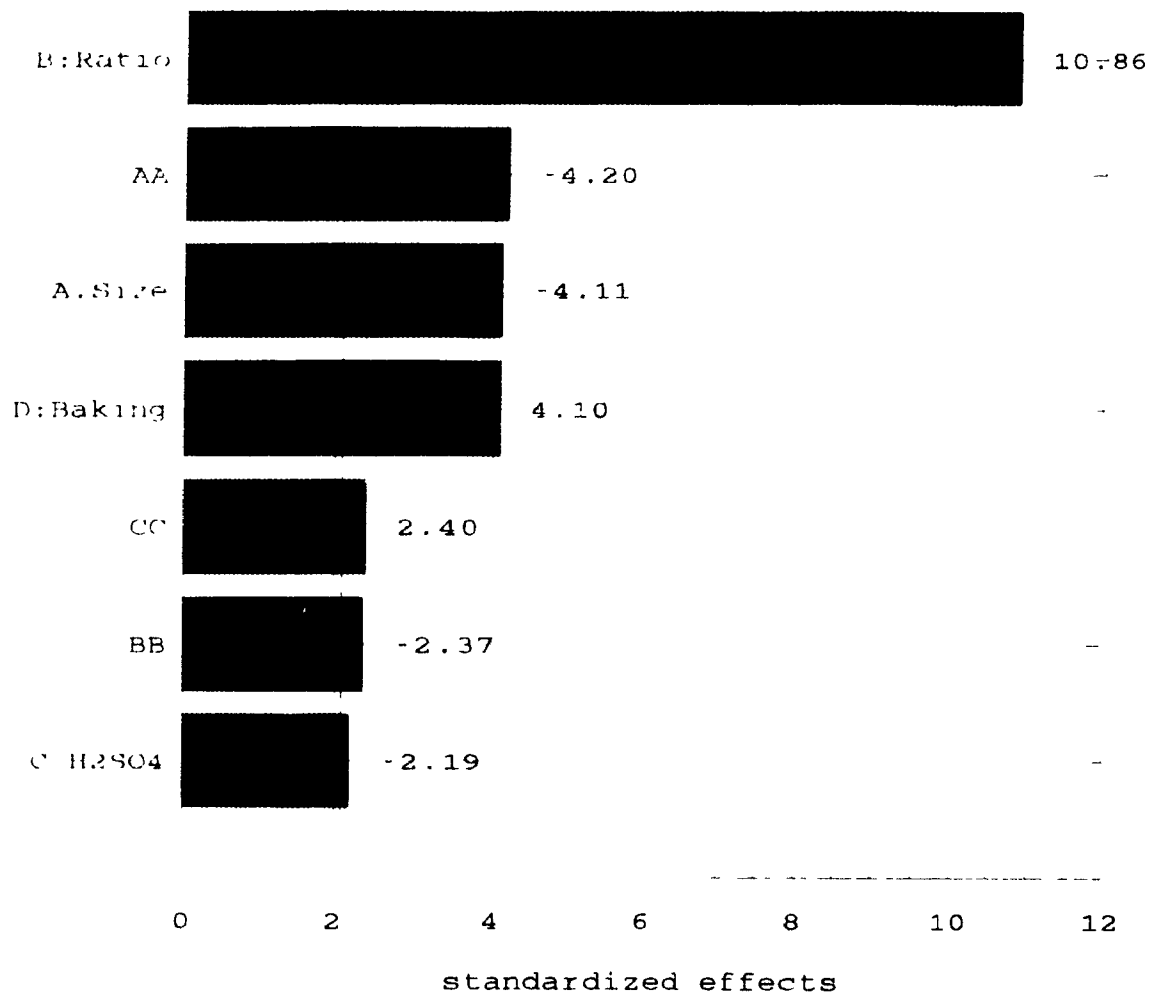


Figure 6.14 : Standardized Pareto Chart for Yield with Significant Effects

Table 6.8 : ANOVA for Yield with Significant Effects

Effect	Sum of Squares	DF	Mean Sq.	F-Ratio	P-value
A:Size	14.1886938	1	14.188694	16.90	.0006
B:Ratio	99.0862059	1	99.086206	118.04	.0000
C:H2SO4	4.0436033	1	4.043603	4.82	.0408
D:Baking	14.1284334	1	14.128433	16.83	.0006
AA	14.7818689	1	14.781869	17.61	.0005
BB	4.7021545	1	4.702154	5.60	.0287
CC	4.8404303	1	4.840430	5.77	.0267
Total error	15.9487031	19	.839405		
Total	174.080000	26			

R-squared = 0.908383 R-squared (adj. for d.f.) = 0.874629

Table 6.9 : Estimated Significant Regression Coefficients for Yield (in real units)

constant	=	848.44
A:Size	=	1.29181
B:Ratio	=	89.3782
C:H2SO4	=	-18.6131
D:Baking	=	0.542654
AA	=	-0.0433248
BB	=	-22.0547
CC	=	0.101186

All this information indicates that the yield is influenced by all four independent parameters studied in this work. The model equation is:

$$Y = 848.44 + 1.29181X_1 + 89.3782X_2 - 18.6131X_3 + 0.542654X_4 - 0.0433248X_1^2 - 22.0547X_2^2 + 0.101186X_3^2 \quad (6.2)$$

where Y : Yield of reaction (%)
 X₁ : Particle size (micron)
 X₂ : Acid/Slag weight ratio
 X₃ : Acid concentration (wt%)
 X₄ : Baking time (hrs)

By order of importance, it is the sulphuric acid/slag ratio, the baking time, the particle size of the slag and the concentration of the acid which most significantly affect the yield.

To determine if the model adequately fits the data, diagnostic plots were used. A plot of the predicted versus observed values was built, Figure 6.15. The plot includes a line with a slope equal to 1 which gives perfect predictions. The plot can be used to detect cases in which the variance is not constant or in which a transformation of the response variable is needed. In the case of the digestion yield, constant scatter around the reference line indicates a constant variance.

A plot of the residuals versus the predicted values, Figure 6.16, shows that the points around the reference line are randomly distributed, which indicates a constant variance. Curvature with respect to the reference line may indicate a missing factor. This was not the case for the digestion yield response.

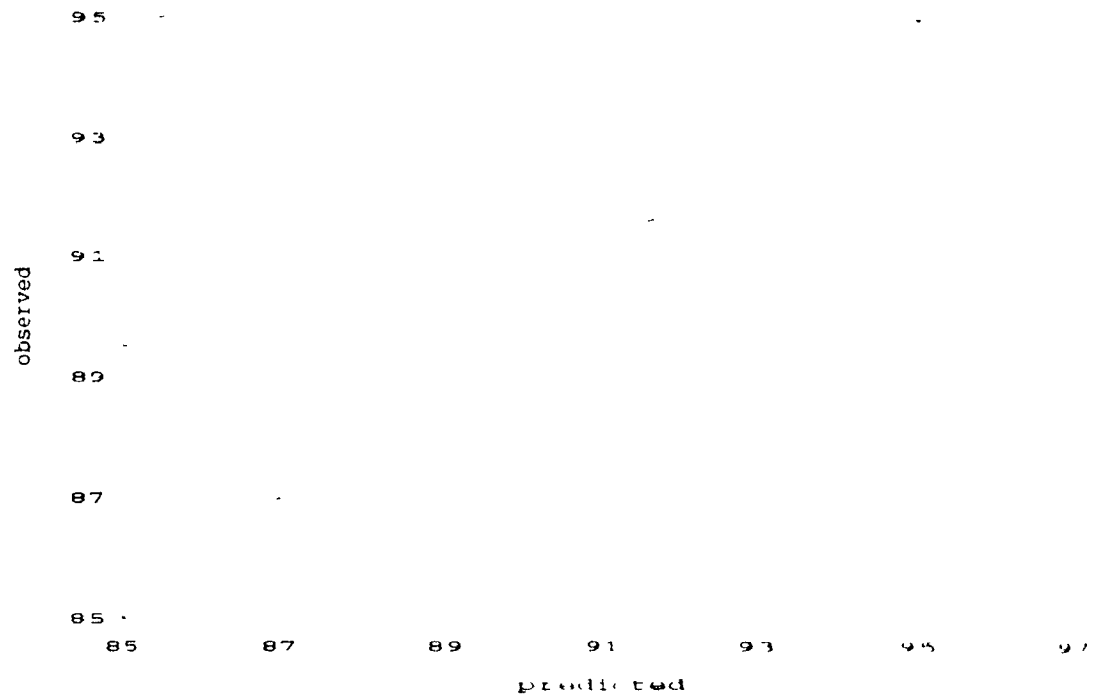


Figure 6.15 : Diagnostic Plot of the Predicted Versus Observed Values for Yield

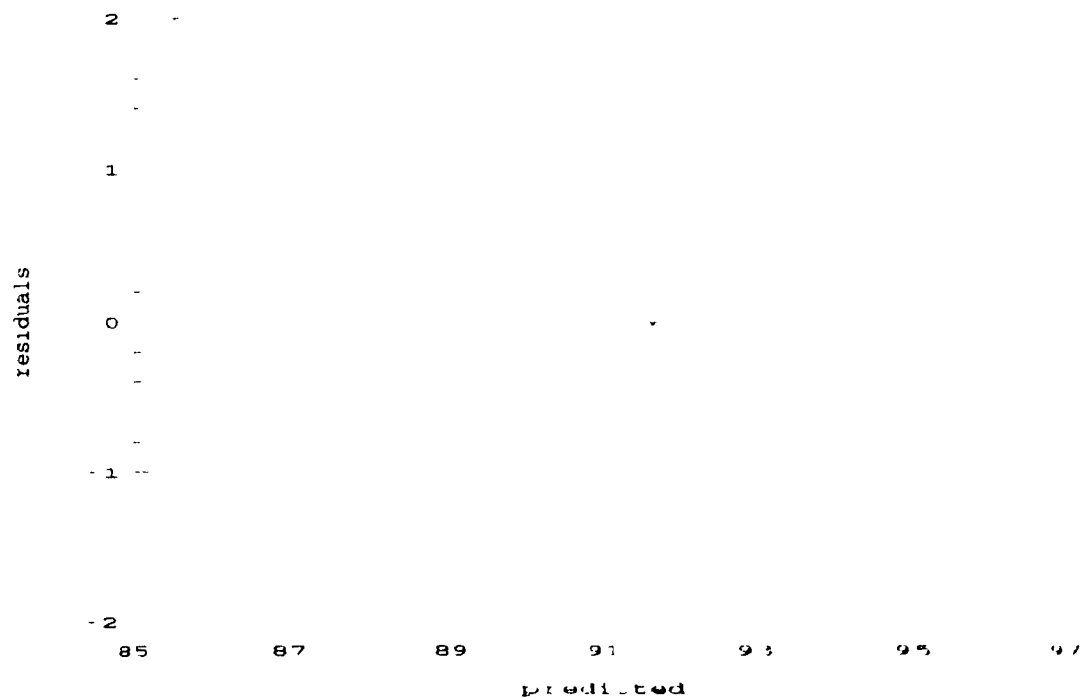


Figure 6.16 : Diagnostic Plot of the Residuals Versus Predicted Values for Yield

A plot of the residuals versus run order (time), Figure 6.17, shows that there is no sequential correlation among the residuals, which indicates no time effect.

A normal probability plot of the residuals was used to verify if the residuals were normally distributed. The residuals fall approximately along a straight line, as shown in Figure 6.18, which indicates that the basic assumption of a normal distribution was true.

To check the model prediction power in the range of this study, an additional run was carried out. This test, called verification run, used a particle size of 17 micron, a sulphuric acid-slag ratio of 1.6, a concentration of 90 % and a baking time of 5 hours. The model equation predicted a yield of 91.6 %, which compares well with the experimental value of 91.7 %. This prediction is within the 1 % error range.

Having verified the model the next step was to generate two or three dimensional graphs of the yield response. When three-dimensional graphs are used, Surface or Contour plots can be produced. The Surface plots represent a three-dimensional grid surface for a function: $Z = f(X,Y)$ and give a good general view of the response. The Contour plots represent a two-dimensional surface similar to a topographical map and are useful to determine a response for specific conditions.

residuals

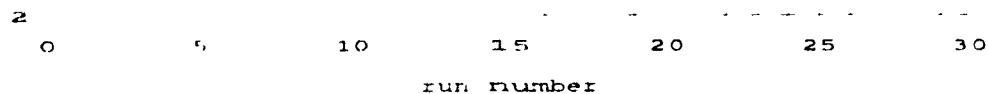


Figure 6.17 : Diagnostic Plot of the Residuals Versus Run Order for Yield

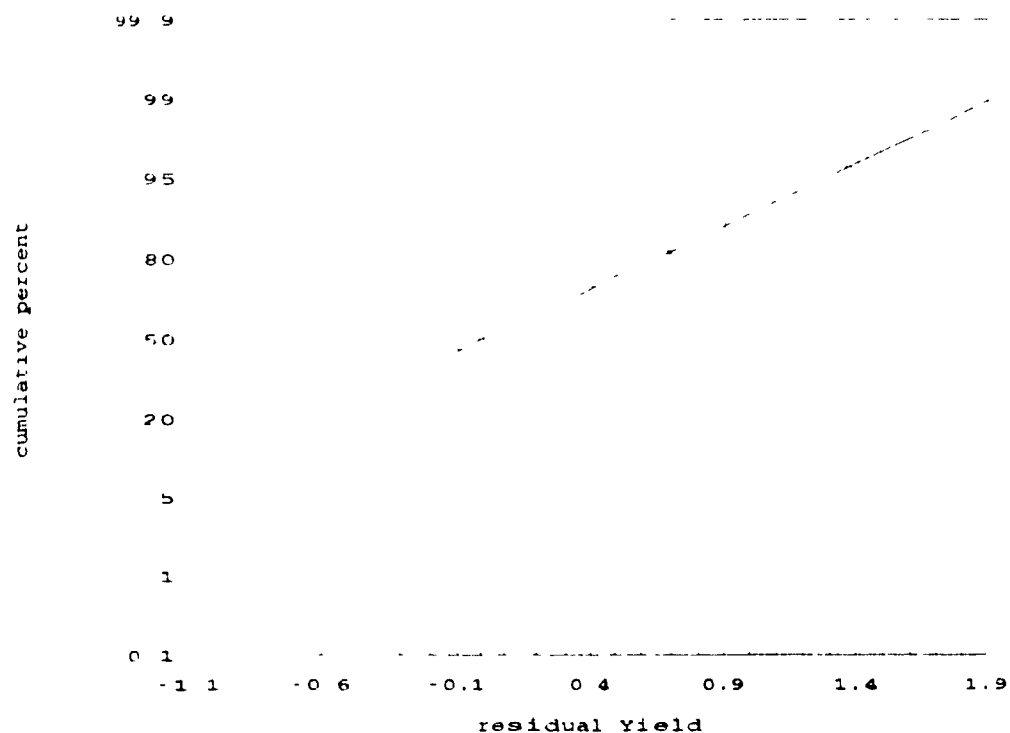


Figure 6.18 : Normal Probability Plot of Residuals for Yield

Figure 6.19 and Figure 6.20 which are, respectively, Surface and Contour plots of the Yield of reaction, show that for a slag with a medium size of 15 micron and an acid concentration of 91 % at attack, the yield of the reaction increases with an increase of the acid/slag ratio. This increase is less important in the high ratio zone, 1.8 to 1.9. With a ratio of 1.5, the amount of sulphuric acid is less than the stoichiometric amount while at much higher ratio (> 1.8) the amount of acid to slag is stoichiometrically in excess resulting in a less significant effect.

Based on this observation, we can say that a reduction of the acid/slag ratio below 1.5 will have a really bad effect on the yield of the reaction while increases over 1.9 will have a negligible effect.

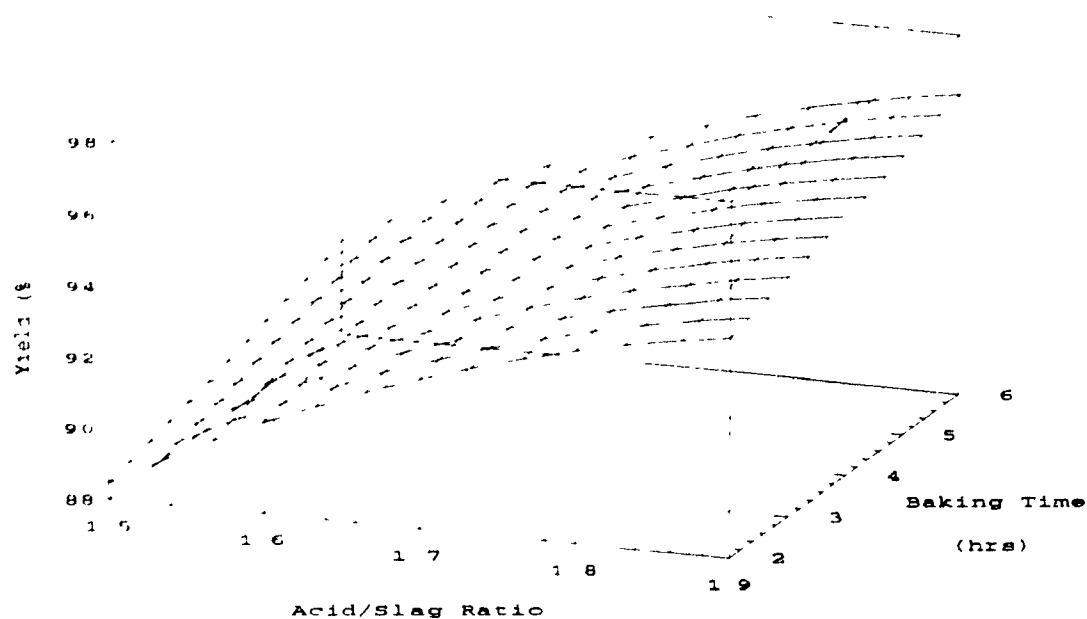


Figure 6.19 : Surface Plot of the Response Function for Yield
with a Fixed Particle Size and Concentration
Particle Size = $15\ \mu\text{m}$, $[\text{H}_2\text{SO}_4] = 91\%$

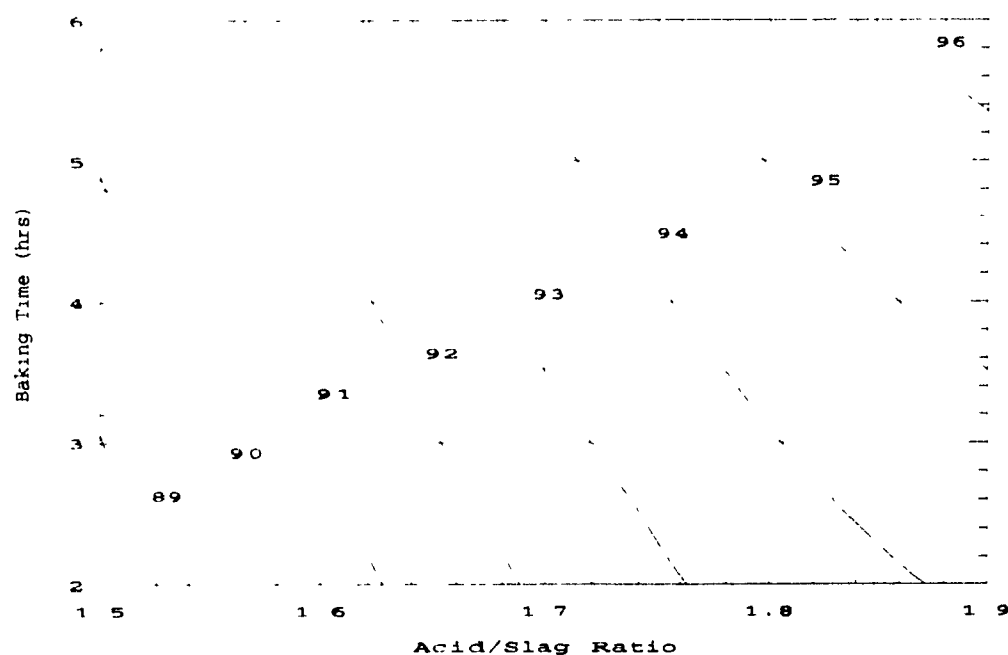


Figure 6.20 : Contour Plot of the Response Function for Yield
with a Fixed Particle Size and Concentration
Particle Size = $15\ \mu\text{m}$, $[\text{H}_2\text{SO}_4] = 91\%$

Figure 6.21 shows the effect of baking time on the reaction yield. Baking provides the time necessary for the slag to react completely with the acid and a long baking time results in higher yield where the first hours are the most important. A baking time longer than 6 hours has an insignificant effect on yield, while a baking time of less than 2 hours sharply reduces the reaction yield. The reaction yield for a simple test performed without baking at all was found to be only 62.3 %.

The reaction yield is also a function of particle size and of acid concentration, but in the range covered by this work these variables are less important than the acid/slag ratio or the baking time. Figures 6.22 and 6.23 show the effect of those two parameters on the reaction yield. The slag with the coarser granulometry, average size = 23 micron, gives low yields but the yield is the best when the slag has a size of 15 micron. Further reductions of the size do not improve the yield of the reaction.

On the other hand the concentration of sulphuric acid has according to Figures 6.22 and 6.23 a rather modest but interesting effect on the yield of the reaction. Yield seems to be at the lowest value at an intermediate acid concentration, but increases at lower and at higher concentrations. An increase in yield with higher acid concentration is understandable but the opposite was

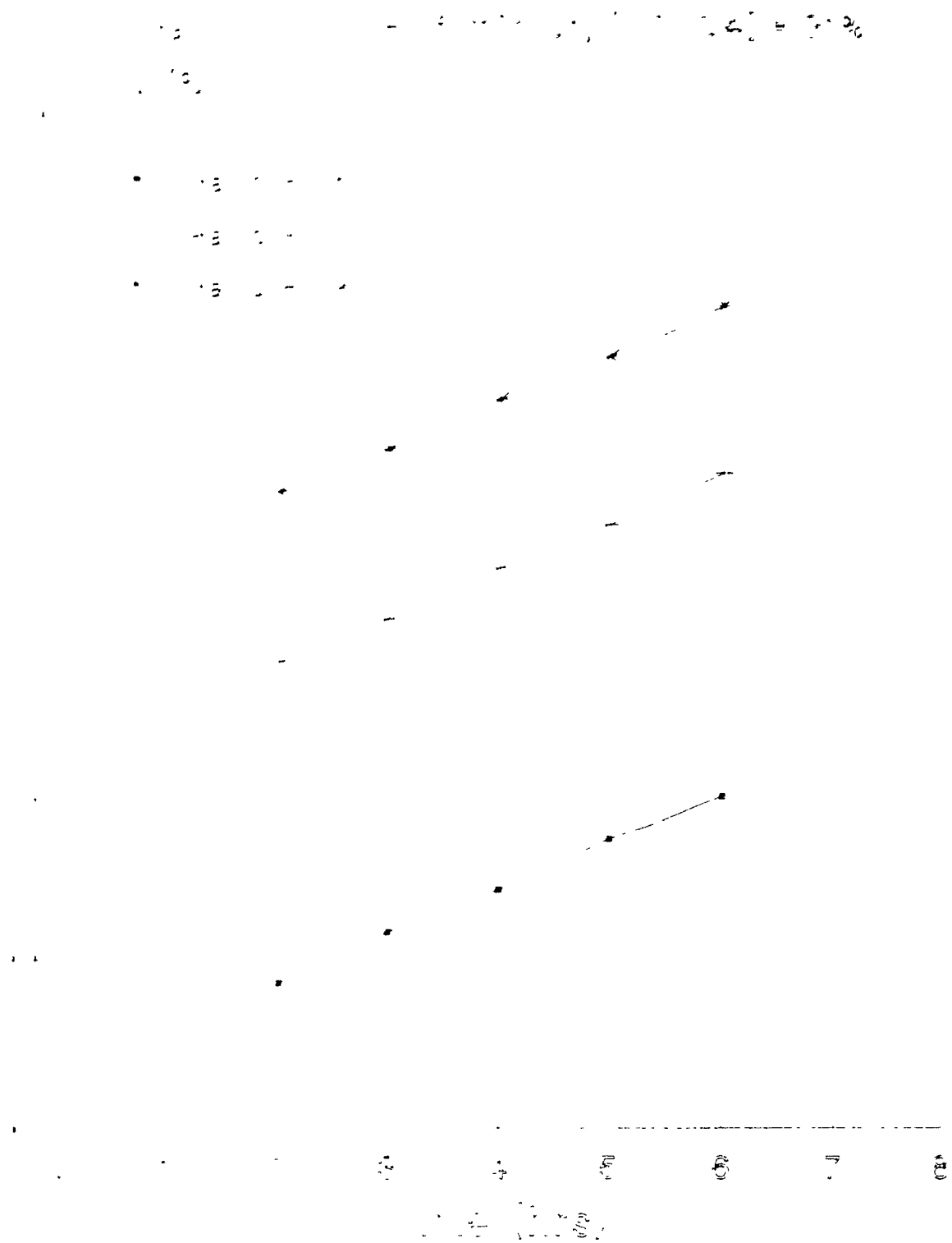


Figure 6.21 : Effect of Baking Time on the Yield of Digestion

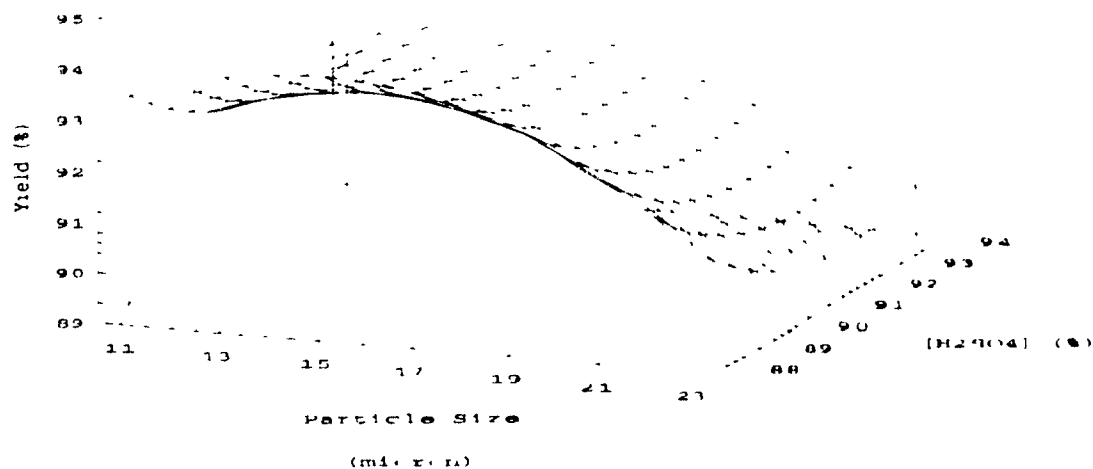


Figure 6.22 : Surface Plot of the Response Function for Yield
with a Fixed Acid/Slag Ratio and Baking Time
Acid/Slag Ratio = 1.7, Baking Time = 4 hours

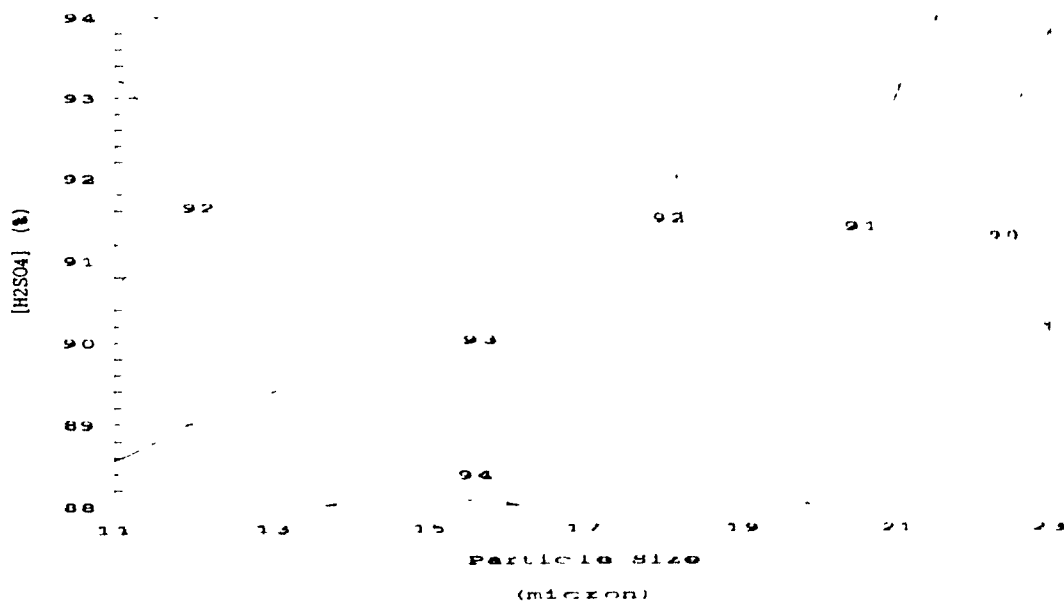


Figure 6.23 : Contour Plot of the Response Function for Yield
with a Fixed Acid/Slag Ratio and Baking Time
Acid/Slag Ratio = 1.7, Baking Time = 4 hours

unexpected. To understand why this happens it was decided to explore further and the Figures 6.24 to 6.27 were generated. As can be seen in these Figures the same trend persists, with the lowest acid concentration (here 88 wt %) giving the highest yield (i.e. 98 % at Ac/SI ratio = 1.9, size = 11 μm and baking 5 hrs; Figure 6.25 and 98 % at Ac/SI ratio = 1.75, size = 11 μm and baking 6 hrs; Figure 6.27).

It seems that because of the extra water carried by the 88 % acid a mass of higher porosity is generated which reacts to a greater degree due to a higher specific surface area.

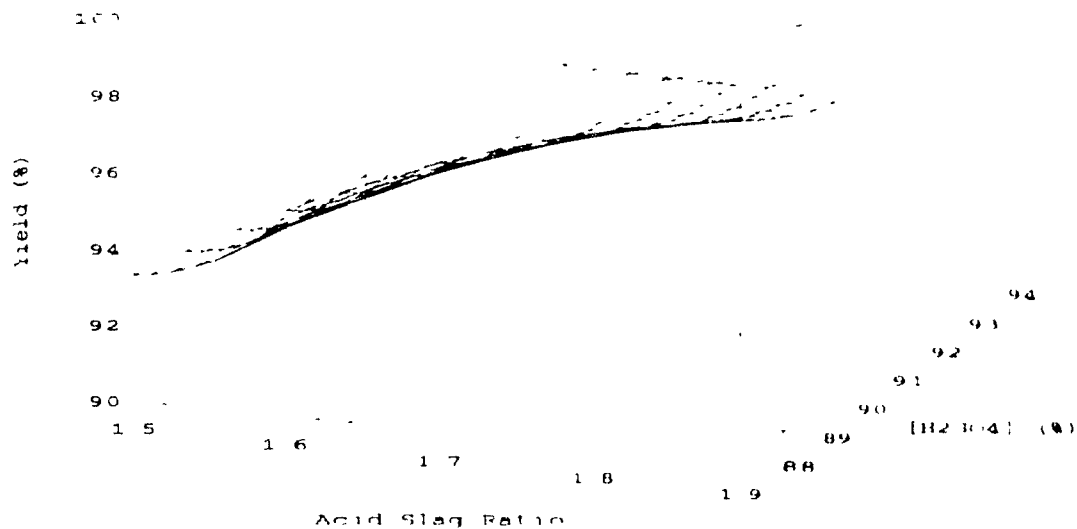


Figure 6.24 : Surface Plot of the Response Function for Yield with a Fixed Particle Size and Baking Time
Particle Size = 11 μ m, Baking Time = 5 hours

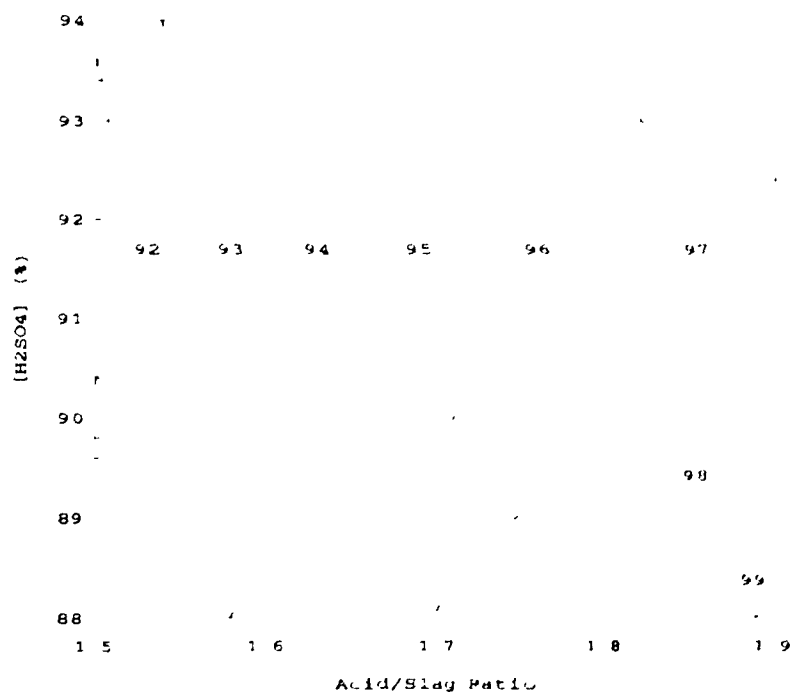


Figure 6.25 : Contour Plot of the Response Function for Yield with a Fixed Particle Size and Baking Time
Particle Size = 11 μ m, Baking Time = 5 hours

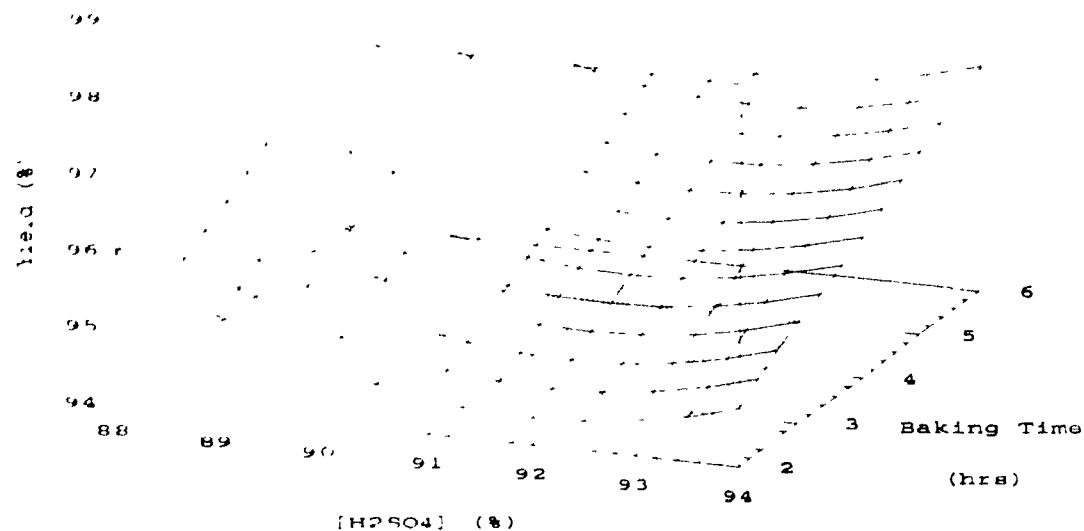


Figure 6.26 : Surface Plot of the Response Function for Yield
with a Fixed Particle Size and Acid/Slag Ratio
Particle Size = $11\ \mu\text{m}$, Acid/Slag Ratio = 1.75

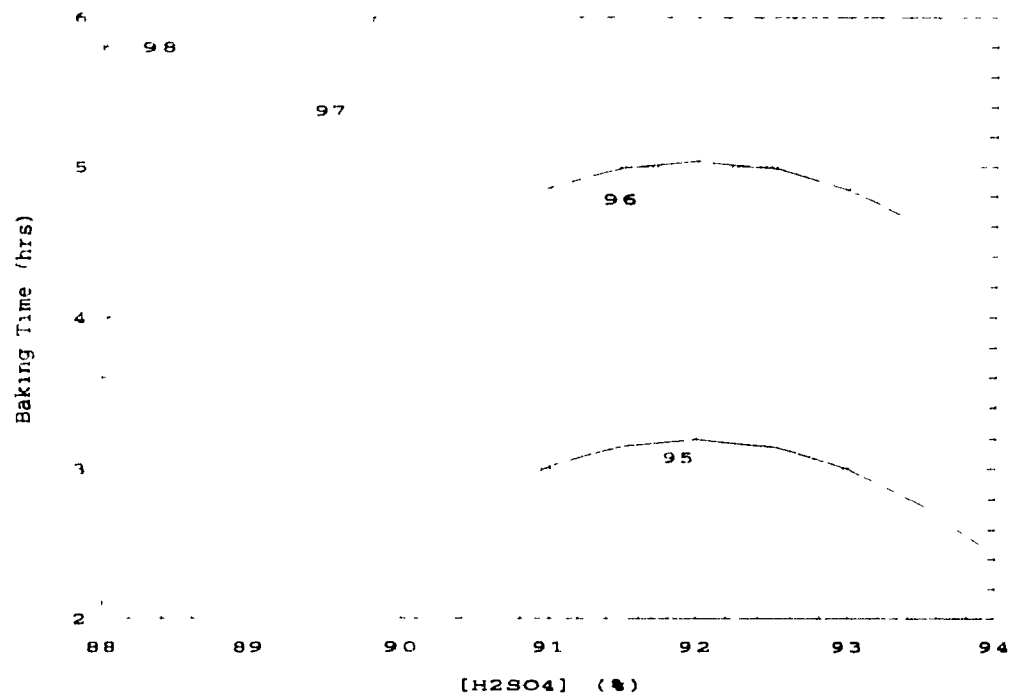


Figure 6.27 : Contour Plot of the Response Function for Yield
with a Fixed Particle Size and Acid/Slag Ratio
Particle Size = $11\ \mu\text{m}$, Acid/Slag Ratio = 1.75

6.4.2 Maximum temperature obtained

The maximum temperature obtained in the digestion reactor was recorded for the 27 experiments. Following the same procedure as for the Yield of reaction, a model equation was developed.

The information indicated that the maximum temperature obtained is influenced only by the concentration of acid. The model equation developed is:

$$Y = -164.886 + 4.055X_3 \quad (6.3)$$

where Y : Maximum Temperature (°C)
 X₃ : Acid concentration (wt %)

Figure 6.28 is a representation of this equation. The concentration of acid has a linear effect on the maximum temperature. A low sulphuric acid concentration will result in a lower temperature as a significant amount of the calories generated by the reactions are used to evaporate the excess water.

The maximum temperature is critical as it is this parameter which controls the baking temperature in commercial scale operations. If the baking temperature is not high enough the yield of the digestion reaction will not be satisfactory.

In the laboratory reactor it was possible to obtain a high yield (>97 %, see Figure 6.25) with only 88 wt%

H_2SO_4 because in the laboratory set-up, the baking was controlled by an auxiliary heating system which permitted the study of each parameter independently. In industry, however, no auxiliary heating is used but instead the process proceeds with no external assistance. Under these conditions and according to model equation 6.3 a high acid concentration is needed to ensure that the maximum temperature and resulting high yield are obtained.

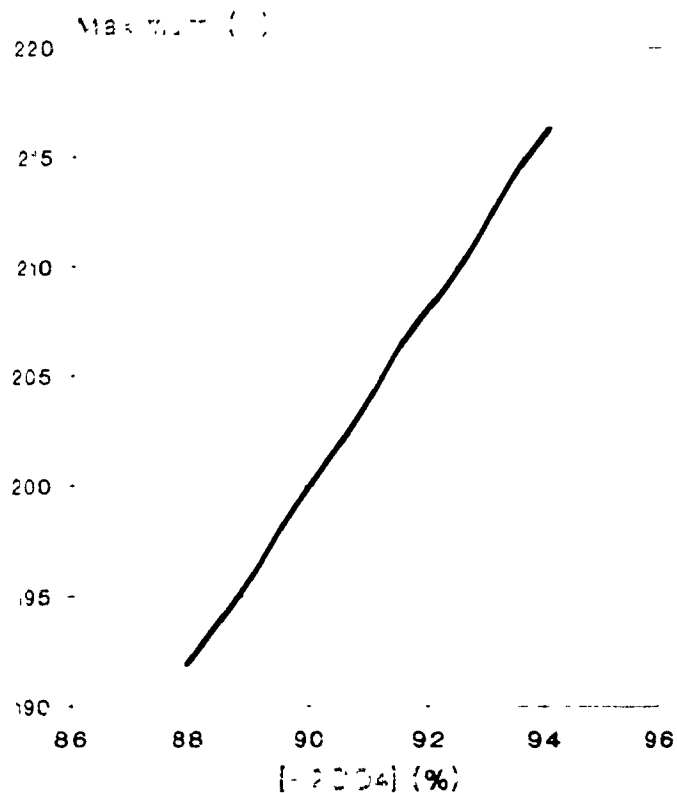


Figure 6.28 : Response Function for Maximum Temperature

To identify optimum conditions giving reasonably high yield and maximum temperature Figure 6.29 was generated. In this Figure the white area indicates where effective maximum temperatures and high yields are obtained. This area is defined by the line 93 % for yield (R1_Lo) which was selected because it is the industrially acceptable minimum value and by the 205°C line for temperature (R2_Lo) because it is high enough to obtain effective baking in commercial operations.

	Response	Units	Lo	Hi	Transform	Model
R1:	Yield	(%)	93.000	100.000		Quadratic
R2:	Maximum	(C)	205.000	250.000		Linear

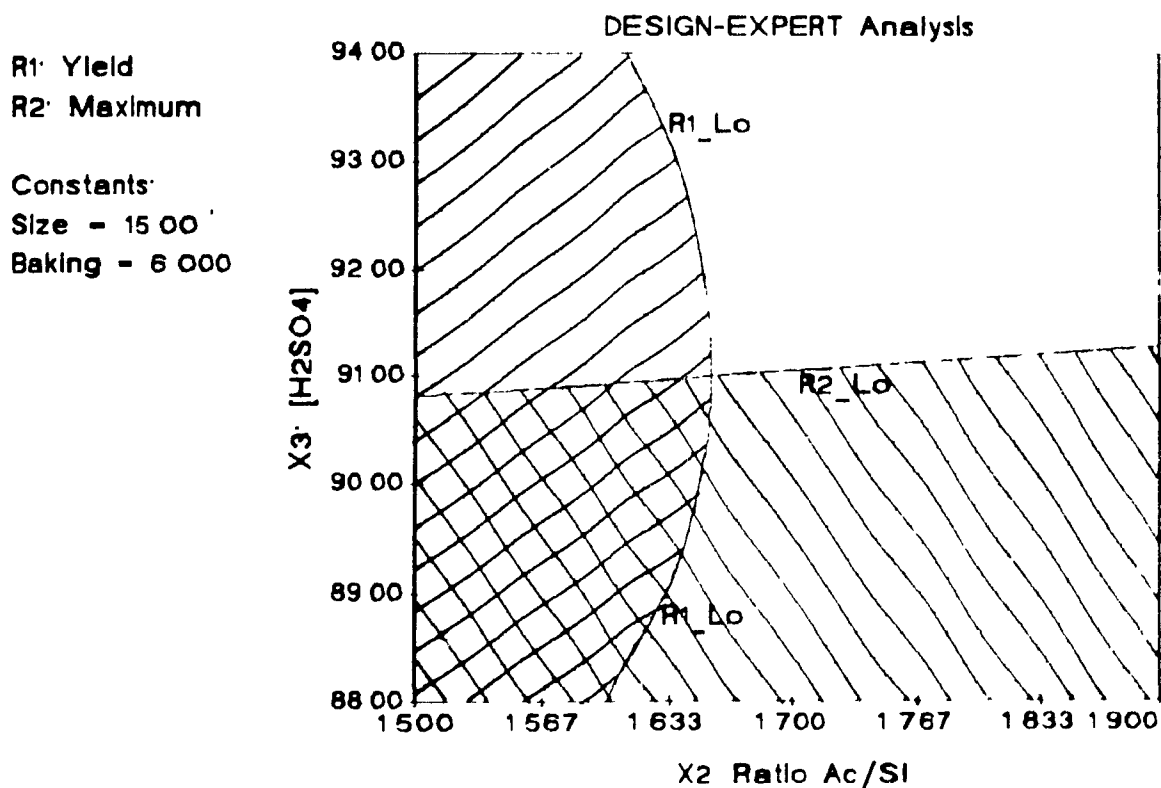


Figure 6 29 : Optimization of Yield and Maximum Temperature with a Fixed Particle Size and Baking Time

6.4.3 Set-up time

The set-up time is the time (in minutes) elapsed between the addition of water to the reactor, at 90°C, and the solidification of the reacting mass. A model equation was developed with set-up time as the response function following the same method as that used for the digestion yield.

$$Y = 4744.16 + 14.6428X_2 - 101.977X_3 + 0.547849X_3^2 \quad (6.4)$$

where Y : Set-up time (minutes)
 X₂ : Acid/Slag weight ratio
 X₃ : Acid concentration (wt %)

According to equation 6.4, the set-up time is affected by two of the four parameters studied: the concentration of the acid and the acid/slag ratio. Figures 6.30 and 6.31 combine the effects of those two variables on the set-up time. A low acid concentration and a high acid/slag ratio delay the set-up. The amounts of water and steam added to dilute the excess sulphuric acid slowdown the solidification process (set-up).

The time at which the set-up of the cake happens affects the safety of the operation and the porosity of the cake. A premature solidification of the slurry before the maximum temperature is reached is dangerous because large quantities of fumes generated at the maximum temperature can be trapped in a non-porous solid, resulting in a high pressure and the possibility of an explosion.

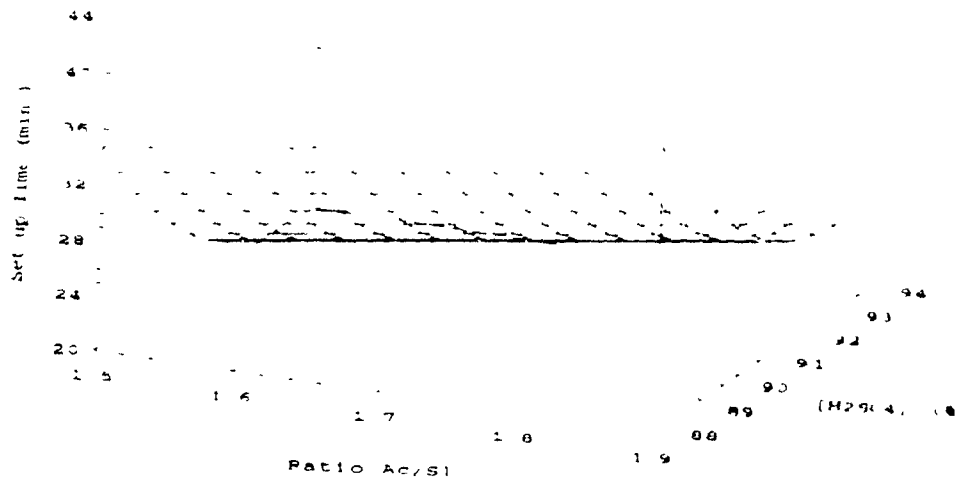


Figure 6.30 : Surface Plot of the Response Function for Set-up Time

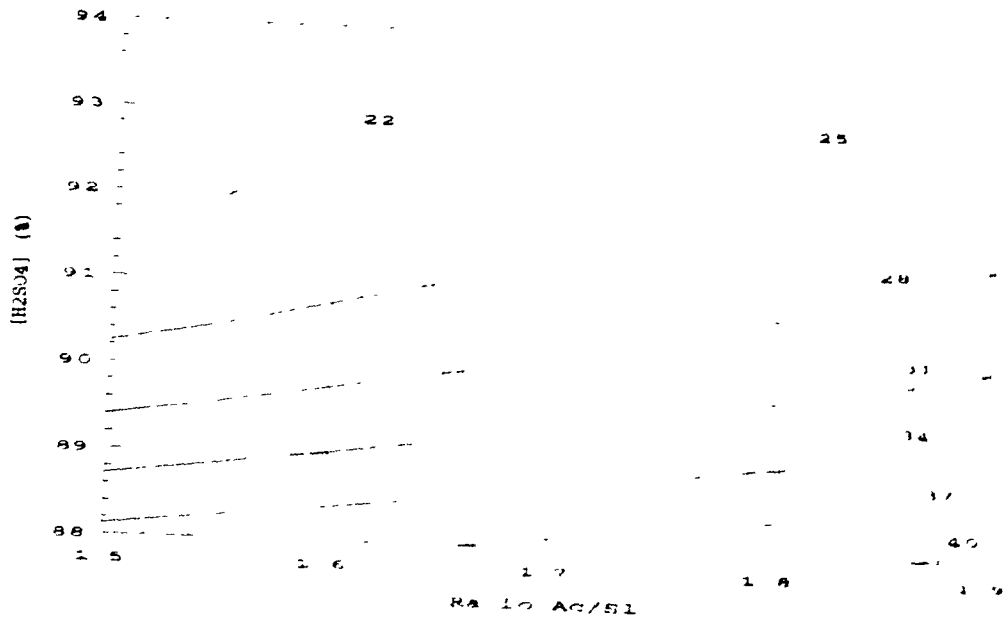


Figure 6.31 : Contour Plot of the Response Function for Set-up Time

On the other hand, when set-up occurs after the maximum temperature has been attained, the maximum amount of fume emission occurs when the slurry is viscous which results in a smoother gas evolution and a uniformly porous cake which is much easier to dissolve.

The present model was developed so that set-up always occurred after the maximum temperature.

6.4.4 Black liquor active acid / titanium ratio

The term "Active Acid" (67) means the total quantity of free acid in the reaction solution plus the acid combined with titanium in the reaction solution. This value divided by the titanium content of the black liquor gives the AAc/Ti ratio, a value which is used in the industry to characterize the liquor for the next step of the process, the hydrolysis.

Following the same technique used for the digestion yield, a model equation was developed.

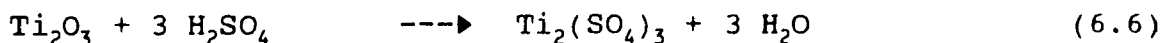
$$Y = 0.0410955 + 1.05773X_2 - 0.0305596X_4 \quad (6.5)$$

where	Y	: Active Acid (g/l)/ TiO ₂ (g/l)
	X ₂	: Acid/Slag weight ratio
	X ₄	: Baking Time (hrs)

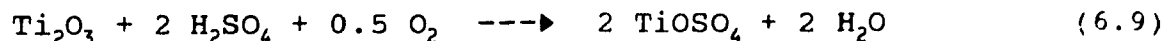
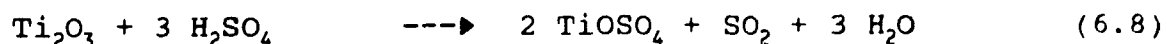
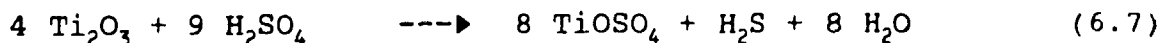
The Active Acid/Titanium ratio is linearly influenced by the acid/slag ratio and the baking time, the former having the strongest effect. Figures 6.32 and 6.33 show that a higher acid/slag ratio results in a higher active acid/Titanium ratio. This is expected as the excess acid used in the mixture ends up in the active acid. The AAc/Ti is inversely proportional to the baking time which is most probably due to the increase of TiO_2 in solution (g/l) with longer baking times (higher yields) and the higher acid losses in the exit gases, (longer baking times generate more gas).

6.4.5 Oxidation of Ti_2O_3 during digestion

Titanium (III) present in the slag reacts with sulphuric acid following different reaction paths. Some of the Ti_2O_3 reacts with sulphuric acid to produce titanous sulphate:



In addition, dititanium trioxide can be oxidized according to the following reactions:



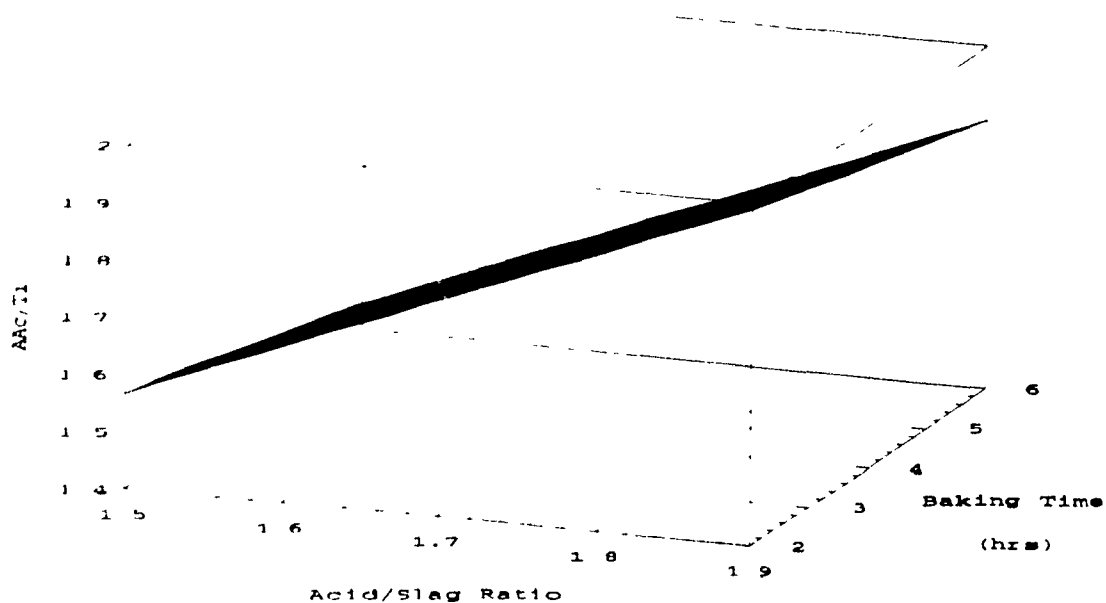


Figure 6.32 : Surface Plot of the Response Function for Active Acid / Titanium Ratio

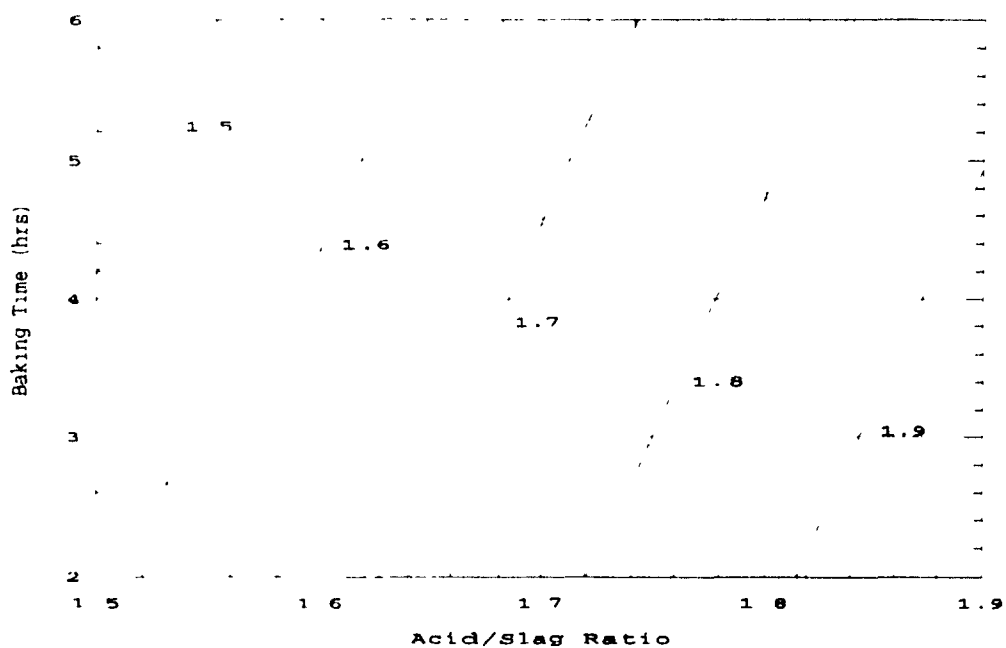


Figure 6.33 : Contour Plot of the Response Function for Active Acid / Titanium Ratio

To evaluate in which proportion these reactions occur, the solids before and after digestion were analyzed for titanium (III) and the exit gas was analyzed for H_2S and SO_2 .

Based on the overall data collected from the 27 experiments, Table 6.10, the average oxidation of Ti_2O_3 was found to be 65 %. This overall percent oxidation is produced by the action of sulphuric acid and by the air used for agitation. According to F*A*C*T air oxidation is more favourable than the corresponding H_2SO_4 oxidation. On the basis of this information and the gas analysis data the yield of each oxidation reaction was estimated: 17.9 % of the Ti_2O_3 was oxidized by sulphuric acid, (8% through reaction 6.7, 9.9 % through reaction 6.8) and 47.1 % by air.

Following the same procedure used for the digestion yield, a model equation for oxidation was developed:

$$Y = 4219.99 - 4.69023X_1 - 89.1841X_3 + 3.87613X_4 - 0.248308X_1X_2 + 0.110818X_1^2 + 0.482603X_3^2 \quad (6.10)$$

where	Y	: Ti_2O_3 Oxidation (%)
	X_1	: Particle size (micron)
	X_2	: Acid/Slag weight ratio
	X_3	: Acid concentration (wt%)
	X_4	: Baking time (hrs)

Table 6.10 : Percentage of the Ti_2O_3 Reacting in Each of the Four Possible Reactions and Total Oxidation Measured in Each Experiment.

RUN	SLAG (Ti_2O_3 g)	REACTION 1 (%)	REACTION 2 (%)	REACTION 3 (%)	REACTION 4 (%)	OXIDATION (%)
1	192	37.7	7.6	9.1	45.6	62.3
2	185	31.4	9.5	4.3	54.8	68.6
3	212	42.6	11.3	7.2	39.0	57.4
4	185	20.2	8.6	14.3	56.9	79.8
5	212	47.8	10.3	6.7	35.3	52.2
6	192	32.6	6.7	10.8	49.9	67.4
7	192	45.2	5.7	9.0	40.1	54.8
8	192	31.2	14.3	9.9	44.6	68.8
9	192	32.0	12.7	13.2	42.2	68.0
10	185	35.0	4.4	12.8	47.8	65.0
11	212	49.7	5.1	3.6	41.7	50.3
12	185	16.5	5.9	14.2	63.4	83.5
13	212	31.8	12.3	6.9	49.0	68.2
14	192	35.4	4.0	9.1	51.4	64.6
15	192	31.5	7.2	6.4	54.9	68.5
16	192	28.2	11.6	10.8	49.4	71.8
17	192	38.8	4.5	8.0	48.7	61.2
18	192	37.5	9.5	15.7	37.4	62.5
19	185	20.3	7.9	14.8	57.0	79.7
20	212	34.9	14.4	10.4	40.3	65.1
21	185	28.1	3.0	15.9	53.0	71.9
22	212	41.2	6.0	9.1	43.6	58.8
23	192	42.9	10.7	8.8	37.6	57.1
24	192	56.0	3.6	7.1	33.3	44.0
25	192	28.6	7.0	5.6	58.8	71.4
26	192	30.6	3.4	11.0	55.1	69.4
27	192	38.4	7.5	12.6	41.6	61.6
AVR	195	35.0	8.0	9.9	47.1	65.0

REACTION 1 $Ti_2O_3 + 3 H_2SO_4 \rightarrow Ti_2(SO_4)_3 + 3 H_2O$

REACTION 2 $4 Ti_2O_3 + 9 H_2SO_4 \rightarrow 8 TiOSO_4 + H_2S + 8 H_2O$

REACTION 3 $Ti_2O_3 + 3 H_2SO_4 \rightarrow 2 TiOSO_4 + SO_2 + 3 H_2O$

REACTION 4 $Ti_2O_3 + 2 H_2SO_4 + 0.5 O_2 \rightarrow 2 TiOSO_4 + 2 H_2O$

All the parameters studied were found to influence the oxidation of Ti_2O_3 , but it was the particle size of the slag and the baking time which had the strongest effect. Figures 6.34 and 6.35 show the percentage of oxidation as a function of two basic parameters slag particle size and baking time. The finer the slag the greater the oxidation as a larger surface area is exposed to acid and air. Longer baking times increase the oxidation as the cake is in contact with air for a longer time.

It is interesting to note that oxidation was slightly better by using the low acid concentration (Figures 6.35 and 6.37). Up to 85 % oxidation was obtained with 88 % acid as opposed to 78 % with 94 % acid (Figure 6.37). This result apparently is due more to the production of a more porous cake (producing a high surface area) with low acid concentration due to water evaporation and less to the air versus acid attack of Ti_2O_3 . In other words the better oxidation at 88 % acid are attributed to the increased surface area which is similar to the particle size effect. This is supported by the results of Figures 6.38 and 6.39.

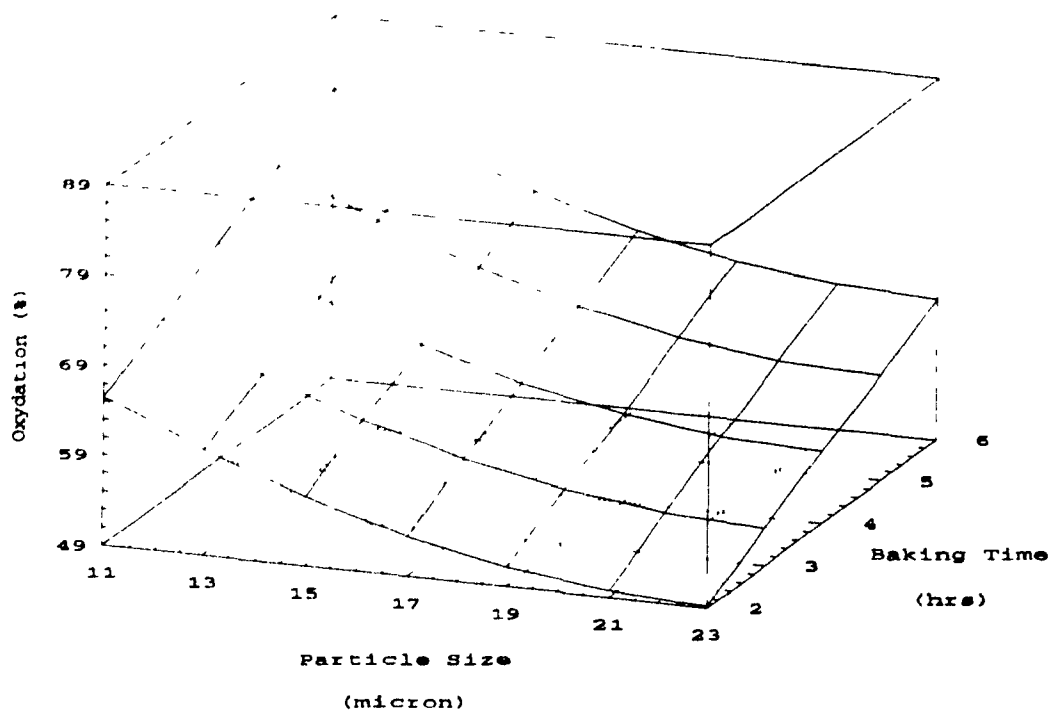


Figure 6.34 : Surface Plot of the Response Function for Oxidation with a Fixed Ratio and Concentration
Acid/Slag Ratio = 1.75, $[H_2SO_4]$ = 91 %

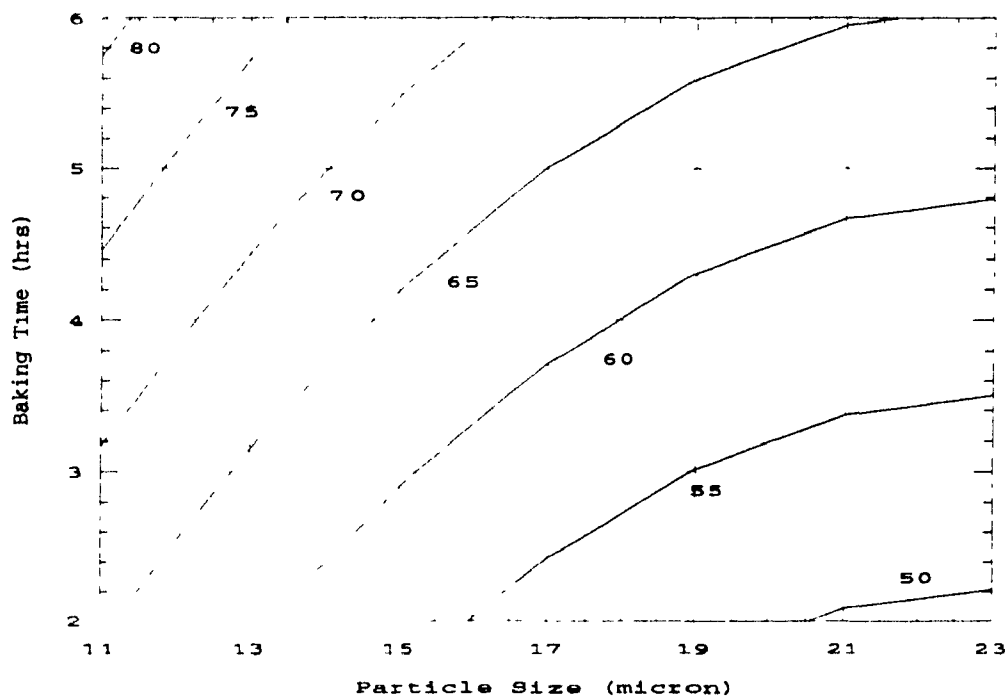


Figure 6.35 : Contour Plot of the Response Function for Oxidation with a Fixed Ratio and Concentration
Acid/Slag Ratio = 1.75, $[H_2SO_4]$ = 91 %

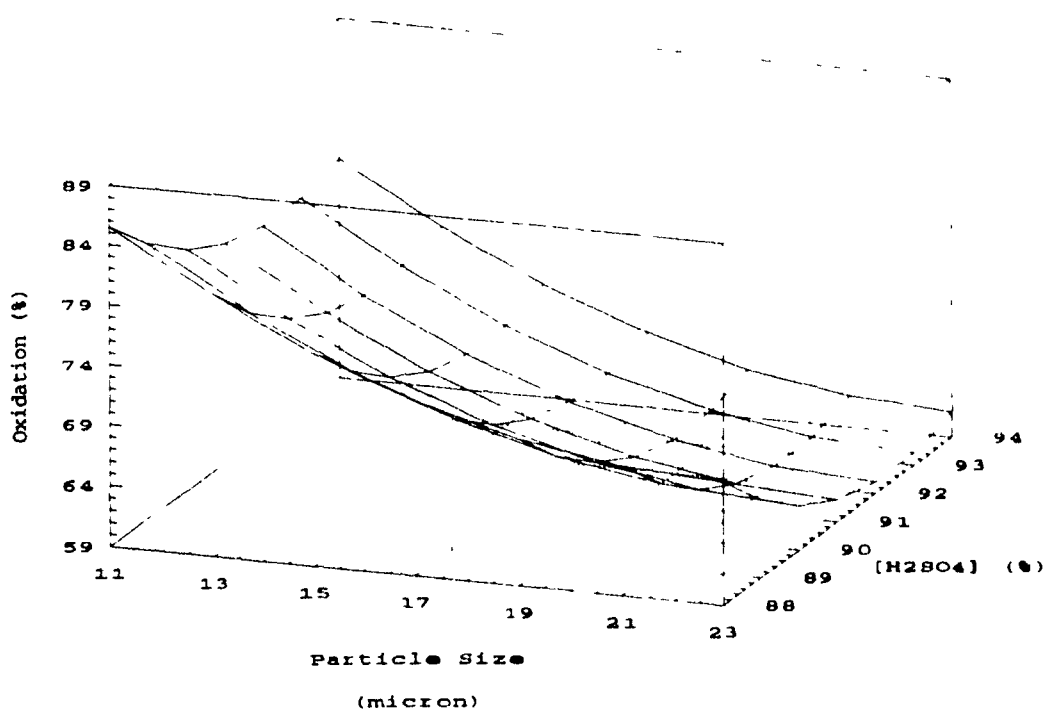


Figure 6.36 : Surface Plot of the Response Function for Oxidation with a Fixed Ratio and Baking Time
Acid/Slag Ratio = 1.75, Baking Time = 5 hours

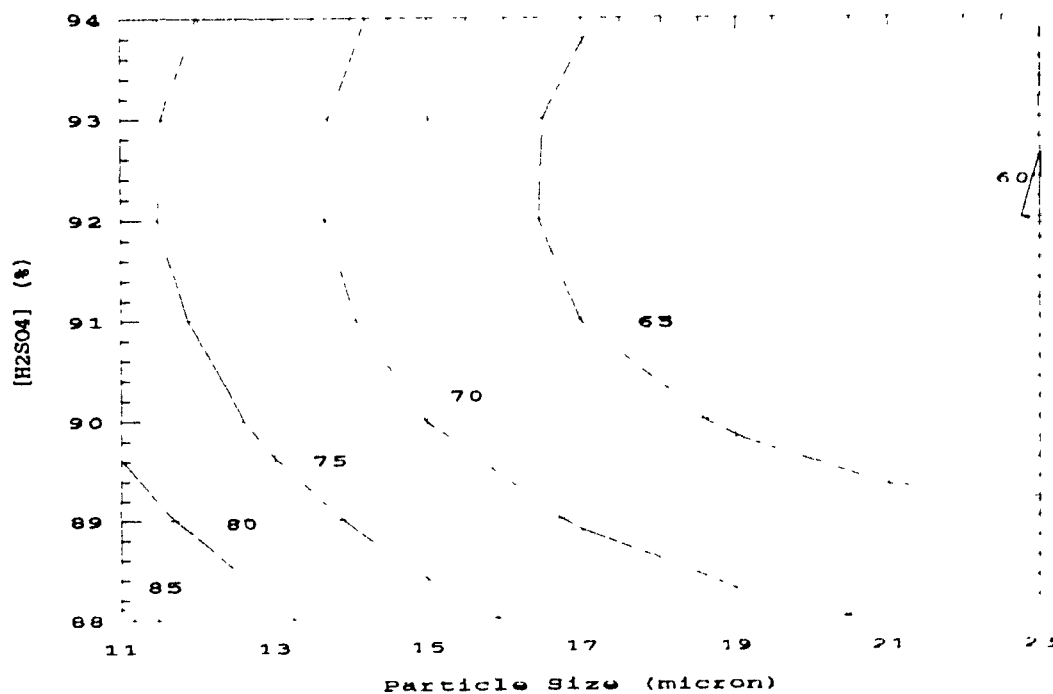


Figure 6.37 : Contour Plot of the Response Function for Oxidation with a Fixed Ratio and Baking Time
Acid/Slag Ratio = 1.75, Baking Time = 5 hours

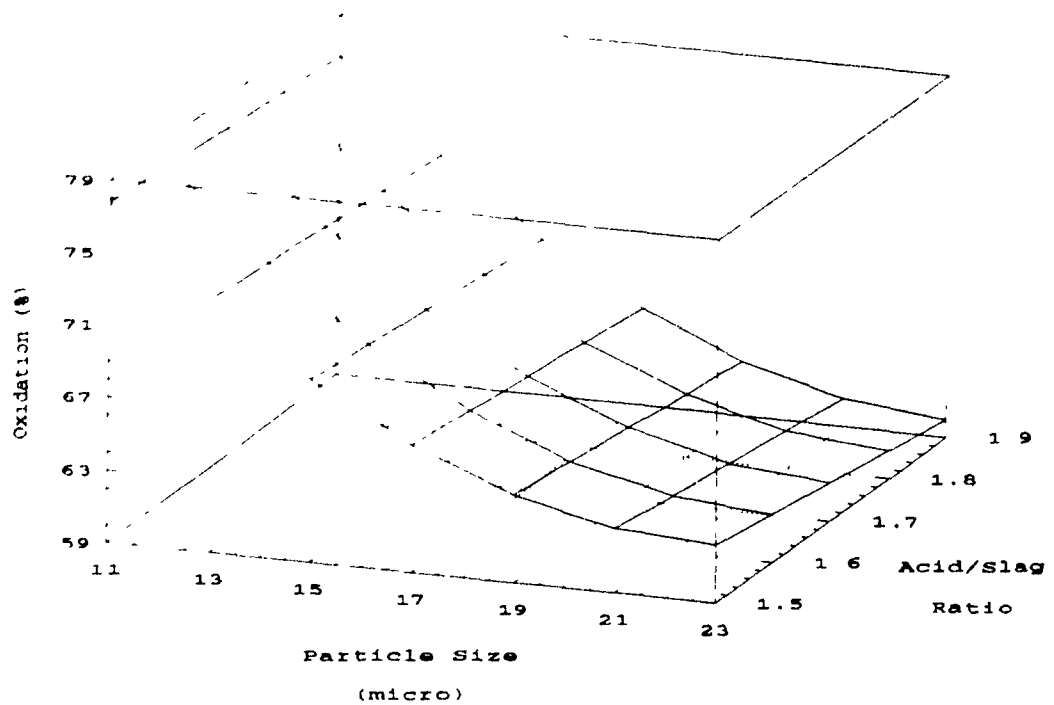


Figure 6.38 : Surface Plot of the Response Function for Oxidation with a Fixed Concentration and Baking $[H_2SO_4] = 91 \%$, Baking Time = 5 hours

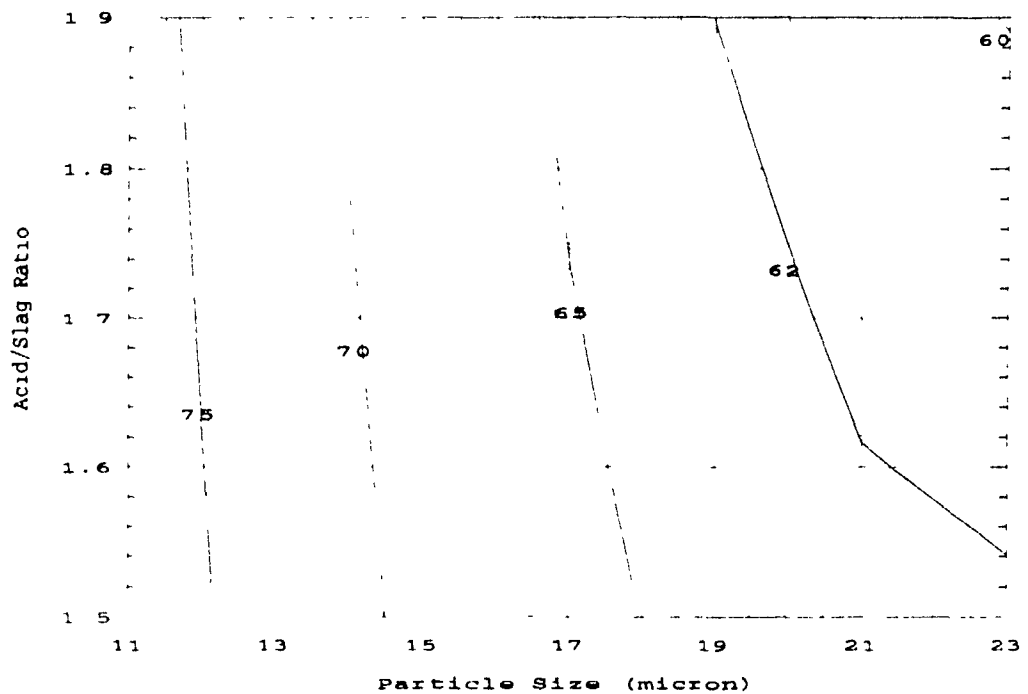
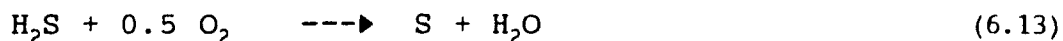
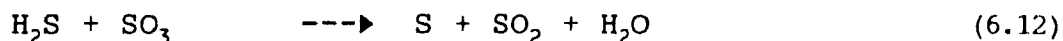
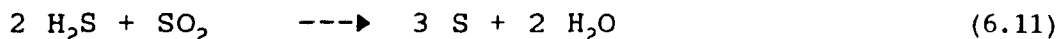


Figure 6.39 : Contour Plot of the Response Function for Oxidation with a Fixed Concentration and Baking $[H_2SO_4] = 91 \%$, Baking Time = 5 hours

Other tests done with the digester proved that titanium (III) can be completely converted to titanium (IV) by continuously supplying air throughout the whole baking period. This technique is described in two patents (38,39).

6.4.6 Sulphuric acid - equivalent losses in the exit gas

Elemental sulphur was detected in the gas collecting system in all tests. The sulphur was most probably produced from H_2S by a secondary reaction. Programs Equilibrium and Reaction in F*A*C*T were used to evaluate some possible reactions:



All these reactions are possible, but at equilibrium, when SO_2 , SO_3 , H_2S and O_2 are present, as in our gas, SO_2 , H_2O and S are the main constituents, which suggest that reaction 6.12 dominates.

The amount of sulphur, H_2S , SO_2 , and SO_3 collected during each of the 27 experiments was converted into the sulphuric acid equivalent (Table 6.11). Following the same procedure used for the digestion yield, a model equation was developed for this H_2SO_4 - equivalent losses.

Table 6.11 : Analysis of the Digestion Fumes

RUN	SULPHUR (g)	H ₂ S (g)	SO ₂ (g)	SO ₃ (g)		H ₂ SO ₄ eq. (g)
1	0.52	0.31	8.78	9.42		27.5
2	0.53	0.47	4.63	19.52		34.0
3	0.79	0.57	8.34	13.99		34.0
4	0.43	0.49	12.59	19.84		46.3
5	0.69	0.56	7.66	16.16		35.2
6	0.39	0.35	9.96	13.58		34.1
7	0.45	0.17	8.59	8.84		25.8
8	0.83	0.74	10.12	15.33		39.0
9	0.57	0.83	12.39	16.61		43.5
10	0.25	0.22	11.05	14.42		36.0
11	0.47	0.13	4.31	7.55		17.7
12	0.27	0.36	12.22	11.76		35.0
13	0.86	0.63	8.25	13.97		34.2
14	0.26	0.18	8.30	22.11		41.1
15	0.51	0.27	6.46	10.41		25.0
16	0.62	0.66	10.43	16.59		40.1
17	0.34	0.15	7.51	11.41		27.0
18	0.31	0.74	13.98	17.14		45.5
19	0.58	0.25	13.32	18.58		45.6
20	0.85	0.91	11.48	17.93		44.7
21	0.25	0.07	13.57	18.11		43.9
22	0.47	0.26	9.56	14.56		34.7
23	0.40	0.78	8.35	11.37		30.2
24	0.39		6.85	9.91		23.8
25	0.53	0.23	5.88	27.37		44.8
26	0.29	0.07	9.95	13.54		32.9
27	0.45	0.37	11.63	13.97		37.4
Av	0.5	0.4	9.5	15.0		35.5

$$Y = 25.3745 + 2.50772X_4 \quad (6.14)$$

where Y : H_2SO_4 - equivalent (g)
 X_4 : Baking time (hrs)

The sulphuric acid loss in the gas was found to be a function of the baking time only. The other parameters were not significant. Figure 6.40 shows the amount of H_2SO_4 lost for different baking times. The acid loss in the gas was determined at the end of the baking period; longer baking periods time allow the gas to be released thus resulting in higher acid equivalent losses.

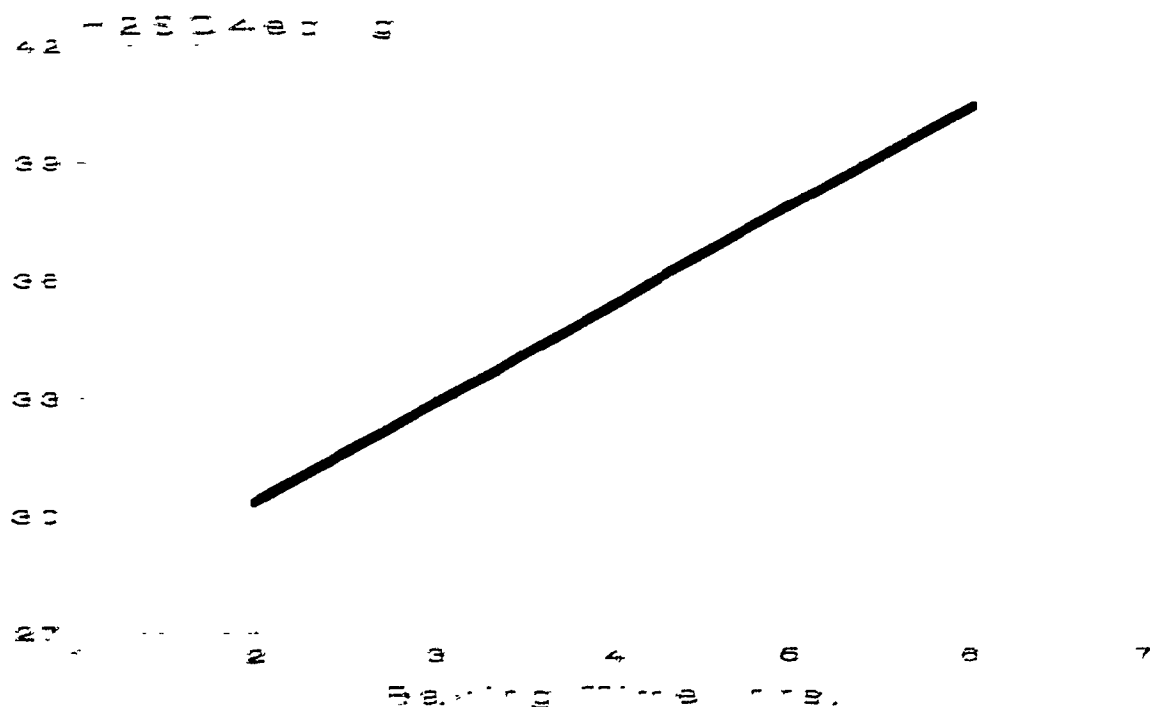


Figure 6.40 : Response Function for H_2SO_4 Equivalent

6.4.7 Digestion cake height

The higher the porosity of the cake the higher the cake height will be. Following the same procedure used with the other responses, a model equation of the cake height was developed.

$$Y = 6.01512 + 0.294346X_1 + 0.133504X_3 - 0.0161007X_1^2 \quad (6.15)$$

where Y : Cake height (cm)
 X₁ : Particle size (micron)
 X₃ : Acid concentration (wt%)

The cake height was found to be significantly affected by the particle size and the acid concentration only. Figures 6.41 and 6.42 show the combined effect of these two parameters.

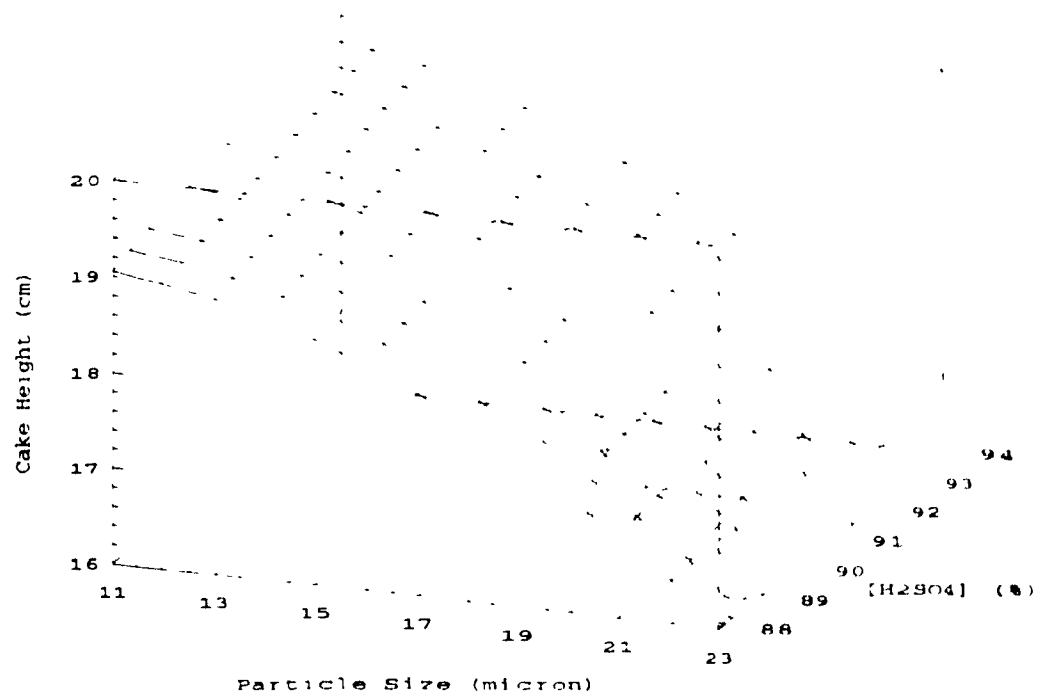


Figure 6.41 : Surface Plot of the Response Function for Cake Height

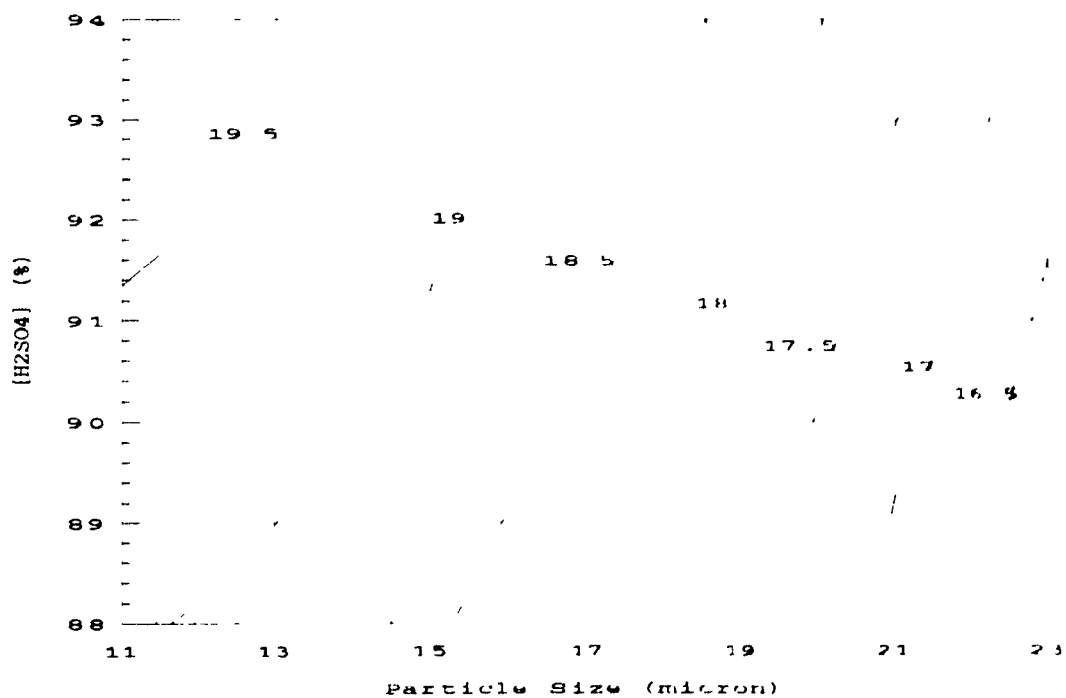


Figure 6.42 : Contour Plot of the Response Function for Cake Height

6.5 Special Conditions and Recommendations

In North America and specially in Quebec, commercial sulphuric acid is delivered with a 93 % concentration, consequently, two extra tests were done using this lower concentration. During these tests set-up occurred before the attainment of the maximum temperature (all the other conditions were similar to those used in a test where the set-up occurred after the maximum). The preliminary results, suggest that when starting with a 96% or higher acid concentration and diluting with water and steam to reach the concentration wanted, there is no set-up problem. However, when started with an initial acid concentration of 93% or less, less water is used to reach the concentration wanted and set-up apparently occurs prematurely. However, more research on the use of low acid concentration should be done as it might open the possibility of using recycled (at low concentration) acid from the downstream hydrolysis step which at the worst has to be disposed of.

Finally, during the tests, it was demonstrated that it is important to introduce the slag slowly into the acid to insure proper wetting of the slag. The ore is so fine that if it is not properly mixed during the reactor loading stage, it will be impossible to achieve complete wetting just with the agitation provided by the air, because slag will form partially wet clots sinking to the bottom or sticking to the walls of the reactor.

CHAPTER 7

CONCLUSIONS AND FUTURE WORK

7.1 Conclusions

A laboratory reactor built to simulate the operation of an industrial slag digestion reactor was successfully tested.

Box-Behnken experimental design was used to plan the digestion tests. The experimental data were subjected to a mass balance evaluation and were considered to be satisfactory. Heat balance calculations were also performed to obtain qualitative information. Finally, using regression analysis, model equations were developed correlating the several responses to the four experimental variables (particle size, acid/slag weight ratio, acid concentration and baking time). The model equations developed are listed below:

The model equation for digestion yield

$$Y = 848.44 + 1.29181X_1 + 89.3782X_2 - 18.6131X_3 + 0.542654X_4 \\ - 0.0433248X_1^2 - 22.0547X_2^2 + 0.101186X_3^2 \quad (7.1)$$

where	Y	: Yield of reaction (%)
	X ₁	: Particle size (micron)
	X ₂	: Acid/Slag weight ratio
	X ₃	: Acid concentration (wt %)
	X ₄	: Baking time (hours)

By order of importance, it is the sulphuric acid/slag weight ratio, the baking time, the particle size of the slag and the concentration of the acid which have the most significant effect on the yield. The highest yields were obtained when acid/slag weight ratio and baking time were at the highest levels. Medium particle size gave best results, while acid concentration had only a modest effect. The model equation was successfully tested.

The model equation for Maximum Temperature

$$Y = -164.886 + 4.055X_3 \quad (7.2)$$

where Y : Maximum Temperature (°C)
 X₃ : Acid concentration (%)

The maximum temperature is influenced only by the concentration of acid. A low sulphuric acid concentration will give a lower maximum temperature.

The model equation for set-up time

$$Y = 4744.16 + 14.6428X_2 - 101.977X_3 + 0.547849X_3^2 \quad (7.3)$$

Y : Set-up time (minute)
 X₂ : Acid/Slag ratio
 X₃ : Acid concentration (%)

Set-up is affected by two of the four parameters studied: the concentration of the acid and the acid/slag ratio. A low acid

concentration and a high acid/slag ratio delay set-up. The amounts of water and steam added to dilute the excess sulphuric acid lengthened the set-up time.

The model equation for the oxidation of Ti_2O_3

$$Y = 4219.99 - 4.69023X_1 - 89.1841X_3 + 3.87613X_4 \\ - 0.248308X_1X_2 + 0.110818X_1^2 + 0.482603X_3^2 \quad (7.4)$$

Y : Ti_2O_3 Oxidation (%)
X₁ : Particle size (micron)
X₂ : Acid/Slag ratio
X₃ : Acid concentration (%)
X₄ : Baking time (hours)

All the parameters studied influence the Ti_2O_3 oxidation but it was the particle size of the slag and the baking time which had the strongest effect. The finer the slag the higher the oxidation as a larger surface area is exposed to acid and air. Longer baking times increase the oxidation in that the cake is in contact with air for a longer period of time.

Model equations for black liquor active acid/titanium ratio, Sulphuric acid - equivalent losses in the exit gas and digestion cake height were also developed and successfully tested.

Microstructure examination of the slag prior to and after

digestion showed the main phase of the slag to be a pseudobrookite phase containing mainly titaniferous oxide with several other oxides. EDS spectra of the reacted samples revealed the presence of both TiOSO_4 and $\text{Ti}(\text{SO}_4)_2$ with these compounds present in the form of aggregates. Some insoluble rutile (TiO_2) and silicates were also detected.

Thermodynamic analysis of the reactions involved in the digestion of Sorelslag with sulphuric acid yielded the following information:

- a) Entropy, heat capacities and heat of formation of TiOSO_4 , $\text{Ti}(\text{SO}_4)_2$ and $\text{Ti}_2(\text{SO}_4)_3$, estimated for the first time, were found to be:

	Entropy $\text{J}/^\circ\text{C}$	Heat capacities $\text{J}/\text{gmol}^\circ\text{C}$	Heat of formation kJ/mole
TiOSO_4 :	95.5	112.5	1637
$\text{Ti}(\text{SO}_4)_2$:	141.5	169.4	2181
$\text{Ti}_2(\text{SO}_4)_3$:	254.1	272.3	3387

- b) All reactions are exothermic with the oxidation of $\text{Ti}(\text{III})$ to $\text{Ti}(\text{IV})$ being the most exothermic.
- c) Simple TiO_2 converts first to TiOSO_4 and does not convert to $\text{Ti}(\text{SO}_4)_2$ even with double the stoichiometric amount of H_2SO_4 . However, when all the constituents of the slag are present then $\text{Ti}(\text{SO}_4)_2$ appears to form.
- d) $\text{Ti}(\text{III})$ thermodynamically is oxidized completely to $\text{Ti}(\text{IV})$ by H_2SO_4 or air.

7.2 Further investigations

The possibility of using the recycled low concentration acid from the downstream hydrolysis step needs to be studied. With environment laws being more and more restrictive the recirculation of the waste acid is an attractive solution.

A detailed thermic balance of the digestion process with the objective of describing the time/temperature profile of the digestion cake would permit an improved simulation of the baking conditions of large scale operations and would be a complement to the present work.

REFERENCES

1. W.M. Peirce, R.K. Waring, and L.D. Fetterolf, Titaniferous Material for Producing Titanium Dioxide, U.S. Patent, No. 2,476,453, July 19, 1949.
2. M. Bergeron, A Mineralogical Study of the Hemo-Ilmenite Ore from Lac Tio, Quebec, QIT-Fer et Titane Inc., Intercompany Communication, 1973.
3. C.S. Hurlbut, Dana's Manual of Mineralogy, Seventeenth Edition, John Wiley & Sons Inc., New York, 1959, pp 295-296.
4. QIT-Fer et Titane Inc., Brochure 1991, Montreal, Canada.
5. H.Y. Lee, J.M. Noy and P. Tarassoff, Beneficiation of Allard Lake Ilmenite, Krivsky 14, pp. 197-209.
6. F. Houle, Condensé sur l'Entreposage et l'Enrichissement, QIT-Fer et Titane Inc., Intercompany Communication, 1987.
7. Quebec Iron and Titanium Corporation, A Study in Growth, Canadian Mining Journal, 1964, Volume 85, Number 11, pp 3-9.
8. R.S. Miller and G.G. Hatch, Smelting of Ilmenite, Canadian Patent, No. 564,642, October 14, 1958.
9. P.J. Ensio, Smelting of Titaniferous Ores, U.S. Patent, No. 2,853,375, September 23, 1958.
10. R. Guimond, Titanium and QIT, Mining in Canada, November, 1964, Volume 37, No. 11, pp 11-16, 19-21.
11. A.W. Knoeri, World's Major Titanium Mine and Smelter Swing into Full-Scale Production, Engineering and Mining Journal, 1959, Vol 153, No. 3, pp 72-79.
12. A. Grau and D. Poggi, Physico-Chemical Properties of Molten Titania Slags, The Metallurgical Society of CIM, 1978, Annual Volume, pp 97-102.
13. G.G. Hatch and P.J. Ensio, Smelting of Ilmenite, Canadian Patent, No. 579,641, July 14, 1959.
14. R.S. McLaren, Production of Acid-Soluble Titania Slags, U.S. Patent, No. 2,537,229, January 9, 1951.

15. J.D. Stephens, Microscopy Characterization of Sorelslag, QIT-Fer et Titane Inc, Intercompany Communication, 1989.
16. S.A. Forman, A.T. Prince, and N.F.H. Bright, The Separation and Identification of the Titaniferous and Siliceous Constituents of Slag From The Quebec Iron and Titanium Corporation, Intercompany Communication, 1954.
17. R.G. Teller, M.R. Antonio, A.E. Grau, M. Guéguin, and E. Kostiner, The Chemistry of Thermal Decomposition of Pseudobrookite Ferrous Titanium Oxides, Journal of Solid State Chemistry, 1990, **88**, pp 351-367.
18. R.G. Teller, M.R. Antonio, A.E. Grau, M. Guéguin, and E. Kostiner, Structural Analysis of Metastable Pseudobrookite Ferrous Titanium Oxides with Neutron Diffraction and Mossbauer Spectroscopy, Journal of Solid State Chemistry, 1990, **88**, pp 334-350.
19. G. Handfield, and G.G. Charette, Viscosity and Structure of Industrial High TiO_2 Slags, Canadian Metallurgical Quarterly, 1971, Volume 10, Number 3, pp 235-243.
20. G. Handfield, Physico-Chemical Properties of High-Titania Slags, Quebec Iron and Titanium Corporation, Intercompany Communication, 1968.
21. M. Guéguin and A. Grau, Upgrading of Titania Slags by Fluidized-bed Selective Chlorination, Extraction Metallurgy '89, The Institution of Mining and Metallurgy, 1989, pp 899-922.
22. E. Schmoll, Recovering Waste Sulphuric Acid from Titanium Dioxide Plants, Escher Wyss News, 2/1978-1/1979, pp 17-20.
23. J.A. Miller, Titanium, A Materials Survey, U.S. Bureau of Mines Circular no. 7791, 1957, pp 82.
24. S.P. Todd, M.L. Meyers, and W.J. Cauwenberg, Production of Titanium Dioxide Pigment from High Titanium Dioxide Content Slags, U.S. Patent, No. 2,531,926, Nov. 28, 1950.
25. T.P. Forbath, TiO_2 Process Taps Sorel Slag for Savings, Chemical Engineering, 1958, Volume 65, No. 2, pp 98-101.
26. W.H. Coates, The Manufacture of Titanium Pigments, Meeting of the Chemical Engineering Group, Soc. Chem. Ind., February 7, 1950, pp 13-25.

27. W.J. O'Brien, Titanium Pigment Industry, Chemical Engineering Progress, 1948, Volume 44, No. 11, pp 809-814.
28. K.W. Heywood, C.R. Trampier and W. Groves, Preparation of Anatase Titanium Dioxide Pigment, U.S. Patent, No. 3,617,217, November 2, 1971.
29. J.J. Libera, E.J. Puetz and Lemay, Preparation of Anatase Titanium Dioxide Pigment, U.S. Patent, No. 3,615,204, October 26, 1971.
30. W. Mecklenburg, Production of Titanium Dioxide, U.S. Patent, No. 1,758,528, May 13, 1930.
31. P. Pascal, Nouveau Traité de Chimie Minérale, Masson et Cie, Paris, 1963, Tome IX, pp 1-210.
32. J. Barksdale, Titanium, The Ronald Press Company, Second Edition, New York, 1966, pp 213-323.
33. B. Jarish, Titanium Dioxide Pigment Processing and Sulphate Pigment Studies, Quebec Iron and Titanium Corporation, Intercompany Communication, 1971.
34. R.W. McKinney, Preparation of Hydrolyzable Titanium Sulphate Solutions, U.S. Patent, No. 2,631,924, March 17, 1953.
35. D.P. Doll, W. Groves and T.S. Griffin, Process for the Sulphuric Acid Digestion of Titaniferous Iron Material, U.S. Patent, No. 3,053,625, September 11, 1962.
36. I. Slama, Decomposition of High-Grade Titanium Slag by Means of Sulphuric Acid, Chemicky Prumysl, 1960, 10(35), No. 7, pp 337-340.
37. R.M. McKinney, and G.S. Reeder Jr., Process for Sulfating Titaniferous Material, U.S. Patent, No. 2,953,434, Sept. 20, 1960.
38. J.H. Weikel, Production of Titanium Dioxide, U.S. Patent, No. 2,589,909, Mar. 18, 1952.
39. J.H. Weikel, Improvements in Production of Titanium Dioxide, U.S. Patent, No. 671,728, Jun 24, 1952.
40. M. Gueguin, Method to Oxidize Ti^{+3} During the Sulphuric Acid Digestion of Titaniferous Slags, U.S. Patent, No. 4,325,920, Apr. 20, 1982.
41. P. Farup, U.S. Patent, No. 1,919,425, July 25, 1933.

42. W.F. Washburn, Recovery of Titanium Compounds, U.S. Patent, No. 1,889,027, Nov. 29, 1933.
43. M.L. Borodina, T.A. Velikoslavinskaja, and B.A. Davidovskaya, Advantages in Using High Concentration Titanium Slags Instead of Ilmenite for the Production of Titanium Dioxide by the Sulphuric Acid Method, Titan i ego Splary, U.S.S.R., 1959, Volume II, pp 73-77.
44. F.Y. Irkov, and V.A. Reznichenko, Production of Titanium Dioxide by Processing Slags Obtained From Smelting Titanium-Magnetite Agglomerates, Titan i ego Splavy, U.S.S.R., 1962, Volume 8, pp 119-123.
45. G.E.P. Box, W.G. Hunter and J.S. Hunter, Statistics for Experimenters: An Introduction to Design, Data Analysis, and Model Building, John Wiley and Sons Inc., New York, 1978, pp 294, pp 510-535.
46. G.E.P. Box and N.R. Draper, Empirical Model-Building and Response Surfaces, John Wiley and Sons Inc, New York, 1987, pp 1-19.
47. P.D. Kondos, Pressure Chloride Leaching of a Complex U/Ra/Ni/As Ore: Statistical Modelling and Solution Chemistry, Ph.D. thesis, McGill University, 1988.
48. W.T. Thompson, A.D. Pelton and C.W. Bale, F.A.C.T. Guide to Operations, McGill University, May 1985.
49. W.M. Latimer, Oxidation Potentials, Second Ed., Prentice-Hall Inc., 1952.
50. Y.K. Rao, Stoichiometry and Thermodynamics of Metallurgical Processes, Cambridge University Press, 1985, pp 65-67.
51. H.H. Kellogg, Application of Fundamental Thermodynamics to Metallurgical Processes, Edited by G.R. Fitterer, Gordon and Breach, New York, 1967, pp 357-366.
52. D.E. Wilcox, A Method for Estimating the Heat of Formation and Free Energy of Formation of Inorganic Compounds, U.S. Department of Commerce, National Technical Information Service, Springfield, VA.22161.
53. O. Kubaschewski, E.L.L. Evans and C.B. Alcock, Metallurgical Thermochemistry, Pergamon Press, Oxford, 1974.

54. Yu.Ya. Bobyrenko, Estimation of the Standard Enthalpies of Formation and of the Free Energies of Titanium(IV) Sulphates and Hydroxides, Russian Journal of Inorganic Chemistry, July 1967, Vol.12, No.7, pp 931-932.
55. Guy Handfield, Physico-chemical properties of high-titania slags, QIT-Fer et Titane Inc., Intercompany Communication, 1968.
56. M. Guéguin, Méthode de digestion des scories, QIT-Fer et Titane Inc., Intercompany Communication, 1985.
57. J.F. Turgeon, Construction d'un nouvel appareil de digestion pour les scories de titane, QIT-Fer et Titane Inc., Intercompany Communication, 1988.
58. A. Turco, "Nuovissimo Ricett Ario Chimico", Ed. Hopeli, 1972, p. 1045-1046.
59. P.A. Schweitzer, Corrosion Resistance Tables, Second Edition, Marcel Dekker Inc., New York, 1986, pp 1098-1099, 1118-1134.
60. M.A. Merdinger, Practical Pilot Plants, short course notes, The Center for Professional Advancement, East Brunswick, New Jersey, 1990, pp B1.
61. G. Falconi, Analytical Method, QIT-Fer et Titane Inc., 1990.
62. Anon., Strategy of Experimentation, E.I. du Pont de Nemours & Co., Applied Technology Division, Wilmington, Delaware, 1975, pp 36.
63. ECHIP Inc, 724 Yorklyn Road, Hockessin, DE 19707, Tel. (302)-239-5429.
64. Stat-Ease Inc, Hennepin Square, Suite 191, 2021 East Hennepin Avenue, Minneapolis, MN 55413, Tel. (612)-378-9449
65. Manugistics Inc, 2115 East Jefferson Street, Rockville, MD 20852, Tel. (301)-984-5000.
66. A. Przepiera and al., Reactivity of titanium slags, Research center of inorganic chemistry, Police, Szcrecin, Poland, Private communication to K. Borowiec.
67. Joseph A. Rahm and Donald G. Cole, Process for Manufacturing Titanium Dioxide, U.S. Patent, No. 4 288 417, September 8, 1981.

68. Smith J.M. and Van Ness H.C., "Introduction to Chemical Engineering Thermodynamics", Fourth Edition, McGraw-Hill, N.Y., 1987, pp. 116-122, 574-579.
69. Perry and Green, Chemical Engineers Handbook, Sixth Edition, McGraw-Hill Book Company, 1984, pp 3-140, 3-145.
70. Robert C. Weast, CRC Handbook of Chemistry and Physics, 64th Edition, CRC Press Inc., Florida, 1984,

APPENDIX A

EXAMPLE OF A TABLE PRODUCED BY "INSPECT"

FORMULA: MG#S#O4

NAME: MAGNESIUM SULFATE

FORMULA WEIGHT: 120.363

PHASE	NAME	CP RANGE (K)
S1	SOLID	298.0 - 1400.0 D H TRANS (1400.00 K) = 14.644 (K J)
L1	LIQUID	1400.0 - 2000.0
AQ	AQUEOUS	298.0 - 473.0

$$CP = A + 1.0E-3B \cdot T(K) + 1.0E5C \cdot T(K)^{-2} + 1.0E-6D \cdot T(K)^{-3}$$

PHASE	DH(298) (K J)	S(298) (J /K)	DENSITY (G/CM ³)	A	B	C	D
----- (J /K) -----							
S1	-1284.906	91.630	2.660	106.437	46.275	-21.899	0.0
L1	-1290.658	60.037	2.660	158.992	0.0	0.0	0.0
AQ	-1755.616	-7.113	-----	-800.784	2715.244	-60.806	0.0

REFERENCE:

"THERMOCHEMICAL PROPERTIES OF INORGANIC SUBSTANCES",
I. BARIN, O. KNACKE, AND O. KUBASCHEWSKI,
SPRINGER-VERLAG, BERLIN, 1977.
(FOR THE NON-AQUEOUS SPECIES)

APPENDED TO:

"HANDBOOK OF THERMOCHEMICAL DATA FOR COMPOUNDS AND AQUEOUS SPECIES",
H.E. BARNER AND R.V. SCHEUERMAN,
WILEY-INTERSCIENCE, NEW YORK, 1978.
(FOR THE AQUEOUS SPECIES)

APPENDIX B

EXAMPLE OF A TABULAR PRINT-OUT FROM "RE/ CTION"

***** ENTER EQUATION *****

?

T1#02 + H2S#04 = T1#08S#04 + H2O

SUBSCRIPTS (OR ENTER /S TO SEE PHASES & RANGES)

?

(T,1,S) (T,1,L) (T,1,S) (T,1)

PRESS RETURN WHEN READY FOR TABULAR OUTPUT

(OR ENTER /H FOR HELP ON HOW TO SPECIFY RANGES AND GRAPHICS)

?

XX

T1#02 + H2S#04 = T1#08S#04 + H2O

(T,1,S) (T,1,L) (T,1,S) (T,1)

CALCULATIONS ARE BASED ON THE INDICATED NUMBER OF GRAM MOLES

(T) (K)	DELTA H (J)	DELTA G (J)	DELTA V (L)	DELTA S (J /K)	DELTA U (J)	DELTA A (J)

?						
298						
-----S1 L = S L-----						
298.0	-163115.6	-150654.8	-8.699E-03	-41.816	-163114.7	-150653.7
?						
348						
348.0	-163735.8	-148523.1	-8.699E-03	-43.715	-163734.8	-148522.1
?						
398						
-----S1 L = S G-----						
398.0	-124795.9	-148969.7	3.263E+01	60.739	-128102.0	-152275.9
?						
448						
448.0	-128324.1	-151796.8	3.673E+01	52.394	-132045.9	-155518.4
?						
498						
498.0	-132115.2	-154214.9	4.083E+01	44.376	-136252.7	-158352.3
?						

APPENDIX C

EXAMPLE OF THE RESULTS OBTAINED BY RUNNING "EQUILIBRIUM"

***** ENTER REACTANTS *****
(OR PRESS 'RETURN' FOR LAST ENTRY)

~~*****~~

ENTER SUBSCRIPTS, ENTER 'HELP', OR PRESS 'RETURN'

298.1, S1 (298.1, L) (298.1, L)

T FROD F FROD DELTA H DELTA G DELTA V DELTA S DELTA U DELTA A
(K) (ATM) (J) (J) (L) (J/K) (J) (J)

---S1 L L -----

298 1

- DATABASES BEING SEARCHED

GASEOUS SPECIES 1 - 34

LIQUID SPECIES 35 - 51

AQUEOUS SPECIES 52 - 80

SOLID SPECIES 81 - 108

Aqueous solution with Pitzer parameters.

< GQ(298K) from F*AC*T >

109 H2O

110 H[+]

111 OH[-]

ENTER CODE NUMBERS, ENTER "LIST" TO DISPLAY, OR ENTER "HELP"

*** (CHANGES TO EQUILIB REQUIRE THE USE OF SLASHES ABOUT GASEOUS SPECIES) ***

LIST

POSSIBLE PRODUCT COMPOUNDS FOUND:

" ---" IDENTIFIES YOUR PRIVATE COMPOUNDS DATA CREATED WITH "DATAENTRY"

" (--S" IDENTIFIES YOUR PRIVATE SOLUTION DATA CREATED WITH "SOLUTION"

UNNUMBERED SPECIES MEANS INCOMPLETE DATA SET

1	TI#S	G1	GAS	298.0 K -	2200.0 K	1
2	TI#O	G1	GAS	298.0 K -	3200.0 K	1
3	TI[+]	G1	GAS	298.0 K -	6000.0 K	2
4	TI	G1	GAS	298.0 K -	300.0 K	1
5	H2S#04	G1	GAS	298.0 K -	2000.0 K	1
6	S2O	G1	GAS	298.0 K -	2000.0 K	1

7	S#03	G1	GAS	298.0 K -	2000.0 K	1
8	S#02	G1	GAS	298.0 K -	1800.0 K	1
9	S#0	G1	GAS	298.0 K -	2000.0 K	1
10	H2S2	G1	GAS	298.0 K -	1000.0 K	1
11	H2S	G1	GAS	298.0 K -	1800.0 K	1
12	S#H	G1	GAS	298.0 K -	6000.0 K	2
13	S8	G1	GAS	298.0 K -	2000.0 K	1
14	S7	G1	GAS	298.0 K -	2000.0 K	1
15	S6	G1	GAS	298.0 K -	2000.0 K	1
16	S5	G1	GAS	298.0 K -	2000.0 K	1
17	S4	G1	GAS	298.0 K -	2000.0 K	1
18	S3	G1	GAS	298.0 K -	2000.0 K	1

19	S2	G1	GAS	298.0	K	-	2000.0	K	1
20	S	G1	GAS	298.0	K	-	2000.0	K	1
21	H2O1	G1	GAS	298.0	K	-	1500.0	K	1
22	H#O2	G1	GAS	298.0	K	-	6000.0	K	2
23	H2O	G1	STEAM	298.0	K	-	2500.0	K	1
24	C#H(+)	G1	GAS	298.0	K	-	6000.0	K	2
25	C#H(-)	G1	GAS	298.0	K	-	6000.0	K	2
26	C#H	G1	GAS	298.0	K	-	6000.0	K	2
27	O2	G1	GAS	298.0	K	-	2000.0	K	1

28	O2(-)	G1	GAS	298.0	K	-	6000.0	K	2
29	O2	G1	GAS	298.0	K	-	3000.0	K	1
30	O(+)	G1	GAS	298.1	K	-	6000.0	K	2
31	O(-)	G1	GAS	298.0	K	-	6000.0	K	2
32	O	G1	GAS	298.0	K	-	3000.0	K	2
33	H2	G1	GAS	298.0	K	-	3000.0	K	1
34	H	G1	GAS	298.0	K	-	6000.0	K	1

35	O7T14	L1	LIQUID	1950.0	K	-	2400.0	K	1
36	T1305	L1	LIQUID	2047.0	K	-	3000.0	K	1
37	T1203	L1	LIQUID	2112.0	K	-	3000.0	K	1
38	T1#02	L1	LIQUID	2143.0	K	-	3000.0	K	1
39	T1#0	L1	LIQUID	2023.0	K	-	3934.0	K	1
40	T1	L1	LIQUID	1933.0	K	-	3575.0	K	1
41	(H2S#04)2(H2O)13	L1	LIQUID	295.0	K	-	300.0	K	1
42	H2S#04(H2O)4	L1	LIQUID	295.0	K	-	300.0	K	1
43	H2S#04(H2O)3	L1	LIQUID	295.0	K	-	300.0	K	1
44	H2S#04(H2O)2	L1	LIQUID	295.0	K	-	300.0	K	1
45	H2S#04(H2O)	L1	LIQUID	295.0	K	-	300.0	K	1
46	H2S#04	L1	LIQUID	298.0	K	-	553.0	K	1

47	S#03	L1	LIQUID	298.0	K	-	310.0	K	1
48	H2S2	L1	LIQUID	240.0	K	-	313.0	K	1
49	S	L1	LIQUID	388.0	K	-	718.0	K	2
50	H2O2	L1	LIQUID	298.0	K	-	431.0	K	1
51	H2O	L1	WATER	273.0	K	-	374.0	K	1

52	H2S208	A1	AQUEOUS	298.0	K	-	298.0	K	1
	H2S204	A1	AQUEOUS						
	H#S204(-)	A1	AQUEOUS						
53	H2S#04	A1	AQUEOUS	295.0	K	-	300.0	K	1
54	H#S#04(-)	A1	AQUEOUS	298.0	K	-	573.0	K	1
55	H2S#02	A1	AQUEOUS	298.0	K	-	477.0	K	1
56	H#S#03(-)	A1	AQUEOUS	298.0	K	-	573.0	K	1
57	S#06(2-)	A1	AQUEOUS	298.0	K	-	573.0	K	1
58	S#06(2-)	A1	AQUEOUS	298.0	K	-	573.0	K	1

59	S206(2-)	A1	AQUEOUS	298.0 K -	573.0 K 1
60	S208(2-)	A1	AQUEOUS	298.0 K -	573.0 K 1
61	S206(2-)	A1	AQUEOUS	298.0 K -	573.0 K 1
62	S205(2-)	A1	AQUEOUS	298.0 K -	573.0 K 1
63	S204(2-)	A1	AQUEOUS	298.0 K -	573.0 K 1

64	S207(2-)	A1	AQUEOUS	298.0 K -	573.0 K 1
65	S204(2-)	A1	AQUEOUS	298.0 K -	573.0 K 1
66	S203(2-)	A1	AQUEOUS	298.0 K -	573.0 K 1
67	S202	A1	AQUEOUS	298.0 K -	298.0 K 1
68	H2S	A1	AQUEOUS	298.0 K -	473.0 K 1
69	H2S(-)	A1	AQUEOUS	298.0 K -	573.0 K 1
70	S3(2-)	A1	AQUEOUS	298.0 K -	573.0 K 1
71	S4(2-)	A1	AQUEOUS	298.0 K -	573.0 K 1
72	S3(2-)	A1	AQUEOUS	298.0 K -	573.0 K 1
73	S2(2-)	A1	AQUEOUS	298.0 K -	573.0 K 1
74	S(2-)	A1	AQUEOUS	298.0 K -	573.0 K 1
75	H2O2	A1	AQUEOUS	298.0 K -	473.0 K 1
76	H2O2(-)	A1	AQUEOUS	298.0 K -	573.0 K 1
77	O2H(-)	A1	AQUEOUS	298.0 K -	573.0 K 1
78	O2	A1	AQUEOUS	298.0 K -	573.0 K 1
79	H2	A1	AQUEOUS	298.0 K -	573.0 K 1
80	H(+)	A1	AQUEOUS	298.0 K -	573.0 K 1

81	T12(S204)3	----	S1	SOLIDE	298.0 K - 500.0 K 1
82	T1*(S204)2	----	S1	SOLIDE	298.0 K - 500.0 K 1

83	T1*O*S204	----	S1	SOLIDE	298.0 K - 500.0 K 1
84	T12S3		S1	SOLID	298.0 K - 310.0 K 1
85	T12S		S1	SOLID	298.0 K - 310.0 K 1
86	T1*S2		S1	SOLID	298.0 K - 310.0 K 1
87	T1*S2		S1	SOLID-A	298.0 K - 420.0 K 1
88	T1*S2		S2	SOLID-B	420.0 K - 1000.0 K 1
89	T1*S		S1	SOLID	298.0 K - 2200.0 K 1
90	O13T18		S1	SOLID	298.1 K - 1500.0 K 1
91	O13T17		S1	SOLID	298.1 K - 1500.0 K 1
92	O11T16		S1	SOLID	298.1 K - 1500.0 K 1
93	O9T15		S1	SOLID	298.1 K - 1500.0 K 1
94	O7T14		S1	SOLID	298.1 K - 1950.0 K 1
95	T1305		S1	SOLID-A	298.0 K - 450.0 K 1
96	T1305		S2	SOLID-B	450.0 K - 2047.0 K 1
97	T1207		S1	SOLID-A	298.0 K - 473.0 K 1
98	T1207		S2	SOLID-B	473.0 K - 2112.0 K 1
99	T1*O2		S1	RUTILE	298.0 K - 2147.0 K 1
100	T1*O2		S2	ANATASE	298.0 K - 2000.0 K 1
101	T1*O		S1	SOLID-A	298.0 K - 1264.0 K 1
102	T1*O		S2	SOLID-B	1264.0 K - 2027.0 K 1
103	T1*H2		S1	SOLID	298.0 K - 2000.0 K 1

VT100 NUM

CAFS

More...
COM1

1 4 71	S1 SOLID-A	298.0 K -	1139.0 K 1
1 5 71	S2 SOLID-B	1139.0 K -	1933.0 K 1
1 6 S8O7	S1 SOLID		
1 6 S	S1 RHOMBIC	298.0 K -	368.0 K 1
1 7 S	S2 MONOCLINIC	368.0 K -	388.0 K 1
1 8 H2O	S1 ICE	290.0 K -	273.0 K 1

Aqueous solution with Pitzer parameters.
 G' 298 from F&A&C&T
 1 9 H2O
 11 H(+)
 111 OH(-)

ENTER CODE NUMBERS, ENTER "LIST" TO DISPLAY, OR ENTER "HELP"
 ****(CHANGES TO EQUILIB REQUIRE THE USE OF SLASHES ABOUT GASEOUS SPECIES)***
 7 8 11 23 46 51 81 82 83 99 100
 PRESS "RETURN" WHEN READY FOR OUTPUT
 ENTER AN OPTION NUMBER, OR ENTER "0" FOR OPTIONS MENU

-----T-----T

**EXCESSIVE TIME ESTIMATED..ASSUMING 60 SERVICE UNITS
 T1#O2 + H2S#O4 + 0.5 H2O
 (298,1,S) (298,1,L) (298,1,L)

1.5000	H2O	
(398.0, 1.00	,G1, 1.0000)
+ 1.0000	T1OS04	<---
(398.0, 1.00	,S1, 1.0000)
+ 0.000000E+00	H2O	
(398.0, 1.00	,L1, 0.44182)
+ 0.000000E+00	S03	
(398.0, 1.00	,G1, 0.000000E+00)	
+ 0.000000E+00	S02	
(398.0, 1.00	,G1, 0.000000E+00)	
+ 0.000000E+00	H2S	
(398.0, 1.00	,G1, 0.000000E+00)	

-----T-----T

+ 0.000000E+00	H2S04	
(398.0, 1.00	,L1, 0.000000E+00)	
+ 0.000000E+00	T12(S04)3	----
(398.0, 1.00	,S1, 0.000000E+00)	
+ 0.000000E+00	T1(S04)2	<---
(398.0, 1.00	,S1, 0.000000E+00)	
+ 0.000000E+00	T1O2	
(398.0, 1.00	,S1, 0.000000E+00)	

DATA ON : PRODUCT SPECIES IDENTIFIED WITH T HAVE BEEN EXTRAPOLATED

DATA ON : PRODUCT SPECIES IDENTIFIED WITH ---- OR ---S HAVE BEEN DRAWN
FROM YOUR PRIVATE DATA COLLECTION

-----T

```

*****
  DELTA H   DELTA G   DELTA V   DELTA S   DELTA U   DELTA A   REACT V
    (J)      (J)      (L)      (J*)      (J)      (J)      (L)
*****
--S1 L L  -----
-104758.2 -150315.7 -0.757E-01  114.466  -104754.6  -150312.1  0.810E-01

```

(02MAR90)

***** ENTER REACTANTS *****
(OR PRESS "RETURN" FOR LAST ENTRY)

?

-----T

VT100 NUM

CAPS

Reading
COM1

APPENDIX D

EXAMPLE OF A TEST SPREADSHEET

DIGESTION NO.: RUN4

DATE: 29 AOUT 1990

ECHANTILLON: SQ1A

OPERATEUR: ALAIN MELANCON

CONDITIONS EXPERIMENTALES

GRANULOMETRIE:

+200:	888	z	-200 A +325:	888	z	-325:	888	z
AC./SC.:	1.70		POIDS SCORIE:	1500	g			
CONC.AC.ATTAQUE:	91.0	z	BOUTEILLE:	96.35	z			
POIDS ACIDE:	2646.6	g	POIDS EAU:	90.0	g	POIDS VAPEUR:	65	g
MELANGE:	15	min.	DEBIT AIR:	120		PRESSION:	30	PSIA
DEBIT A L ATTAQUE:	80		TEMPERATURE VAPEUR:	122	C	PRESSION:	15	PSIA

TEMPERATURE

ARRET VAPEUR:	142	C	TEMPS:	3.5	min.			
DEPART REACTION:	90	C						
PRISE:	202	C	TEMPS:	24.5	min.			
MAXIMUM:	208	C	TEMPS:	13	min.			
TEMPS MURISSEMENT:	240	min.	TEMPERATURE:	215	C	DEBIT AIR:	0	
REFROIDISSEMENT:	17	hres	TEMPERATURE FINAL:	74	C	DEBIT AIR:	0	
HAUTEUR DU GATEAU:	15.5	cm						

DISSOLUTION

TEMPS DISSOLUTION:	6	hres	TEMPERATURE	75	C	DEBIT AIR:	100
FLOCULANT:	DIAFLOC		CONCENTRATION:	0.3	g/l	VOLUME:	150
TEMPS DECANTATION:	30	min.	VOLUME:	0	ml	POIDS Fe:	0
							g

FILTRATION

POIDS LIQUEUR:	4476	g	VOLUME:	2692	ml	DENSITE:	1.663
POIDS LIQUEUR:	1429	g	VOLUME:	859	ml	DENSITE:	1.663
POIDS RESIDU:	166.35	g	STABILITE:	>500		BOUES:	888
POIDS RESIDU:	0	g					mg
VOLUME LAVAGE:	4200	ml	ACIDE ACTIF:	19.78	ml	PAR TITRATION (NaOH 0.5 N)	
VOLUME LAVAGE:	2050	ml					

ANALYSES

=====

SCORIE	TiO2:	77.3 %	Ti2O3:	14.2 %	Fe Total:	8.8 %
LIQUEUR	TiO2:	16.9 %	Ti2O3:	1.36 %	Fe Total:	1.95 %
NON-DISSOUT	TiO2:	16.75 %				
LAVAGE	TiO2:	15.2 g/l				
NON-DISSOUT	TiO2:	4.5 g/l				
RESIDU	TiO2:	39.8 %				
NON-DISSOUT	TiO2:	0 %				

CALCULS

=====

BILAN DE MATIERE POUR LE TiO2

AU DEPART:	1159.5 g	DANS LES PRODUITS:	1135.1 g	PERTES:	24.4 g
					2.11 %
RENDMENT SANS NON-DISSOUT	ICI ON CONSIDERE LES PERTES DANS LE RESIDU				
RESIDU:	92.2 %	LIQUEUR:	92.2 %		
RENDMENT AVEC NON-DISSOUT		PERTE TiO2 NON-DISSOUT:	0 g		
RESIDU:	0.0 %	LIQUEUR:	0.0 %		

LIQUEUR	BOUES APRES FILTRATION:		0 mg/l
TiO2:	281.0 g/l	Ti2O3:	22.6 g/l
		FeSO4:	88.2 g/l
ACIDE ACTIF:	484.61 g/l		
Fe Tot./TiO2 Tot.:	0.115	Ti2O3/TiO2 Tot.:	8.05 %
		FeSO4/TiO2:	0.314

DIGESTION NO.: RUM4

DATE: 29 AOUT 1990

ECHANTILLON: SQ1A

OPERATEUR: ALAIN MELANCON

GAZ

SOUFRE SOLIDE

PIEGES+BALLON: 0.15425 g LAVAGE: 0.37006 g H2S CORRESPONDANT: 0.56 g

TITRATION

SOLUTION NaOH: 5.14 M

PIEGE 1: 200 ml 1028 meq.

TITRATION H2SO4 1N

pH 9: 77.8 ml pH 7: 91.8 ml

H2SO4 CONTENU: 5.39 g SO2 + H2S: 140 meq.

PIEGE 2: 25 ml 129 meq.

TITRATION H2SO4 1N

pH 9: 12.1 ml pH 7: 12.8 ml

H2SO4 CONTENU: 0.02 g SO2 + H2S: 7 meq.

PIEGE 3: 25 ml 128.5 meq.

TITRATION H2SO4 1N

pH 9: 12.85 ml pH 7: 13.2 ml

H2SO4 CONTENU: -0.17 g SO2 + H2S: 3.5 meq.

PIEGE 4: 25 ml 128.5 meq.

TITRATION H2SO4 1N

pH 9: 12.9 ml pH 7: 13.2 ml

H2SO4 CONTENU: -0.17 g SO2 + H2S: 3 meq.

BALLON: 200 ml 1028 meq.

TITRATION H2SO4 1N

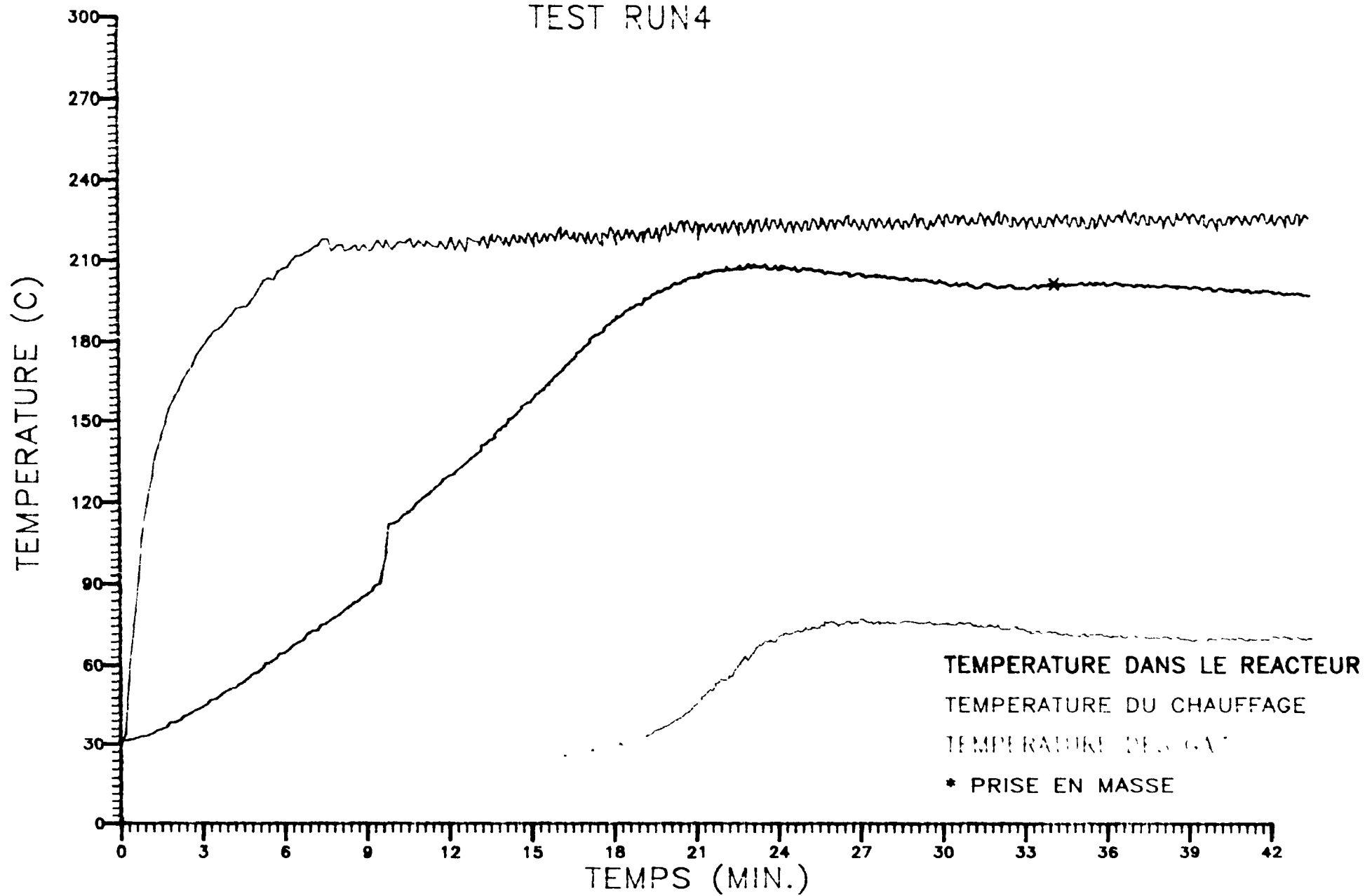
pH 9: 77.05 ml pH 7: 89.6 ml

H2SO4 CONTENU: 6.47 g SO2 + H2S: 125.5 meq.

TOTAL

POIDS RESIDU:	2.14912 g	% SOUFRE:	1.35	H2S SOLUBLE:	0.308 g
SO2 + H2S:	279 meq.	SO2:	274 meq.	SO2:	8.78 g
				H2SO4:	11.54 g
				H2S:	0.866 g

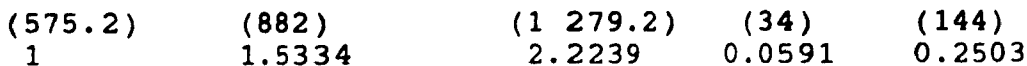
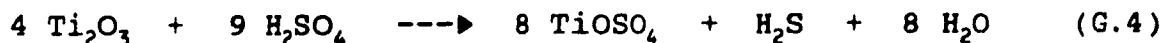
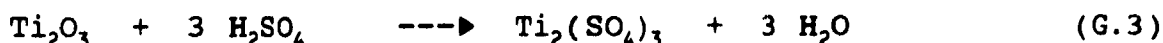
TEST RUN 4



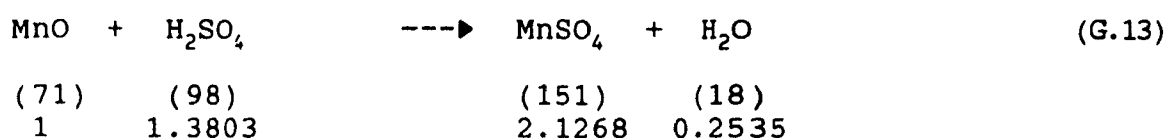
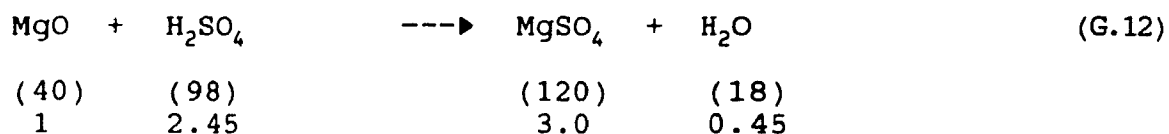
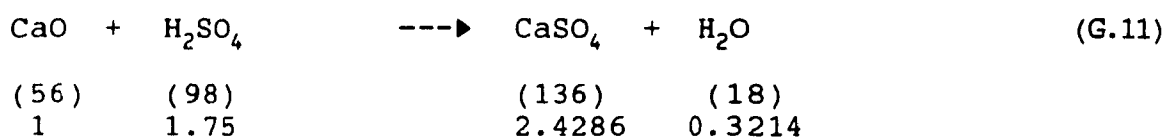
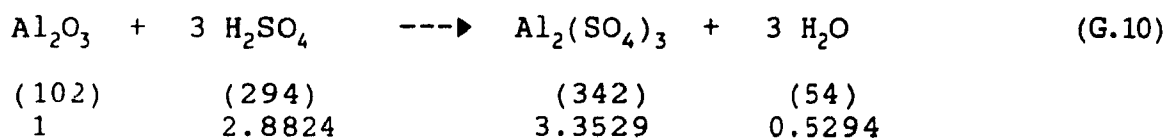
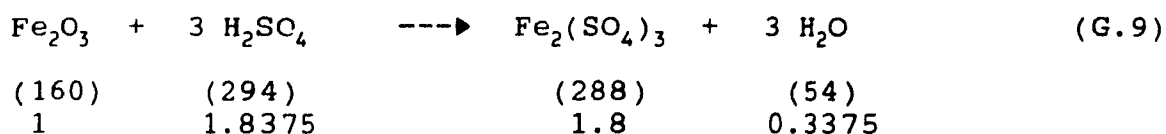
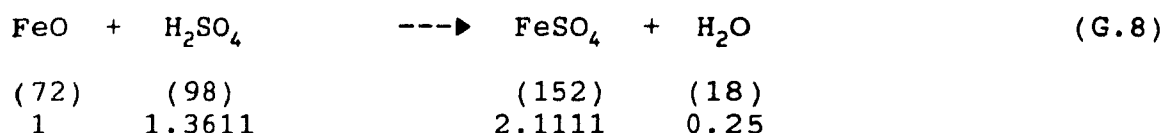
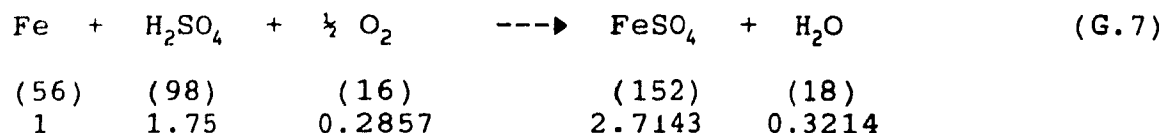
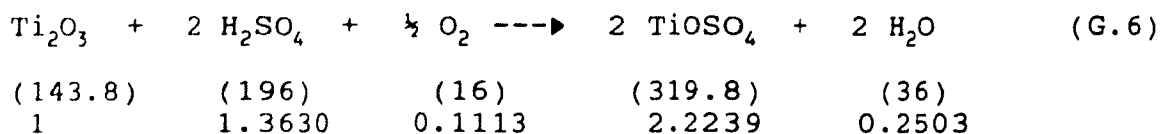
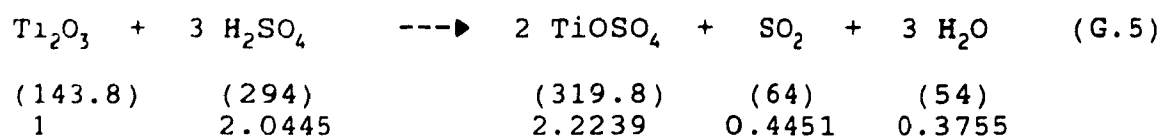
APPENDIX E

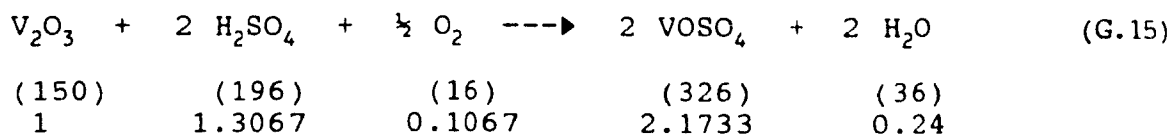
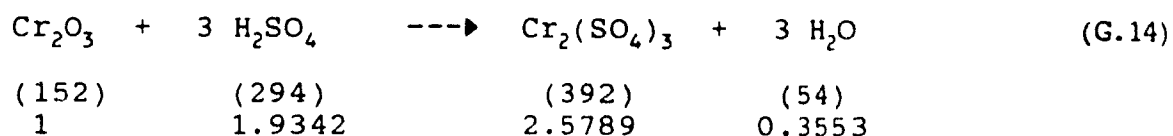
DETAILS OF THE MASS AND HEAT BALANCES CALCULATIONS

In this Appendix, details of the work which led to the preparation of Tables 6.3, 6.4 and 6.5 are provided. Table 6.3 contains the stoichiometric amounts of reactants and products obtained for 95 % digestion efficiency. To calculate the amount of sulphuric acid necessary to react with the various components of the slag SQ1B (see chemical analysis Table 4.2) and to evaluate the amount of sulphate and water produced, the following reactions were used:



***The molecular weight of each compound is given in parenthesis. The numbers below represent the stoichiometry in weight units.





The slag contain a fraction of TiO_2 which does not react with sulphuric acid, this is called insoluble TiO_2 . This fraction reports directly to the non-reacted product. The soluble TiO_2 may react with sulphuric acid via either or both of reactions G.1 or G.2. For this case, in order to obtain an acid/slag ratio of 1.7 and 100 % conversion of the acid into sulphate salts, we have assumed 44.77 % of the soluble TiO_2 to have reacted following reaction G.1 and 55.23 % following reaction G.2.

For all the reactions, except the Ti_2O_3 and Fe metal reactions, 95 % conversion was used. Ti_2O_3 and Fe metal were considered to transform completely into sulphate salts.

Ti_2O_3 may react with sulphuric acid via reaction G.3, G.4, G.5 or G.6. To decide at which degree each of these reactions occur the average data of the 27 experiments were used as reference (see Table 6.10). Thus for the theoretical mass balance we have taken 35 % of Ti_2O_3 to have reacted following reaction G.3, 8 % following G.4, 9.9 % following G.5 and 47.1

% following G.6 (refer to section 6.4.5).

The heat of reaction was calculated at 175°C for each of the reactions using the program F*A*C*T. In Table G.1 the obtained data are given. The total heat of reaction was calculated by adding the heat of each reaction except the reaction of Fe metal. This is so because Fe metal is assumed to react with sulphuric acid only during dissolution when the concentration of sulphuric acid is low.

Table G.1 : Heats of Reaction Obtained with F*A*C*T at 175°C

Reaction	Heat of Reaction (kJ/mol)
G.1	-128.3241
G.2	-108.6438
G.3	-175.4774
G.4	-1 722.3350
G.5	-360.0251
G.6	-626.9211
G.7	-363.8557
G.8	-93.2504
G.9	-65.1083
G.10	-62.6653
G.11	-235.6745
G.12	-118.8099
G.13	-115.1889
G.14	-84.7176
G.15	-266.5558

The mass balance calculations (Table 6.4)

REACTANTS

SLAG:

1500 g was used as in the experiment

H₂SO₄ 96 %:

The amount of 100 % H₂SO₄ was calculated in Table 6.3 according to the reaction stoichiometry; using this value the mass of 96 % H₂SO₄ was obtained:

$$\text{Mass of 100 \% H}_2\text{SO}_4 \div 0.96 = \text{Mass of 96 \% H}_2\text{SO}_4$$

DILUTION WATER:

It is the mass of water required to give a sulphuric acid concentration of 91 % at the attack.

$$(\text{Mass of 100 \% H}_2\text{SO}_4 \div 0.91) - \text{Mass of 96 \% H}_2\text{SO}_4 = \\ \text{Mass of Dilution Water}$$

OXYGEN:

It is the stoichiometric amount of O₂ used in reactions G.6, G.7 and G.15.

PRODUCTS

SULPHATES:

The amount of sulphate salts was calculated in Table 6.3 from the stoichiometry.

RESIDUE:

It is the non-reacted product calculated in Table 6.3. The insoluble TiO₂, SiO₂ and 5 % of the other oxides were assumed not to react.

REACTION WATER:

It is the stoichiometric amount of water produced by the reaction.

DILUTION WATER:

Water contained in the sulphuric acid.

$$\text{Mass of 100 \% H}_2\text{SO}_4 \div 0.91 = \text{Mass of Dilution Water}$$

SO₂ and H₂S:

Stoichiometric amounts of SO₂ and H₂S produced by reactions G.4 and G.5 respectively.

EVAPORATION OF WATER DURING DIGESTION:

It is the mass of water lost in the fumes.

$$\text{Total water} \times 0.60 = \text{Steam Loss}$$

The heat balance calculations (Table 6.5)

HEAT GENERATED

TOTAL HEAT OF REACTION AT 175°C:

It is the total heat of reaction calculated in Table 6.3 with the program F*A*C*T.

SULPHURIC ACID DILUTION:

It corresponds to the heat generated by diluting H₂SO₄. The heat evolved when one kilogram of sulphuric acid is diluted with water from 96 % to 91 % is 22.8 kcal (69). Thus:

$$2.55 \text{ kg of 100 \% H}_2\text{SO}_4 \times 22.8 \text{ kcal} = 58.14 \text{ kcal or } 243.3 \text{ kJ}$$

STEAM AT 122°C:

The specific internal energy of steam at 122°C is 2 531.1 kJ/kg and the specific internal energy of water at 20°C is 83.86 kJ/kg (68), by difference the heat introduced by the steam in the system is obtained.

$$2\,447.24 \text{ kJ/kg} \times 0.065 \text{ kg of steam} = 159.1 \text{ kJ}$$

HEAT ABSORBED

SLAG FROM 20 TO 175°C:

The specific heat of the slag was calculated from the specific heat of its various components using a lotus program. C_p was assumed constant between 20 and 175°C. At 20°C $C_p = 166.13 \text{ cal/kg}^\circ\text{C}$ or $0.6951 \text{ kJ/kg}^\circ\text{C}$.

$$1.5 \text{ kg of slag} \times 0.6951 \text{ kJ/kg K} \times 155 \text{ K} = 161.6 \text{ kJ}$$

SULPHURIC ACID FROM 20 TO 175°C:

The specific heat of 96 % sulphuric acid at 20°C is $0.3487 \text{ cal/g}^\circ\text{C}$ or $1.459 \text{ J/g}^\circ\text{C}$ (69).

$$2656.3 \text{ g of } 96 \% \text{ H}_2\text{SO}_4 \times 1.459 \text{ J/g}^\circ\text{C} \times 155^\circ\text{C} = 600.7 \text{ kJ}$$

WATER FROM 20 TO 175°C:

The specific internal energy of water at 175°C is 740.05 kJ/kg and the specific internal energy of water at 20°C is 83.86 kJ/kg (68), by difference the heat absorbed by the water in the system is obtained.

$$0.1459 \text{ kg of water} \times 740.05 \text{ kJ/kg} = 108.0 \text{ kJ}$$

AIR FROM 20 TO 175°C:

The specific heat of air is $0.24 \text{ cal/g}^\circ\text{C}$ or $1 \text{ J/g}^\circ\text{C}$ (70). 2.7 l/min. of air are used to agitate the mass during the digestion. The density of air is 1.2928 g/l at 20°C (70) if an average mixing of 45 minutes is used, the heat absorbed by the air is:

$$2.7 \text{ l/min.} \times 45 \text{ min.} \times 1.2928 \text{ g/l} \times 1 \text{ J/g}^\circ\text{C} \times 155^\circ\text{C} = 24.3 \text{ kJ}$$

FUMES (STEAM):

The specific internal energy of steam at 175°C is 2 578.55 kJ/kg and the specific internal energy of water at 20°C is 83.86 kJ/kg (68), by difference the heat loss when the steam leaves the reactor is:

$$0.4319 \text{ kg of steam} \times (2578.55 - 83.86) \text{ kJ/kg} = 1077.5 \text{ kJ}$$